Identification of processes that control the stable isotope composition of rainwater in the humid tropical West-Central Africa

B. Nlend, H. Celle-Jeanton, Camille Risi, Benjamin Pohl, F. Huneau, S. Ngo Boum-Nkot, G. Seze, Pascal Roucou, Pierre Camberlin, J. Etame, et al.

Elsevier Editorial System(tm) for Journal of Hydrology or its open access mirror
Manuscript Draft

Manuscript Number: HYDROL31370R1

Title: Identification of processes that control the stable isotope composition of rainwater in the humid tropical West-Central Africa

Article Type: Research paper

Keywords: δ18O; water vapor; convective activity; GPCP precipitation; air back trajectory.

Corresponding Author: Mr. Bertil NLEND,

Corresponding Author's Institution: Université de Bourgogne Franche-Comté; UMR 6249 Chrono-Environnement

First Author: Bertil NLEND

Order of Authors: Bertil NLEND; Helene CELLE-JEANTON, Professor; Camille RISI, Dr.; Benjamin POHL, Dr.; Frederic HUNEAU, Professor; Suzanne Ngo BOUM-NKOT, Dr.; Genevieve SEZE, Dr.; Pascal ROUCOU, Associate Professor; Pierre CAMBERLIN, Professor; Jacques ETAME, Professor; Beatrice Ketchemen-Tandia, Associate Professor

Abstract: This study interprets 11 years (2006 to 2016) and 6 months (March to August in 2017) of respectively monthly and daily isotopic (δD and δ18O) monitoring of rain at Douala (Cameroon), a humid tropical station in Western Africa. The main scope is to analyze the climate controls on precipitation isotopes at different timescales. Firstly, we examine the annual cycles of δ18O. Over the 11 years of survey, the annual cycle exhibits a W shape that is quite reproducible from year to year, with two minima in spring and autumn periods. Based on back trajectory calculations and remote sensing observations of water vapor isotopic composition, we show that the observed depletion in spring and autumn is due to strong convective activity along air mass trajectories. The same effect of convective activity can be observed at the daily timescale. At seasonal and daily time scales, the isotopic composition is also strongly tied to the convective organization and cloud types. More depleted precipitation is associated with larger areas of high clouds. Very low to low clouds are observed in July-August, mid-level to high clouds are dominant in June and high to very high clouds characterize March-April-May, thus explaining the enriched (depleted) values in summer (spring). Finally, this paper highlights the importance of large scale meteorological conditions controls on precipitation stable isotope composition in the Gulf of Guinea.

Suggested Reviewers: Luis Araguas Araguas
l.araguas@iaea.org

Naoyuki Kurita
nkurita@nagoya-u.jp

Robert Van Geldern
Erlangen-Nürnberg University, Germany

Zbynek Hrkal
Institute of Hydrogeology, Engineering Geology and Applied Geophysics;
Charles University, Prague

Gabriel Bowen
gabe.bowen@utah.edu

Abstract

This study interprets 11 years (2006 to 2016) and 6 months (March to August in 2017) of respectively monthly and daily isotopic (δD and $\delta^{18}O$) monitoring of rain at Douala (Cameroon), a humid tropical station in Western Africa. The main scope is to analyze the climate controls on precipitation isotopes at different timescales. Firstly, we examine the annual cycles of $\delta^{18}O$. Over the 11 years of survey, the annual cycle exhibits a W shape that is quite reproducible from year to year, with two minima in spring and autumn periods. Based on back trajectory calculations and remote sensing observations of water vapor isotopic composition, we show that the observed depletion in spring and autumn is due to strong convective activity along air mass trajectories. The same effect of convective activity can be observed at the daily timescale. At seasonal and daily time scales, the isotopic composition is also strongly tied to the convective organization and cloud types. More depleted precipitation is associated with larger areas of high clouds. Very low to low clouds are observed in July-August, mid-level to high clouds are dominant in June and high to very high clouds characterize March-April-May, thus explaining the enriched (depleted) values in summer (spring). Finally, this paper highlights the importance of large scale meteorological conditions controls on precipitation stable isotope composition in the Gulf of Guinea.

Keywords: $\delta^{18}O$, water vapor, convective activity, GPCP precipitation, air back trajectory.

***Declaration of Interest Statement**

Declaration of interests

☒ The authors declare that they have no known competing financial interests or personal relationships that could have appeared to influence the work reported in this paper.

☐The authors declare the following financial interests/personal relationships which may be considered as potential competing interests:

Response to Revision Request

The authors would like to thanks all the reviewers for their comments and suggestions for improvements which helped us to propose a new corrected version of the manuscript.

Here below is a point to point answer to comments.

Reviewer #2

1- I have some reservation about the explanation on the intra-seasonal time scale. For example, the authors have used the TES derived hydrogen vapor isotope data and compared their result of precipitation δ^2H variability. Though the absolute values of these two different datasets are not comparable as correctly mentioned by the authors, however a qualitative match is expected. According to Fig. 7 the seasonal characters are similar, but a considerable mismatch is observed during the later period of the year. For example, from Jan to Sep the precipitation isotope maintains a more or less constant positive offset relative to the vapor isotopic record, which is expected. But in the month of Oct the offset nearly vanishes and surprisingly in the month of Nov the offset value turns negative! This behavior defies the principle of isotopic fractionation. It may so happen that within the limits of analytical uncertainties, this negative offset is not significantly different from zero. But this aspect needs to be discussed in detail, especially why the offset values differ consistently in the months of Oct and Nov. Which atmospheric processes drive such kind of anomalous behavior?

In Figure 7, δD_V and δD_P do not have the same y-axis. For instance, in October (November) δD_V is approximately equal to -100‰ (-45‰) while δD_P equal to -30‰ (-10‰). So, there is always a positive offset between the isotopic composition of water vapor and precipitation despite the fact that we observe on Figure 7 that the two curves are bringing together. Moreover, once again, it is clearly mentioned in the text that we can't compare absolute values obtained from TES with observed precipitation isotopes. Concerning the processes involved in the variability of δD_V and δD_P, on Figure 7, the seasonal variability of δD_P - δD_V provides information on rainwater – water vapor interactions and it is demonstrated that post-condensational effects are negligible.

However, regarding this comment from the reviewer, to avoid misunderstanding, **we added in the title of Figure 7 a precision concerning the y-axis and precision in the text (lines 364-365) about the positive offset between δD_V and δD_P.**

Other issues

2- Line: 372: It is known that the process of condensation is an equilibrium process; if so, then why 'there is no reason for the precipitation to be in equilibrium with the vapor'?

We removed this sentence to avoid misunderstanding and confusion.

3- Line 376: Pls provide a complete description of the relationship between dDp and dDv. It has been reported that the slope for this kind of relation is closer to 1 (Conroy et al. 2016). But, the authors get a very high value of slope, 1.68. The reason for such a large deviation should be explained. In this context, it is also suggested to use the q-dD diagram (Conroy et al. 2016) in order to characterize the moisture sources.

Many thanks for bringing this to our attention and for the reference which has been taken in account (see lines 378 – 379). **We corrected it** and putted now the right value of the slope (see line 375).

4- In order to study the effect of continental recycling, the authors have calculated "the percentage of time of the air parcel over the continent during the last 3 days along the trajectory" (Line 404-405), termed as Fland. Two issues are important in this context. Firstly, the method of calculation of Fland is not provided. Secondly, and more importantly, at what height the trajectories have been calculated? If the trajectories have been calculated for a single height, then they do not necessarily represent a major amount of moisture transport to the sampling site, since moisture is typically transported at a spectrum of heights. A detailed quantitative calculation of moisture transport for different heights is expected to be presented here. Without this exercise the conclusion of 'poor continental recycling' could be misleading.

The method of calculation of F_{land} was added in the text; see lines 405-408. About the second issue, we thank the reviewer for his comment which helped us to improve this section of the manuscript. Indeed, **we calculated air back trajectories at different heights: 800, 850, 900, 950 and 980 hPa.** We have not performed investigation at more than 800 hPa because it is the boundary layer that feeds the convection and it is with the water vapor from the low layers that the rain is re-evaporated. By calculating trajectories at these different heights, we observed that there is no difference between them, especially since we focus only on air back trajectory at 3 days before Douala. Therefore, our conclusion of "poor continental recycling" in the study region can be considered as correct. **Detailed precision on this issue were added in section 4.3.2 (see lines 408 to 414).**

5- Line 457: how do you define the parameter "cloud surface"? How it is measured? How do you take care of the uncertainties in measurement?

Information concerning this is well detailed in section 3.3, line 238 and lines 240-241. Nevertheless thanks to this comment, to ensure the methodology described in the text is more understandable and robust, **we added more precision in lines 238, 240-241.**

6- One of the highlights "Local site precipitation <delta>18O of Douala was found to represent large-scale meteorology" may be confusing. I suggest rewording as 'Local site precipitation <delta>18O of Douala appears to respond to large-scale metrology".

Done.

7- The title of the MS is slightly misleading. Use of the word "and" in 'Western and Central Africa' may mean that the study sites are situated at both the western and central Africa. It

may be slightly modified as "Identification of processes that control the stable isotope composition of rainwater in the humid tropical West-Central Africa".

Done. Thank you for this suggestion.

Minor issues

8- Line 179: Ratios of d18O/d16O or d2D/D1H is not technically correct. Better use "ratios of 18O/16O or 2H/1H".

Done.

9- Line 212: Lekshmy et al. 2014 used TRMM derived rainfall data, not the GPCP products.

Corrected as suggested.

10- Line 270: Pls replace 'delta' by 'precipitation isotopes'.

Done. It is now line 269.

11- The MS is full of grammatical mistakes; use of the article is poorly done. I have mentioned some of them, but this is only an indicative list. It is suggested to get the MS examined by a native English speaker, or take the help of a professional service provider on the English language.

Done. Syntax errors have been corrected. In general, the English of the document has been improved and we thank the reviewer who encouraged us.

12- Line 282: 'regional scale' should be followed by "on a".

Done. It is now line 281

13- Line 296-97: please check for typos in the citations.

Done.

14- Line 311: English problem: "trajectories come…" is awkward. Trajectories are not object, but some kind of attribute. In this context, it may be replaced by moisture. Similar kind of errors is there in Line 313, 316, 318.

Corrected.

15- Line: 318: typo

Corrected.

16 - Line 321: "monsoon winds become less influent.." is not a good English. May be written as "strength of monsoon winds weaken.

Done.

17 - Line 327: The wording like "GPCP precipitation increases" may be replaced by 'the GPCP precipitation data show an increasing trend…'.

Done.

18 - Line 333: 'rainfall is most depleted' may mean that rainfall intensity is less. Better write "isotopic value of rainfall is depleted in spring….'.

Corrected as suggested. It is now line 332.

19 - Line 358: 'given' should be replaced by "provided".

Done. It is now line 357.

20 - Line 360: trajectories should be followed by 'the'.

Done. It is now line 359

Reviewer #3

1- Please avoid lumped references. Please talk about the specific points of each reference.

This remark has been considered and we would like to reassure the editors and the reviewers that each reference in the manuscript concerns a specific point or aspect.

2- How is the reproducibility of <delta>18O seasonal cycle from year to year?

This fact is clearly detailed and explained in section 4.1. The Figure 2 also discuss about it.

3- what is the correlation between monsoon and the transition to the dry season?

General comments on climate dynamic in the study area are given in section 2. There is no correlation between monsoon and the transition toward the dry season period, except that the second occurs when the first one ends. The monsoon is a SW wet wind which is most predominant at Douala from April to August. As the ITCZ begins its southward withdrawal in September until November the monsoon wind become less efficient, giving way to the Harmattan (NE dry wind) and the transition toward the dry period often correspond to the end of October – November. This is stated in section 2 and in section 4.2.2 by looking the pattern of air back trajectories.

Reviewer #4: Manuscript ID: HYDROL31370

Manuscript Title: Identification of processes that control the stable isotope composition of rainwater in the humid tropical Western and Central Africa

The paper is in order and can be recommended for publishing in present format.

Thank you very much for your positive comment.

***Highlights (3 to 5 bullet points (maximum 85 characters including spaces per bullet point)**

Highlights

- $\delta^{18}O$ was measured in precipitation in Douala (West Central Africa) at daily and monthly scales.
- key factors controlling stable isotope ratios of meteoric waters in humid tropical areas of Africa were identified thus contributing to the understanding of atmospheric processes
- Temporal variations of $\delta^{18}O$ are controlled by the intensity of upstream convection, the size of convective systems and clouds elevation
- Local site precipitation $\delta^{18}O$ of Douala appears to respond to large-scale meteorology

Identification of processes that control the stable isotope composition of rainwater in the humid tropical West-Central Africa

B. Nlend [a,f,g*], H. Celle-Jeanton [a], C. Risi [b], B. Pohl [c], F. Huneau [d,e], S. Ngo Boum-Nkot [f], G. Seze [b] , P. Roucou [c], P. Camberlin [c], J. Etame [f], B. Ketchemen-Tandia [f]

[a] Université de Bourgogne Franche-Comté, CNRS, UMR 6249 Chrono-Environnement, 16 route de Gray, F-25030 Besançon cedex, France

[b] Laboratoire de Météorologie Dynamique, IPSL, Sorbonne Universités UPMC, CNRS, Paris, France

[c] Centre de Recherches de Climatologie, UMR 6282 Biogéosciences CNRS/Université de Bourgogne Franche-Comté, Dijon, France

[d] Université de Corse Pascal Paoli, Département d'Hydrogéologie, Campus Grimaldi, BP 52, F-20250 Corte, France

[e] CNRS, UMR 6134 SPE, BP 52, F-20250 Corte, France

[f] University of Douala, Faculty of Sciences, P.O BOX 24157, Douala, Cameroon

[g] Cameroonian Institute for Geological and Mining Research, Hydrological Research Center, P.O BOX 4110, Yaoundé, Cameroon

*Corresponding author:
Bertil NLEND
Université de Bourgogne Franche-Comté,
CNRS, UMR 6249 Chrono-Environnement,
16 route de Gray, F-25030 Besançon cedex, France
Tel: 03 81 66 20 10 / 06 33 59 01 04
(from abroad: +33 3 81 66 20 10 / +33 6 33 59 01 04)
e-mail: bertil.nlend@univ-fcomte.fr / Nlendbertil@yahoo.fr

Abstract

This study interprets 11 years (2006 to 2016) and 6 months (March to August in 2017) of respectively monthly and daily isotopic (δD and $\delta^{18}O$) monitoring of rain at Douala (Cameroon), a humid tropical station in Western Africa. The main scope is to analyze the climate controls on precipitation isotopes at different timescales. Firstly, we examine the annual cycles of $\delta^{18}O$. Over the 11 years of survey, the annual cycle exhibits a W shape that is quite reproducible from year to year, with two minima in spring and autumn periods. Based on back trajectory calculations and remote sensing observations of water vapor isotopic composition, we show that the observed depletion in spring and autumn is due to strong convective activity along air mass trajectories. The same effect of convective activity can be observed at the daily timescale. At seasonal and daily time scales, the isotopic composition is also strongly tied to the convective organization and cloud types. More depleted precipitation is associated with larger areas of high clouds. Very low to low clouds are observed in July-August, mid-level to high clouds are dominant in June and high to very high clouds characterize March-April-May, thus explaining the enriched (depleted) values in summer (spring). Finally, this paper highlights the importance of large scale meteorological conditions controls on precipitation stable isotope composition in the Gulf of Guinea.

Keywords: $\delta^{18}O$, water vapor, convective activity, GPCP precipitation, air back trajectory.

1. Introduction

The atmosphere is an essential hydrological environment. It contains all the water vapor (0.001% of all the water of the Earth; Delmas et al. 2005) that forms the clouds by condensation which can then generate precipitations (liquid/solid) as a function of air temperature. The atmosphere is also an essential place of transfer and exchange for the global functioning of the Earth system. Its multiple interactions with the oceans, the continent and the biosphere make it an important study environment for understanding global changes. According to IPCC (1998), these global changes must affect tropical regions which are among the most vulnerable to possible anthropogenically induced climatic changes.

During the last decade, the scientific community, environmental institutions, governments, and local communities have increased their awareness of the importance of current tropical climate variability, based on the premise that, under increasing anthropogenic influence on the climate, changes in regional and global circulation may lead to an intensification of extreme events (i.e. floods or severe droughts: e.g., Pohl et al. 2017). In parallel, the use of stable isotopes of water, both δD and $\delta^{18}O$ has provided insights in the study of atmospheric water cycle (e.g., Rozanski et al. 1993, Araguas - Araguas et al. 2000, Celle-Jeanton et al. 2004); the key to understand the future climate changes or global changes. Relationship between δD and $\delta^{18}O$ in natural meteoric waters serves as a foundational reference to determine regional and local deviations from equilibrium processes and the potential origin of the water vapor. Moreover, water losses due to evaporation, incorporation of recycled atmospheric moisture, and/or mixing between isotopically distinct reservoirs leave a unique water fingerprint that can be used for climate-reconstructions (Moerman et al. 2013). Recently, isotopic composition of tropical meteoric water has also proven its usefulness as an indicator of modern climate variability (Vuille and Werner 2005; Ishizaki et al. 2012; Sanchez-Murillo 2015).

84 While in extra-tropical climates, stable isotope variations in meteoric
85 waters have been successfully explained by air temperature variability (Dansgaard 1964;
86 Rozanski et al. 1993), the case of tropical humid regions proved to be very much complex
87 since temperature variability is much weaker. The amount effect occurs as a result of
88 convective precipitation and can be nonlocal (Vimeux et al. 2005; He et al. 2015). The degree
89 of organization of convective systems has been shown to impact the atmospheric conditions at
90 the large-scale (Tobin et al. 2012; Wing et al. 2017). Consistently, it also impacts the isotopic
91 composition of water vapor and precipitation. Many additional factors can potentially play a
92 role, such as orographic effects, continental recycling or moisture origin combined with
93 complex microclimates (Rozanski et al. 1993, Lachniet and Paterson 2009).

94 These problematics are of major importance for the paper. What are the key factors
95 controlling stable isotope ratios of meteoric waters in humid tropical areas of West and
96 Central Africa? Answers to this question will contribute to the understanding of atmospheric
97 processes in the study region. Unlike arid and semi-arid African areas, where isotopic
98 variability has already been assessed in previous work (e.g; Taupin et al. 1997, Celle-Jeanton
99 et al. 2001; Risi et al. 2008b, 2010; Lutz et al. 2011, Tremoy 2012; Tremoy et al. 2014), the
100 Gulf of Guinea (GOG) region and tropical humid areas in Central Africa (Figure 1) are still
101 under-documented in isotopic data. There, the atmospheric cycle of water remains poorly
102 documented and isotopic data may help improve their knowledge. Indirectly, the paper will
103 help to understand rainfall variability in Douala and the origin of precipitated water through
104 isotopic analysis. In this objective, we took advantage of the long term monthly monitoring
105 set up in Douala, Cameroon (Figure 1) as part of the Global Network for Isotopes in
106 Precipitation (GNIP) framework (IAEA/WMO 2018) from 2006. In parallel, a daily sampling
107 has been carried out in 2017. This article represents the first valuation of precipitation isotope
108 data in the region. Datasets of other GNIP stations in the GOG and Central Africa (Figure 1)

109 are also integrated in this study, together with remote sensing data that document water vapor
110 isotopic composition, convective activity and cloud properties.

111

112 Figure 1.

113

114 **2. Regional climate: the West African Monsoon (WAM) dynamic**

115 Seasonality in the tropics is mostly determined by the seasonal migrations of the Inter
116 Tropical Convergence Zone (ITCZ, Preston-White and Tyson 1988; Schott et al. 2003), a
117 highly energetic feature of earth climate that is associated with deep convection. The ITCZ or
118 meteorological equator in Africa is the result of convergence between the Harmattan
119 (northeasterly dry wind) and Monsoon (southwesterly wet wind) in low levels of the
120 atmosphere (Sultan and Janicot 2000, Fink et al. 2018). Nicholson and Grist (2003) have
121 shown that the rain belt over Western and Central Africa is positively correlated with the
122 migration of the ITCZ. During the boreal spring (Mar-Apr-May), ITCZ holds a position of
123 about 5°N; half of the rain belt is located over the continent and the other one on the ocean
124 (Waliser and Gautier 1993). The mean rainfall amount calculated for this period, according to
125 GNIP measurements, is 232 mm for Douala, 138.4 mm for Cotonou, 137.7 mm for Sao-Tome
126 and 114.1 mm for Bangui. The relative humidity increases significantly over the continent
127 and sea surface temperatures (SST) present their annual peak (>27°C) during this period
128 (Dezfuli and Nicholson 2013). Then, ITCZ abruptly shifts from 5°N to 10°N in June-July
129 (Sultan and Janicot 2003). The so-called monsoon jump causes a subsidence in the southern
130 part of the GOG and the development of a cold tongue complex (Gu and Adler 2004). Low
131 SSTs suppress then partly or totally rainfall as e.g. in Sao-Tome (Figure 3). However, in the

Gulf of Biafra (Figure 1), SSTs remain high enough (>26°C) to partly maintain convection (Odekunle and Eludoyin 2008). Moisture increases over land and enhances rainfall there. Simultaneously, convective activity migrates to the North, and the monsoon flow crosses the Equator from South (GOG) to North (Guinean and then Sahelian Africa). At this time of the year (Jun-Jul-Aug), a rainfall peak is observed (Figure 3) in Douala (618.3 mm) and Bangui (145.5 mm). In Cotonou, Ogu et al. (2016) have also shown a good correlation between SSTs and precipitation, connecting rainfall amount in June to anomalously warm waters of the Gulf of Benin.

The abruptness of the northward progression of the ITCZ is in sharp contrast to its withdrawal, which appears as a more progressive southward progression. Like most regions in the equatorial latitudes, the Guinean Coast/Central Africa thus benefits from a double passage of the ITCZ in spring and autumn.

The unimodal distribution and the highest rainfall amount (~ 4000 mm/year) observed in Douala (Figure 3) is very particular as the whole region is generally characterized by a bimodal distribution with two precipitation maxima in April-May (or May-June) and October-November (or September-October), with a total amount lower than 2000 mm/year. The concave shape of the Gulf of Biafra may induce a convergence of southwesterly winds and topographic ascents forced by the relief of Mount Cameroon (> 4000 m, Figure. 1). This mesoscale convergence and orographic influence (Vondou et al. 2017) are all the more marked if the monsoon flow is intense and thick, which is the case in the core of the summer monsoon, when the ITCZ is far to the North. These regional features can explain the unimodal regime observed at Douala while further west (in Cotonou), and in southern hemisphere (Sao-Tome), the annual cycle is bimodal.

155 ## 3. Data and methods

156 ### *3.1. Rainfall sampling and isotopes analyses*

157 This paper makes use of the 106 monthly samples of rainwater that have been collected from
158 July 2006 to December 2016 at the GNIP station of Douala (see details of the GNIP stations
159 in Table 1 and Figure 1). The sampling followed the standard protocols (IAEA 2012).
160 Samples were collected by using a rain gauge which consists of a plastic funnel (diameter =
161 10 cm) coupled with a filter mesh to prevent contaminations by debris. A 5 cm layer of
162 mineral oil has been systematically added into the rain collector to avoid fractionation of the
163 collected rainwater. For each month, total rainfall was collected. Samples were taken
164 regularly, stored in a totalizer and kept at 4°C before being transferred in 50 ml amber glass
165 bottles, tightly capped and sent to the International Atomic Energy Agency (IAEA) laboratory
166 in Vienna, Austria for stable isotopes determinations. Stable isotopes of hydrogen and oxygen
167 were then analyzed by laser absorption spectroscopy following the method described by
168 Penna et al. (2010).

169 Table 1

170

171 The rainwater daily survey was conducted from March to August 2017 at the campus of the
172 University of Douala (X= 9.7461; Y= 4.062; Z= 17 m.a.s.l.), approximately at 7 km from the
173 GNIP station. Seventy samples were collected using a Palmex rain gauge that presents the
174 advantage to avoid evaporation without using medicinal paraffin oil (Gröning et al. 2012).
175 Daily samples were stored using the same protocols as for monthly rainfall. Isotopes analyses
176 were performed at the Hydrogeology Department of the University of Corsica, France, by

using a liquid-water stable isotope analyzer DLT-100 Los Gatos Research (Aggarwal et al. 2006; Penna et al. 2010).

Ratios of $^{18}O/\delta^{16}O$ and $^{2}H/^{1}H$ are expressed in delta units (‰, parts per mil) relative to Vienna Standard Mean Ocean Water (V-SMOW). The analytical precision is ±0.1‰ for oxygen-18 and ±1‰ for deuterium.

Local meteorological settings (precipitation amount and duration, air temperatures, vapor pressure) were provided by the National Weather Direction of Cameroon.

3.2. Tropospheric Emission Spectrometer (TES) data

With the advent of new technology in stable water isotopes, such as spectrometer on-board satellite, it has become easier to analyze isotopic composition of water vapor based on indirect laser measurement (Aemisegger et al. 2012). TES instrument on board on the Aura satellite is a nadir-viewing infrared Fourier transform spectrometer from which the deuterium content of water vapor (δD_v) can be retrieved (Worden et al. 2006; Worden et al 2007). The sensitivity of the retrieval is typically larger between 900 hPa and 400 hPa with a peak at 700 hPa. On average, δDv retrieved over these levels has a precision of 1.5% or about 15 parts per thousand (per mile) relative to Standard Mean Ocean Water. Uncertainties are reduced by averaging several measurements (Worden et al. 2006; Risi et al. 2013). Then the precision is sufficient for characterizing the global distribution of evaporation and condensation processes (Worden et al. 2006).

There is on average 1.8 degrees of freedom for δDv retrievals in the tropics (Worden et al. 2012), meaning that vertical profiles bear information on more than one level. To ensure good data quality, we selected only the measurements for which the quality flag is set to unity and for which the degree of freedom of the signal is higher than 0.5 (Risi et al. 2013). Here, to document the water vapor composition as close as possible to the surface, we use the δD

values retrieved by TES at 900 hPa from 2004-2008 at a monthly scale and we focus on a multi-year mean seasonal cycle and temporal variations rather than absolute values.

3.3. Convection and cloud datasets

Convective activity associated with the West African Monsoon (WAM) was analyzed using the Global Precipitation Climate Project one degree daily (GPCP-1dd; Huffman et al. 2001) data. The same dataset is used for both monthly and daily analyses. Data were retrieved from the National Oceanic and Atmospheric Administration (NOAA) website (https://www.esrl.noaa.gov/psd/cgi-bin/data/composites/printpage.pl). The robustness of GPCP products has been demonstrated in many studies (e.g.; Huffman et al. 1995, 1997; Adler et al. 2017) through a comparison with other proxies of convection or by multi-proxy studies: OLR (Outgoing Longwave Radiation) and TRMM (Tropical Rainfall Measurement Mission). GPCP products are a combination of precipitation data provided by a multiple sources of satellite-gauge (SG). They are obtained by optimally merging precipitation estimates computed from microwave, infrared, sounder data observed by the international constellation of precipitation-related satellites, and rain gauge analyses, taking advantage of the strengths of each data type. Mean SG products are computed by combining multi-satellite estimates with rain gauge analysis (Huffman et al. 2001). In this study, we use the GPCP-1dd (1-degree grid over the entire globe at 1-day) both for monthly and daily analyses.

To document the cloud types and convection organization in Western Central Africa, we use a cloud type (CT) product issued from geostationary MSG (Meteosat Second generation) satellite data and developed by SAFNWC (Satellite application facilities in support to nowcasting) /MSG algorithms (for more information see http://www.nwcsaf.org/web/guest/scientific-documentation). Clouds types are determined from their top temperature or pressure and, for high level clouds from their opacity (Dommo

et al. 2018; Seze 2015). The SAFNWC CT offers a classification of clouds into 12 classes: free land, free sea, very low clouds, low clouds, medium clouds, high clouds, very high clouds, thin cirrus, medium cirrus, thick cirrus, fractional clouds and semi-transparent above low or medium clouds, at 3-km spatial resolution for regions close to MSG sub-satellite point (0N, 0E) and a time step of 15-min. For our study purposes, focus is given to the altitude of clouds (low, medium, high, etc.) and their organization (as measured by the spatial extent of connected cloud pixels) to seek links with the isotopic contents of rainfall. Data are extracted for the region bounded by latitudes 10S–10N and longitudes 0E–20E, for the period from March to June 2017.

Based on these images, very high clouds areas (corresponding to very organized convective system) around Douala were calculated for each event using ArcGis mapping software, through the tool "measure". Indeed, since the contours of cloud masses or pixels are approximated to geometric forms (circle, rectangular, trapezoidal shape, etc.), the areas were calculated based on these forms. This calculation was performed after a zoom of the image at 100% in order to limit uncertainties or errors by using the tool of the software. For events with duration of more than 15 min, we have taken the maximum cloud area throughout the duration of rainfall.

3.4. Back trajectories

In order to assess the influence of air masses pathways on the isotopic composition of precipitation, and the importance of the location of convective activity in the region, we compute air back trajectories at 6h time steps, 10 days prior to arrival in the sampling site. This operation was performed for monthly and daily scales when isotopic data is available. Winds (at 900 hPa) were simulated by using the general circulation model LMDZ5A (Hourdin et al. 2013) guided by reanalysis products (ERA-Interim, Dee et al. 2011) of the

European Centre for Medium-Range Weather Forecasts (ECMWF). Back trajectories (speed and direction) were then computed with a 2D algorithm (similar to Vimeux et al. 2005) in order to approximate the moisture transport near the ground surface.

4. Results and discussion

4.1.Annual cycles of isotopes (δ) in precipitation of Douala

Figure 2 presents the seasonal variations of $\delta^{18}O$ from 2006 to 2016. The annual cycle of δ is quite reproducible from year to year. It exhibits a W shape most of the time, with minima in spring and autumn periods. Because of this rather good reproducibility of $\delta^{18}O$ seasonal cycle from year to year; we further consider a multi-year mean seasonal cycle in the section 4.2, and investigate the factors associated with this W cycle of δ.

However, the magnitude varies widely from one year to another for a given month. Such inter-annual variability could either reflect variations (i) in the climate seasonal background, or (ii) in synoptic / intra-seasonal variability, which could modify seasonal mean fields through upscaling processes, or eventually affect isotopic variations. These hypotheses are tested and discussed below.

Figure 2.

4.2. Factors responsible for precipitation isotopes variations at seasonal scale

4.2.1. Highlighting of a regional context

Seasonal variations of $\delta^{18}O$ and precipitation amount for GNIP stations in GOG and Central Africa region are presented in Figure 3.

Figure 3.

Similarities can be observed in the seasonal evolution of $\delta^{18}O$ at Cotonou, Bangui, Douala and Sao-Tome (Figure 3): (i) from January-February to April-May, $\delta^{18}O$ decreases; (ii) an enrichment in isotopic content is observed in summer (in June, July or August depending on the station); (iii) isotope contents then decrease until September or October and (iv) a new increase occurs until December. This relative homogeneity suggests that isotopic seasonality is controlled by mechanisms of, at least, on regional scale.

Correlation coefficients between $\delta^{18}O$, precipitation and temperature are very low for all the stations (Table 2). The weak correlation between $\delta^{18}O$ and air temperature (Table 2) highlights the lack of temperature effect in the GOG and Central Africa regions. Despite the fact that, in tropical maritime stations, a local amount effect is often observed (Rozanski et al. 1993), the poor correlation between $\delta^{18}O$ and local precipitation amount shows that this effect does not dominate the isotopic seasonality in Central Western Africa. Therefore, it is clear that, the local climate parameters do not control the seasonal variation of δ in precipitation. Thus we hypothesize that convective activity at the regional scale could be involved. This hypothesis is tested in the next section for the Douala station.

Table 2.

4.2.2. Influence of regional convective activity

Many studies in China (e.g., Gao et al. 2013; He et al. 2015 ; Yu et al. 2016; Guo et al. 2017; Shao et al. 2017; Gao et al. 2018), India and Indo-Pacific region (e.g., Chakraborty et al. 2015; Rahul and Gosh 2016; Cai et al. 2016; He et al. 2018), South America (e.g., Hoffmann et al. 2003;Vimeux et al. 2005; Villacis et al. 2008, Samuels-Crow et al. 2014) and Sahelian Africa (e.g., Risi et al. 2008b; Risi et al. 2010b; Tremoy et al. 2012) based on both

observations and models, have shown that convective activity, that occurs upstream the pathway of air parcels, is a major control of rainwater isotope composition in the tropics at daily, seasonal and inter-annual timescales.

Convective activity is known to deplete water vapor through 3 main processes: i) precipitating downdrafts, either at the convective-scale or at the meso-scale (Risi et al. 2008a, Kurita 2013), bring down depleted water vapor from the mid-troposphere to the boundary layer; ii) rain evaporation, when concerning a small proportion of each raindrop, adds depleted water vapor to the lower troposphere (Worden et al. 2007, Risi et al. 2010); iii) rain-vapor diffusive exchanges in a saturated atmosphere can also deplete the water vapor (Lawrence et al. 2004).

GPCP precipitations are used to examine convective activity upstream the sampling site of Douala. Figure 4 presents monthly mean precipitation and back trajectories calculated for each month. As expected, moisture comes from the Atlantic Ocean most of the time and precipitation, at this timescale, is entirely controlled by the seasonal migration of the ITCZ.

In November and December, moisture comes from the North-East without undergoing any convection. From December to January, there is an abrupt shift of air parcel from North-Easterly to South-Westerly, in line with the beginning of long northward migration of the ITCZ. From March to May (spring season), air masses undergo strong convective activity over the Gulf of Guinea. During the period June - August, air parcels still travel over the Gulf of Guinea, but air masses undergo a weak convective activity because the ITCZ has shifted further north over the Sahel region. From September to October (autumn period), the ITCZ retreats to the South so that air masses undergo strong convective activity once again. The shift between October and November trajectories marks the transition to the dry season when the strength of monsoon winds weakens.

Figure 5 by presenting the variability of monthly mean GPCP precipitation along the back trajectory over time (in hours), towards Douala station for May (spring period), August

(summer period), October (autumn period) and January (winter period) shows a quantitative analysis. It reveals where, along the trajectories, convective activity becomes higher and thus impacts $\delta^{18}O$ of Douala rainfall. Overall, the GPCP precipitation data show an increasing trend from the Southern Atlantic to Douala. Along the air back trajectories, at 7 days (168 hours) to the sampling site, precipitation is higher in August and May. First significant changes are observable at 120 hours, when a decrease (increase) of GPCP precipitation occurs in January (October). It substantially increases in May and August. At 3 days (72 hours) before Douala, convective activity is stronger in October (and to a lesser extent in May) than August and January. Since isotopic value of rainfall is depleted in spring and autumn (Figures 2-3), $\delta^{18}O$ seems to be mostly sensitive to convective activity only in the past few days before reaching Douala. This is consistent with the "memory" of convection in the isotopic composition of water as discussed by Risi et al (2008a), Tuinenburg et al (2015) and Gao et al (2013). Stable isotopes are imprint of convection along air parcel trajectories, and in the case of Douala, precipitation seems to acquire its signature on average 72h before reaching the station. Figure 6 shows the precipitation averaged over the past 72h (3 days) along the backward trajectories, for each month. The precipitation $\delta^{18}O$ is significantly anti-correlated with this average precipitation (r^2=0.60). This supports our hypothesis that convective activity along trajectories significantly controls the seasonality of precipitation $\delta^{18}O$ in Douala.

In summary, the moisture "source" at Douala is most of the year in the GOG. Two seasonal precipitation maxima along the trajectories (Figure 6) are related to the seasonal migration of the ITCZ. Thus, even if precipitation in Douala shows a unimodal regime with a rainfall peak in August, $\delta^{18}O$ records bimodal cycle as in the "source" area. This suggests that the regional convective activity is the main control of the isotopic composition of precipitation in Douala.

In the following section, we use the isotopic information of the water vapor to provide additional insights about the main processes controlling the isotopic composition of precipitation.

Figure 4.

Figure 5.

Figure 6.

4.2.3. Information from the isotopic composition of water vapor (δv)

The isotopic composition of the water vapor provided by the TES instrument can help to understand the variation of δ in precipitation: it allows separating the relative effect of processes acting along the trajectories of the water vapor (δDv) and local post-condensational processes (δDp – δDv) following the equation below:

$$\delta Dp = \delta Dv + (\delta Dp - \delta Dv) \quad (1).$$

δD_v and δD_P (Figure 7a) show a similar seasonality (r^2 = 0.57). Both δD_v and δD_P present depleted values in April-May and September-October (Figure 7a), corresponding to more active convection in the GOG. In addition, there is always a positive offset between the isotopic composition of water vapor and precipitation. Thus, the isotopic information on the advected water vapor is preserved in the isotopic composition of the rain.

Figure 7.

However, absolute values of δDp and TES δDv should not be directly compared. TES was calibrated using in-situ measurements on local sites (Worden et al 2012) but not specifically in West Africa. In addition, TES data at 900hPa represent an average over several vertical levels in the lower troposphere. Therefore, focus is given instead to temporal variability. Yet, assuming that the vertical δD gradient between 1000 and 900hPa is constant, δDp-δDv variations can be interpreted as variations in the rain-water vapor interaction processes.

The regression between δD_p and δD_v gives a slope of a1 = 1 whereas the values for δD_p and δD_p-δD_v are a2 = -0.68 and r^2 = 0.18. This insignificant r^2 attests that the rain-water vapor interaction processes do not control the δDp variations. Based on the slope a1, δD_v accounts for 100% of the δD_p variability. A similar case has been reported in western tropical Pacific (Conroy et al. 2016). This confirms that the seasonal variability of the isotopic composition of rainfall is predominantly influenced by δD_v, i.e. by the processes that affect water vapor along the trajectories. This means that the variability of δD_p-δD_v acts only to dampen and to blur the variability of δD_p. For instance, the evolution of δDp-δDv presents a maximum in spring (Figure 7b) and autumn, when δDv is most depleted.

4.3. Main controls of precipitation isotopic composition at daily scale

4.3.1. Temporal evolution of δ and link with upstream convection

Daily $\delta^{18}O$ in Douala varies from -0.3‰ to -7.4‰, with a mean value of -3.0‰ close to the monthly weighted mean of -2.8‰ calculated for the 2006-2016 period. These daily data appear then to be representative of the 2006-2016 mean seasonal cycles. Moreover, as for the seasonal scale, daily rainwater (Figure 8) is most depleted in spring (April-May) and more enriched in summer (July-August).

Figure 8.

In order to investigate upstream convection effects, we calculated the correlation between the $\delta^{18}O$ of rainfall and the precipitation recorded at 1 to 3 days earlier, along back trajectories (Table 3). In March, April and August, the correlations are significant (≥ 95%), suggesting that, like for the seasonal timescale, the daily evolution is driven by convection along trajectories. Yet, this mechanism is insufficient to explain completely the variability of δ in daily precipitation, especially in May, June and July.

Table 3.

4.3.2. Factors besides the upstream convection intensity: continental recycling and organization of convective systems

Continental recycling?

The goal of this section is to test whether continental recycling has significant influence on $\delta^{18}O$ at the daily time scale. To that end, we calculated the percentage of time of the air parcel over the continent during the last 3 days (72h) along the trajectory, hereafter F_{land}. This calculation was relatively simple since air back trajectories have been computed at 6h time steps and then for instance, the travel time of 36h of air mass over the continent will correspond to F_{land} equal to 50%. However, for this issue, we calculated air back trajectories at different heights: 800, 850, 900, 950 and 980 hPa since moisture is typically transported at a spectrum of heights. As it is the boundary layer that feeds the convection and it is with the water vapor from low layers that the rain is re-evaporated, investigation was not performed above 800 hPa. Results from this quantitative calculation (not shown here) of moisture transport for different heights show that there is no difference between them, especially since we focus only on air back trajectory at 3 days before Douala. In June, July and August, F_{land} is 0% for all rainy days (except on June 11th when F_{land} = 25%). Table 4 presents the detailed

results for spring period and shows an anti-correlation between $\delta^{18}O$ and F_{land}. Precipitation are thus more depleted, when the transit time of air parcels over the continent is long, during the last 3 days along the back trajectory This is in contradiction with the expected effect of a continental recycling.

Table 4.

Since δ is controlled in spring by a convection upstream the sampling site, the fact that $\delta^{18}O$ is more depleted with the increase of F_{land}, suggests a significant influence of convection intensity over the continent. Indeed, Xu and Zipser (2012) demonstrated that convection is generally more intense over the land than over the ocean. The more intense the convection along trajectories, the more depleted the water vapor. Therefore, moisture origin has only an indirect effect on isotopic composition of precipitation, depending on whether air mass goes through regions of a strong convection. The positive and significant correlation between F_{land} and GPCP precipitation confirms this mechanism.

Therefore, we suggest that, δ variations at a daily timescale are partly controlled by the intensity of the convection along air parcel trajectories and that continental recycling is not involved.

Influence of the organization of convective systems?

Several studies have shown that convective systems deplete the low-level water vapor more efficiently when they are more organized (Lawrence et al. 2004, Risi et al. 2008, Tremoy et al 2014), probably because moister air in larger systems allows for more efficient rain-vapour diffusive exchanges (Risi et al. 2008a). In addition, convective systems deplete more vapor as they extend to the upper troposphere (Lacour et al 2018) and as the extent of their anvils

(measured by the fraction of stratiform clouds) is large (Aggarwal et al. 2016). These features are typically associated with higher degrees of organization.

Here, we test whether the type of convective organization has a significant impact on the $\delta^{18}O$ observed at Douala. By using satellite image from the SAF classification, we define 3 classes of clouds in the region from March to August according to their altitude: (i) very low to low; (ii) medium to high and (ii) very high clouds. The low cloud class is mostly observed in July-August (Table 5 and Figure 9). The mid-level to high cloud class is dominant in June and the very high clouds are mostly present in spring (Figure 9). The area of cloud systems increases throughout spring, reaching a maximum in May, and decreases again from June. In July-August, the areas are too small to be calculated.

Figure 9.

Spatial organization of convective systems also determines rainfall event duration. The latter increases globally from March to August (Figure 10), ranging from 12 minutes to 1278 min (i.e. more than 21 hours).

Figure 10.

Combining this information on cloud altitude, cloud area and rainfall duration; we can infer that in March-April, most convective systems correspond to deep mesoscale convective systems (MCS; Mapes and Houze 1993; Laing and Fritsch 1997; Mathon et al. 2001; Fink et al. 2006; Tremoy et al. 2014). In May-June, convective systems are MCS that become even larger and organized, but extend less deep in altitude (in June). In contrast, in July-August,

462 convective systems are isolated; characterized by small cumulonimbus in the middle of low-
463 to-medium clouds (Figure 9b) that follow one another throughout the day, explaining the
464 apparent long durations of rain events.

465 The type of convective organization emerges then as an important control on the precipitation
466 isotopic composition. Cloud surface shows a significant negative correlation with
467 precipitation $\delta^{18}O$ from March to June (Table 5). The larger the cloud area, the more depleted
468 the precipitation. In addition, the more the convective system is organized, the longer is the
469 duration of the event (Laurent and Machado 2002, Fiolleau et al. 2013). Consistently, event-
470 scale $\delta^{18}O$ is anti-correlated with event duration in March (r^2 = 0.44), April (r^2 = 0.54), May
471 (r^2 = 0.64) and more weakly in June (r^2 = 0.34). The longer is the convective system, the more
472 depleted is the precipitation.

473 These different types of convective organization can also explain the isotopic evolution at the
474 seasonal scale. In spring, the organized, deep MCS deplete the water vapor efficiently,
475 leading to the observed precipitation $\delta^{18}O$ minimum. In contrast, in July-August, the
476 shallower, small isolated cumulonimbus clouds deplete the water vapor less efficiently,
477 leading to the observed precipitation $\delta^{18}O$ maximum in spite of the local precipitation
478 maximum observed at Douala.

479 Surprisingly, the r^2 between cloud area and $\delta^{18}O$ are close and even higher (in May and June)
480 than that observed between $\delta^{18}O$ and upstream precipitation (Table 3). After verifying that
481 upstream convection (GPCP precipitation recorded at 72h to Douala along the trajectory) and
482 cloud area are uncorrelated (Table 5), we can assert that two independent parameters control
483 $\delta^{18}O$: upstream convection intensity and the size of the convective system (both at local scale
484 and at upstream, see the Table 5).

Table 5.

5. Conclusion and outlook

This study aims at investigating the processes controlling the year-to-year (inter-annual), month-to-month (seasonality) and day-to-day (intra-seasonal) variability of rainfall isotopic composition in the Gulf of Guinea (GOG) region and especially in Douala (Cameroon). We observed that the annual cycle of δ is quite reproducible. Most years presents a W shape with minima in spring and autumn. $\delta^{18}O$ and δD_v appear to be mainly controlled by upstream convection and by the size of convective systems. We identified that the continental recycling doesn't impact the rainwater isotopes in the humid tropical area of the GOG. In particular, the $\delta^{18}O$ minima in spring and autumn are associated with strong convective activity in the GOG and large, long-lived and deep mesoscale convective systems, whereas the $\delta^{18}O$ maximum in July-August is associated with reduced convective activity in the GOG and isolated shallow convective systems. The importance of upstream convective activity in controlling the $\delta^{18}O$ of precipitation at various time scales is in line with a large body of recent research in different tropical regions influenced by a monsoon system. The importance of the type of convective system (size, organization, vertical extension) is also consistent with a growing number of recent studies but this is the first time that it is demonstrated through a detailed analysis of such a large number of individual convective systems. The findings of this study (obtained by integrating in situ and satellite measurements) advance our understanding of the temporal variation of precipitation stable isotopes in humid tropical area such as Douala, and shed a

new light on the importance of large scale meteorological conditions controls on precipitation stable isotope composition in the GOG.

Notwithstanding, numerical climate modelling could be a useful complementary approach to further analyse the factors controlling rainfall isotopic composition in and around Douala

Moreover, the climate in Douala being representative of a small area with monomodal rainfall regime surrounded by area with bimodal rainfall, high resolution modelling is necessary to correctly capture such particularity. More robust conclusions could be obtained with larger samples, which could be obtained by extending the length of the record. To better understand the role of convective organization on the isotopic composition, sampling at the intra-event scale is necessary. Finally, measuring the isotopic composition in the water vapor in addition to precipitation would be useful to isolate the post-condensation effects.

Acknowledgements

This paper constitutes a part PhD study of the first author, who was supported by a doctoral scholarship from the French Ministry of Foreign Affairs. The authors thank the French Embassy to the Republic of Cameroon for all mobility facilities provided during the study. Thanks also to the anonymous reviewers whose comments have substantially helped to improve the manuscript.

Funding: This research did not receive any specific grant from funding agencies in the public, commercial, or not-for-profit sectors.

References

Adler, R.F., Sapiano, M.R.P., Huffman, G.J., Wang, J., Gu, G., Bolvin. D., Chiu, L., Schneider, U., Becker, A., Nelkin, E., Xie, P., Ferraro, R., Shin, D-B., 2017. The Global Precipitation Climatology Project (GPCP) Monthly Analysis (New Version 2.3) and a Review of 2017 Global Precipitation. *Atmosphere* 2018, 9, 138; doi:10.3390/atmos9040138

Aemisegger, F., Sturm, P., Graf, P., Sodemann, H., Pfahl, S., Knohl,A., and Wernli, H.: 2012. Measuring variations of $\delta^{18}O$ and $\delta^{2}H$ in atmospheric water vapour using two commercial laser-based spectrometers: an instrument characterization study, *Atmos. Meas.Tech*., 5, 1491–1511, doi:10.5194/amt-5-1491-2012, 2012

Aggarwal, P., Ahmad, T., Gröning, M., Manish, G., Owano, Th., Baer, D., 2006. Laser spectroscopic analysis of stable isotopes in natural waters: a low-cost, robust technique for the use of environmental isotopes in hydrological and climate studies. *AGU Fall Meeting* Abstracts.

Aggarwal, P. K., Romatschke, U., Araguas-Araguas, L., Belachew, D., Longstaffe, F. J., Berg, P., ... & Funk, A. (2016). Proportions of convective and stratiform precipitation revealed in water isotope ratios. *Nature Geoscience, 9*(8), 624.

Aemisegger, F., Pfahl, S., Sodemann, H., Lehner, I., Seneviratne, S.I., Wernli, H., 2014. Deuterium excess as a proxy for continental moisture recycling and plant transpiration. *Atmos. Chem. Phys*. 14, 4029–4054

Araguas-Araguas, L., Froehlich, K., Rozanski, K., 2000. Deuterium and oxygen-18 isotope composition of precipitation and atmospheric moisture. *Hydrol. Process*. 14, 230-244

Benetti, M., Reverdin, G., Pierre, C., Merlivat, L., Risi, C., Steen-Larsen, H. C., & Vimeux, F., 2014. Deuterium excess in marine water vapor: Dependency on relative humidity and

surface wind speed during evaporation. *Journal of Geophysical Research: Atmospheres*, *119*(2), 584-593.

Benetti, M., Lacour, J. L., Sveinbjörnsdóttir, A. E., Aloisi, G., Reverdin, G., Risi, C., & Steen Larsen, H. C., 2018. A framework to study mixing processes in the marine boundary layer using water vapor isotope measurements. *Geophysical Research Letters*, *45*(5), 2524-2532.

Bony, S., Risi, C., and Vimeux, F., 2008. Influence of convective processes on the isotopic composition ($\delta^{18}O$ and δD) of precipitation and water vapor in the tropics: 1. Radiative-convective equilibrium and Tropical Ocean-Global Atmosphere-Coupled Ocean-Atmosphere Response Experiment (TOGA-COARE) simulations, *J. Geophys. Res*., 113, D19305, doi:10.1029/2008JD009942

Cai, Z., & Tian, L., 2016. Processes governing water vapor isotope composition in the Indo-Pacific region: convection and water vapor transport. *Journal of Climate*, *29*(23), 8535-8546.

Celle-Jeanton, H., Zouari, K., Travi, Y., Daoud, A., 2001. Caractérisation isotopique des pluies en Tunisie. Essai de typologie dans la région de Sfax. *C. R. Acad. Sci*. Paris, Sciences de la Terre et des planètes / Earth and Planetary Sciences 333 (2001) 625–631

Celle-Jeanton, H., Gonfiantini, R., Travi, Y., Sol B., 2004. Oxygen-18 variations of rainwater during precipitation: Application of the Rayleigh model to selected rainfalls in Southern France. *J. Hydrol*.289: 165–177

Chakraborty, S., Sinha, N., Chattopadhyay, R., Sengupta, S., Mohan, P.M., Datye, A., 2016. Atmospheric controls on the precipitation isotopes over the Andaman Islands, Bay of Bengal. *Scientific Reports* | 6:19555 | DOI: 10.1038/srep19555.

576 Conroy, J. L., Noone, D., Cobb, K.M., Moerman, J.W. & Konecky, B.L., (2016), Paired
577 stable isotopologues in precipitation and vapor: A case study of the amount effect within
578 western tropical Pacific storms, J. Geophys. Res. Atmos., 121, 3290-3303,
579 doi:10.1002/2015JD023844.

580 Dansgaard, W., 1964. Stable isotopes in precipitation. *Tellus* 16 (4), 436-468.

581 Dee, D.P., Uppala, S.M., Simmons, A.J., Berrisford, P., Poli, P., Kobayashi, S., Andrae, U.,
582 Balmaseda, M.A., Balsamo, G., Bauer, P., Bechtold, P., Beljaars, A.C.M., van de Berg, L.,
583 Bidlot, J., Bormann, N., Delsol, C., Dragani, R., Fuentes, M., Geer, A.J., Haimberger, L.,
584 Healy, S.B., Hersbach, H., Hólm, E.V., Isaksen, L., Kållberg, P., Köhler, M., Matricardi,
585 M., Mcnally, A.P., Monge-Sanz, B.M., Morcrette, J.J., Park, B.K., Peubey, C., de Rosnay,
586 P., Tavolato, C., Thépaut, J.N., Vitart, F., 2011. The ERA-interim reanalysis:
587 configuration and performance of the data assimilation system. Q. J. R. Meteorol. Soc.
588 137, 553–597. https://doi.org/10.1002/qj.828

589 Delmas, R., Mégie, G., & Peuch, V-H., 2005. Physique et chimie de l'atmosphère. Belin

590 Derrien, M., and Le Gléau, H., 2005. MSG/SEVIRI cloud mask and type from SAFNWC. *Int.*
591 *J. Remote Sens*., 26, 4707–4732, https://doi.org/10.1080/01431160500166128D

592 ——, and ——, 2010: Improvement of cloud detection near sunrise and sunset by temporal-
593 differencing and region-growing techniques with real-time SEVIRI. *Int. J. Remote Sens*.,
594 31, 1765–1780, https://doi.org/10.1080/01431160902926632.

595 Dezfuli, A.K., Nicholson, S.E., 2013. The Relationship of Rainfall Variability in Western
596 Equatorial Africa to the Tropical. *Journal of Climate,* Vol 26. DOI: 10.1175/JCLI-D-11-
597 00686.1

598 Dommo, A., Philipon, N., Vondou, D.A., Seze, G., Eastman, R., 2018. The June–September
599 Low Cloud Cover in Western Central Africa: Mean Spatial Distribution and Diurnal
600 Evolution, and Associated Atmospheric Dynamics. *JCLI*, 1-19; DOI: 10.1175/JCLI-D-17-
601 0082.1

602 Fiolleau, T., and Roca, R., 2001. Composite life cycle of tropical mesoscale convective
603 systems from geostationary and low Earth orbit satellite observations: Method and
604 sampling considerations. *Quart. J. Roy. Meteor. Soc*., 139, 941–953,
605 doi:https://doi.org/10.1002/qj.2174.

606 Fink A., Vincent D., Ermert V., 2006. Rainfall types in the West African Sudanian zone
607 during the summer monsoon 2002. *Mon. Wea. Rev*., 134(8) : 2143–2164.

608 Fink AH., Engel T., Ermert V., Van der Linden R., Schneidewind M., Redl R., Afiesimama
609 E., Thiaw W., Yorke C., Evans M., Pohl B., Camberlin B. & Roucou P., 2018. «Chapitre
610 1 : Climat Moyen et Cycle Annuel » dans DJ Parker et M Diop-Kane (Eds.), Météorologie
611 de l'Afrique de l'Ouest Tropicale, Manuel du Prévisionniste. EDP Sciences, pp. 27-82
612 (ISBN: 978-2-7598-2108-2)

613 Gao, J., Masson-Delmotte, V., Risi, C., He, Y., and Yao, T., 2013. What controls precipitation
614 δ18O in the southern Tibetan Plateau at seasonal and intra-seasonal scales? A case study
615 at Lhasa and Nyalam, *Tellus B*, 65, 21043, doi:10.3402/tellusb.v65i0.21043

616 Gao, J., He, Y., Masson-Delmotte, V., & Yao, T., 2018. ENSO effects on annual variations of
617 summer precipitation stable isotopes in Lhasa, southern Tibetan Plateau. *Journal of*
618 *Climate*, *31*(3), 1173-1182.

Gat, J. R. and Matsui, E., 1991. Atmospheric water balance in the Amazon basin: An isotopic evapotranspiration model, *J. Geophys. Res*, 96, 13179–13188, doi:10.1029/91JD00054, 1991.

Gimeno, L., Drumond, A., Nieto, R., Trigo, R. M., and Stohl, A., 2010. On the origin of continental precipitation, *Geophysical Research Letters*, 37, 2010

Gonfiantini, R., 1996. « On the isotopic composition of precipitation ». In Jean Charles Fontes (1936-1994), Un Souvenir, Proceedings, International Symposium, déc. 1995. European Geologist, 2: 5-8.

Gröning, M., Lutz, H.O., Roller-Lutz, Z., Kralik, M., Gourcy, L., Pöltenstein, L., 2012. A simple rain collector preventing water re-evaporation dedicated for δ18O and δ2H analysis of cumulative precipitation samples. *Journal of Hydrology* 448–449 (2012) 195–200

Gu, G., and Adler, R.F., 2004. Seasonal evolution and variability associated with the West African Monsoon System. *J. Climate* 17: 3364–3377.

Guo, X., Tian, L., Wen, R., Yu, W., & Qu, D. (2017). Controls of precipitation δ18O on the northwestern Tibetan Plateau: A case study at Ngari station. *Atmospheric Research*, *189*, 141-151.

Gupta, P., Noone, D., Galewsky, J., Sweeney, C., Vaughn, B.H., 2009. Demonstration of high-precision continuous measurements of water vapor isotopologues in laboratory and remote field deployments using wavelength-scanned cavity ring-down spectroscopy (WS-CRDS) technology. Rapid Commun. Mass Spectrom. 23 (16), 2534-2542. http://dx.doi.org/10.1002/rcm.4100

He, Y., Risi, C., Gao, J., Masson-Delmotte, V., Yao, T., Lai, Ch-T., Ding, Y., Worden, J., Frankenberg, Ch., Chepfer, H., Cesana, G., 2015. Impact of atmospheric convection on

642 south Tibet summer precipitation isotopologue composition using a combination of in situ
643 measurements, satellite data and atmospheric general circulation modeling, *J. Geophys.*
644 *Res. Atmos*., 120, 3852–3871, doi:10.1002/2014JD022180

645 He, S., Goodkin, N. F., Kurita, N., Wang, X., & Rubin, C. M., 2018. Stable isotopes of
646 precipitation during tropical Sumatra Squalls in Singapore. *Journal of Geophysical*
647 *Research: Atmospheres*, *123*(7), 3812-3829.

648 Hoffmann, G., Ramirez, E., Taupin, J.-D., Francou, B., Ribstein, P., Delmas, R., Durr, H.,
649 Gallaire, R., Simoes, J., Schoterer, U., Stievenard, M. and Werner, M., 2003. "Coherent
650 Isotope History of Andean Ice Cores over the Last Century". *Geophys. Res. Lett*., 30(4),
651 1179, doi:10.1029/2002GL014870.

652 Hourdin, F., Foujols, MA., Codron, F. et al. 2013. Impact of the LMDZ atmospheric grid
653 configuration on the climate and sensitivity of the IPSL-CM5A coupled model *Clim Dyn*
654 (2013) 40: 2167. https://doi.org/10.1007/s00382-012-1411-3

655 Huffman, G. J., Adler, R. F., Rudolf, B., Schneider, U., & Keehn, P. R., 1995. Global
656 precipitation estimates based on a technique for combining satellite-based estimates,
657 rain-gauge analysis, and Nwp model precipitation information. *Journal of Climate*, 8(5),
658 1284–1295.

659 Huffman, G. J., Adler, R. F., Arkin, P., Chang, A., Ferraro, R., Gruber, A., Janowiak, J.,
660 McNab, A., Rudolf, B. and Schneider, U., 1997. The Global Precipitation Climatology
661 Project (GPCP) Combined Precipitation Dataset. *Bulletin of the American Meteorological*
662 *Society*, 78(1), 1997, pp. 5-20.

663 Huffman, G.J.; Adler, R.F.; Morrissey, M.; Bolvin, D.; Curtis, S.; Joyce, R.; McGavock, B.;
664 Susskind, J., 2001. Global Precipitation at One-Degree Daily Resolution from Multi-
665 Satellite Observations. *J. Hydrometeorol*. 2001, 2, 36–50.

666 IAEA, 2012. Technical Procedures for GNIP Stations. Vienna, Austria, p. 12. Available at.
667 http://www-naweb.iaea.org/napc/ih/IHS_resources_gnip.html.

668 IAEA/WMO, 2018. Global Network of Isotopes in Precipitation. The GNIP Database.
669 Accessible at: https://nucleus.iaea.org/wiser

670 Ishizaki, Y., Yoshimura, K., Kanae, S., Kimoto, M., Kurita, N., Oki, T., 2012. Interannual
671 variability of H18 2 O in precipitation over the Asian monsoon region. *J. Geophys. Res*.
672 117, D16308. http://dx.doi.org/10.1029/2011JD015890.

673 IPCC 1998. The regional impacts of climate change'. A special report of IPCC Working
674 Group II. Eds. R. T. Watson, M. C. Zinyow-era, R. H. Moss and D. J. Dokken. Cambridge
675 University Press

676 Kurita, N., 2013. Water isotopic variability in response to mesoscale convective system over
677 the tropical ocean, *J. Geophys. Res*., 118, 10,376-10,390, doi:10.1002/jgrd.50754

678 Lachniet, M., Paterson, W., 2009. Oxygen isotope values of precipitation and surface waters
679 in northern Central America (Belize and Guatemala) are dominated by temperature and
680 amount effects. *Earth Planet. Sci. Lett*. 284, 435-446.

681 Lacour, J.-L., Clarisse, L., Worden, J., Schneider, M., Barthlott, S., Hase, F., Risi,
682 C.,Clerbaux, C., Hurtmans, D., Coheur, P.-F., 2015. Cross-validation of IASI/MetOp
683 derived tropospheric δD with TES and ground-based FTIR observations. *Atmos. Meas.*
684 *Tech*. 8, 1447–1466. https://doi.org/10.5194/amt-8-1447-2015.

685 Lacour, J-L., Risi, C., Worden, J., Clerbaux, C., Coheur, P.F., 2018. Importance of depth and
686 intensity of convection on the isotopic composition of water vapor as seen from IASI and
687 TES δD observations. *Earth and Planetary Science Letters* 481: 387–394.
688 https://doi.org/10.1016/j.epsl.2017.10.048.

689 Laing, A., and J. M. Fritsch, 1997: The global population of mesoscale convective complexes.
690 *Quart. J. Roy. Meteor. Soc*.,123,389–405.

691 Laurent, H., and Machado, L.A.T., 2002. Characteristics of the convective cloud system
692 organization during WETAMC/LBA – Comparison with West African convective
693 systems. Second international LBA science conference, Manaus, 7-10 July 2002.

694 Lawrence, J. R., Gedzelman, S.D., Dexheimer, D., Cho, H.K., Carrie, G.D., Gasparini, R.,
695 Anderson, C. R., Bowman, K. P., and Biggerstaff, M. I., 2004. Stable isotopic
696 composition of water vapor in the tropics, *J. Geophys. Res*., 109,
697 D06115,doi:10.1029/2003JD004046

698 Lee, JE., Fung, I., 2008. 'Amount effect' of water isotopes and quantitative analysis of post
699 condensation processes. *Hydrol. Processes* 22: 1–8.

700 Lutz, A., Thomas, J.M., Panorska, A., 2011. Environmental controls on stable isotope
701 precipitation values over Mali and Niger, West Africa. *Environ Earth Sci* (2011) 62:1749–
702 1759. DOI 10.1007/s12665-010-0655-7

703 Mathon, V., and Laurent, H., 2001. Life cycle of Sahelian mesoscale convective cloud
704 systems. *Q. J. R. Meteorol. Soc*., 127(572): 377–406.

705 Mapes, B. E., and Houze, Jr., 1993. Cloud clusters and superclusters over the Oceanic warm
706 pool, *Mon. Wea. Rev*., 121, 1398–1415.

Merlivat, L., and Jouzel, J., 1979. Global climatic interpretation of the deuterium-oxygen 18 relationship for precipitation, *J. Geophys. Res*., 84, 5029–5033

Moerman, J.W., Cobb, K.M., Adkins, J.F., Sodemann, H., Clark, B., Tuen, A., 2013. Diurnal to interannual rainfall δ18O variations in northern Borneo driven by regional hydrology. *Earth Planet. Sci. Lett*. 369e370, 108-119. http://dx.doi.org/ 10.1016/j.epsl.2013.03.014

Moyer, E. J., Irion, F.W., Yung, Y.L., and. Gunson, M. R., 1996. ATMOS stratospheric deuterated water and implications for troposphere-stratosphere transport, *Geophys. Res. Lett*., 23(17), 2385–2388, doi:10.1029/96GL01489.

Nicholson, S.E., Grist, J.P., 2003. The seasonal evolution of the atmospheric circulation over west africa and equatorial Africa. *J Climate* 16(7):1013–1030

Odekunle, T.O. and Eludoyin, A.O., 2008. Sea Surface Temperature Patterns in the Gulf of Guinea: Their Implications for the Spatio-Temporal Variability of Precipitation in West Africa. *International Journal of Climatology*, 28, 1507-1517. http://dx.doi.org/10.1002/joc.1656

Ogou, F.K., Batebana, K., Ogwang, B.A., Sein, Z.M.M., Ongoma, V., Ngarukiyimana, J.P., 2016. Investigation of the influence of Atlantic Ocean on rainfall variability over Benin Republic, West Africa. *Ethiopian Journal of Environmental Studies & Management* 9 (1): 70 – 79, 2016. ISSN:1998-0507 doi: http://dx.doi.org/10.4314/ejesm.v9i1.7

Penna, D., Stenni, B., Sanda, M., Wrede, S., Bogaard, T.A., Gobbi, A., Borga, M., Fischer, B.M.C., Bonazza, M., Charova, Z., 2010. On the reproducibility and repeatability of laser absorption spectroscopy measurements for δ^2H and $\delta^{18}O$ isotopic analysis. *Hydrol. Earth Syst. Sci. Discuss*., 7, 2975–3014, 2010. www.hydrol-earth-syst-sci-discuss.net/7/2975/2010/doi:10.5194/hessd-7-2975-2010

730 Pfahl, S., and Wernli, H., 2009. Lagrangian simulations of stable isotopes in water vapor – an
731 evaluation of non-equilibrium fractionation in the Craig-Gordon model, *J. Geophys. Res*.,
732 114, D20108, doi:10.1029/2009JD012054.

733 Pohl, B., Macron, C., & Monerie, P.A., 2017. Fewer rainy days and more extreme rainfall by
734 the end of the century in Southern Africa. Sci. Rep. 7, 46466; doi: 10.1038/srep46466.

735 Preston-Whyte, R., Tyson, P., 1988. The atmosphere and weather of Southern Africa. *Oxford*
736 *University Press*, Cape Town, pp 334

737 Rahul, P., Ghosh, P., & Bhattacharya, S. K., 2016. Rainouts over the Arabian Sea and
738 Western Ghats during moisture advection and recycling explain the isotopic composition
739 of Bangalore summer rains. *Journal of Geophysical Research: Atmospheres*, *121*(11),
740 6148-6163.

741 Ren, W., Yao, T., & Xie, S.,2017. Key drivers controlling the stable isotopes in precipitation
742 on the leeward side of the central Himalayas. *Atmospheric Research*, *189*, 134-140.

743 Risi, C., Bony, S., Vimeux, F., 2008a. Influence of convective processes on the isotopic
744 composition (δ18O and δD) of precipitation and water vapor in the tropics: 2. Physical
745 interpretation of the amount effect. *J. Geophys. Res*. 113, D19306.
746 http://dx.doi.org/10.1029/2008JD00943

747 Risi, C., Bony, S., Vimeux, F., Descroix, L., Ibrahim, B., Lebreton, E., Mamadou I., Sultan,
748 B., 2008b. What controls the isotopic composition of the African monsoon precipitation?
749 Insights from event-based precipitation collected during the 2006 AMMA field campaign.
750 *Geophysical Research Letters*, Vol. 35, L24808, doi: 10.1029/2008GL035920

751 Risi, C., S. Bony, F. Vimeux, M. Chong, L. and Descroix, L., 2010a. Evolution of the water
752 stable isotopic composition of the rain sampled along Sahelian squall lines, *Quart. J. Roy.*
753 *Meteor. Soc*., 136, 227–242.

754 Risi, C., Bony, S., Vimeux, F., Frankenberg, C., Noone, D., & Worden, J., 2010b.
755 Understanding the Sahelian water budget through the isotopic composition of water vapor
756 and precipitation. *Journal of Geophysical Research: Atmospheres*, *115*(D24).

757 Risi, C., Noone, D., Worden, J., Frankenberg, C., Stiller, G., Kiefer, M., Funke, B., Walker,
758 K., Bernath, P., Schneider, M., Wunch, D., Sherlock, V., Deutscher, N., Griffith, D.,.
759 Wennberg, P.O., Strong, K., Smale, D., Mahieu, E., Barthlott, S., Hase, F., García, O.,
760 Notholt, J., Warneke, T., Toon, G., Sayres, D., Bony, S., Lee, J., Brown, D., Uemura, R.,
761 and Sturm, C., 2012.Process evaluation of tropospheric humidity simulated by general
762 circulation models using water vapor isotopologues: 1. Comparison between models and
763 observations, *J. Geophys. Res*., 117, D05303

764 Risi, C., Noone, D., Frankenberg, C., and Worden, J., 2013. Role of continental recycling in
765 intraseasonal variations of continental moisture as deduced from model simulations and
766 water vapor isotopic measurements, *Water Resour. Res*., 49, 4136–4156,
767 doi:10.1002/wrcr.20312.

768 Rozanski, K., Araguas-Araguas, L., and Gonfiantini, R., 1993. Isotopic patterns in modern
769 global precipitation, in Climate Change in Continental Isotopic Records, *Geophys.*
770 *Monogr. Ser*., vol. 78, edited by P. K. Swart et al., pp. 1 –36, AGU, Washington, D. C

771 Salamalikis, V., Argiriou, A. A., & Dotsika, E., 2015. Stable isotopic composition of
772 atmospheric water vapor in Patras, Greece: A concentration weighted trajectory approach.
773 *Atmospheric research*, *152*, 93-104.

774 Salati, E., Dall'Olio, A., Matsui, E., and Gat, J., 1979. Recycling of water in the Amazon
775 basin: An isotopic study, *Water Resour. Res*, 15, 1250–1258, doi:
776 10.1029/WR015i005p01250.

777 Samuels Crow, K. E., Galewsky, J., Hardy, D. R., Sharp, Z. D., Worden, J., & Braun, C.,
778 2014. Upwind convective influences on the isotopic composition of atmospheric water
779 vapor over the tropical Andes. *Journal of Geophysical Research: Atmospheres*, *119*(12),
780 7051-7063.

781 Sanchez-Murillo, R., Birkel, C., Welsh, K., Esquivel-Hernandez, G., Corrales-Salazar, C.,
782 Boll, J., Brooks, E., Roupsard, E., Saenz-Rosales, O., Katchan, I., Arce-Mesen, R.,
783 Soulsby, C., Araguas-Araguas, L.J., 2015. Key drivers controlling stable isotope
784 variations in daily precipitation of Costa Rica: Caribbean Sea versus Eastern Pacific
785 Ocean moisture sources, *Quaternary Science Reviews*
786 http://dx.doi.org/10.1016/j.quascirev.2015.08.028

787 Schott, F., Carton, J., Hazeleger, W., Johns, W., Kushnir, Y., Reason, C., Xie, SP., 2003.
788 White paper on a tropical atlantic climate experiment (t.a.c.e.) CLIVAR Atlantic
789 Implementation Panel, US Clivar, Washington

790 Sèze, G., Pelon, J., Derrien, M., Le Gléau, H., Six, B., 2015. Evaluation against CALIPSO
791 lidar observations of the multigeostationary cloud cover and type dataset assembled in the
792 framework of the Megha-Tropiques mission. *Quart. J. Roy. Meteor. Soc*., 141, 774–797,
793 https://doi.org/10.1002/qj.2392.

794 Shao, L., Tian, L., Cai, Z., Cui, J., Zhu, D., Chen, Y., & Palcsu, L., 2017. Driver of the
795 interannual variations of isotope in ice core from the middle of Tibetan Plateau.
796 *Atmospheric Research*, *188*, 48-54.

797 Stewart, M. K., 1975. Stable isotope fractionation due to evaporation and isotopic exchange
798 of falling water drops: Applications to atmospheric processes and evaporation of lakes.
799 *Journal of Geophysical Research*, *80*(9), 1133-1146.

800 Sultan. B., Janicot, S., 2000. Abrupt shift of the ITCZ over West Africa and intra-seasonal
801 variability. *Geophys Res Lett* 27:3353–3356

802 Sultan, B., Janicot, S., 2003. The West African monsoon dynamics. Part II: the ‘‘pre-onset’’
803 and ‘‘onset’’ of the summer monsoon. *J Clim* 16:3407–3427

804 Taupin, J.-D., R. Gallaire, and Y. Arnaud., 1997. Analyses isotopiques et chimiques des
805 précipitations sahéliennes de la région de Niamey au Niger: Implications climatologiques,
806 Hydrochemistry, 244, 151– 164, *IAH Congress*.

807 Tobin, I., Bony, S., & Roca, R., 2012. Observational evidence for relationships between the
808 degree of aggregation of deep convection, water vapor, surface fluxes, and radiation.
809 *Journal of Climate*, *25*(20), 6885-6904.

810 Tremoy, G., 2012. Etude de la composition isotopique (deutérium et oxygène 18) de la vapeur
811 d’eau à Niamey (Niger): vers une meilleure compréhension des processus atmosphériques
812 en Afrique de l’Ouest, Ph.D. thesis, Université de Versailles Saint-Quentinen-Yvelines

813 Tremoy, G., Vimeux, F., Mayaki, S., Souley, I., Cattani, O., Risi, C., ... & Oi, M., 2012b. A 1
814 year long $\delta^{18}O$ record of water vapor in Niamey (Niger) reveals insightful atmospheric
815 processes at different timescales. *Geophysical Research Letters*, *39*(8).

816 Tremoy, G., Vimeux, F., Soumana, S., Souley, I., Risi, C., Favreau, G., Oï, M., 2014.
817 Clustering mesoscale convective systems with laser-based water vapor $\delta^{18}O$ monitoring in
818 Niamey (Niger). doi: 10.1002/2013JD020968

819 Tuinenburg, O. A., Risi, C., Lacour, J.L., Schneider, M., Wiegele, A., Worden, J., Kurita, N.,
820 Duvel, J.P; Deutscher, N; Bony, S,.Coheur, P.F., and C. Clerbaux., 2015. Moist processes
821 during MJO events as diagnosed from water isotopic measurements from the IASI
822 satellite, *J. Geophys. Res. Atmos*., 120, 10,619–10,636, doi:10.1002/2015JD023461.

823 Villacís, M., Vimeux, F. and Taupin, J.-D., 2008. "Analysis of the Climate Controls on the
824 Isotopic Composition of Precipitation (d18O) at Nuevo Rocafuerte, 74.58W, 0.98S, 250
825 m, Ecuador." *C. R. Geosciences* 340(1): 1-9

826 Vimeux, F., Gallaire, R., Bony, S., Hoffmann, G., Chiang, J., Fuertes, R., 2005. What are the
827 climate controls on isotopic composition (δD) of precipitation in Zongo Valley (Bolivia)?
828 Implications for the Illimani ice core interpretation, *Earth Planet. Sci. Lett*. 240 (2005)
829 205–220

830 Vondou, D.A., Yepdo, Z.D., Djiotang Tchotchou, L.A., 2017. Diurnal Cycle of Convective
831 Cloud Occurrences over Cameroon during June–August. *Journal of the Indian Society of*
832 *Remote Sensing* https://doi.org/10.1007/s12524-017-0747-x

833 Vuille, M., Wermer, M., 2005. Stable isotopes in precipitation recording South American
834 summer monsoon and ENSO variability: observations and model results. Clim. Dyn. 25,
835 401-413. http://dx.doi.org/10.1007/s00382-005-0049-9.

836 Wing, A. A., Emanuel, K., Holloway, C. E., & Muller, C. (2017). Convective self-
837 aggregation in numerical simulations: a review. In *Shallow Clouds, Water Vapor,*
838 *Circulation, and Climate Sensitivity* (pp. 1-25). Springer, Cham.

839 Worden, J., and Coauthors. 2006. Tropospheric Emission Spectrometer observations of the
840 tropospheric HDO/H2O ratio: Estimation approach and characterization. *J. Geophys. Res*.,
841 111, D16309,

842 Worden, J, D. Noone, K. Bowman, and the Tropospheric Emission Spectrometer science team
843 & data contributors. 2007. Importance of rain evaporation and continental convection in
844 the tropical water cycle, *Natur*e, 445, doi:10.1038.

845 Worden, J., Kulawik, S., Frankenberg, C., Payne, V., Bowman, K., Cady-Pereira, K., Wecht,
846 K., Lee, J.-E., Noone, D., 2012. Profiles of CH4, HDO, H2O, and N2O with improved
847 lower tropospheric vertical resolution from aura TES radiances. *Atmos.Meas. Tech*. 5,
848 397–411. https://doi.org/10.5194/amt-5-397-2012.

849 Xu, W. and Zipser, E.J., 2012. Properties of deep convection in tropical continental, monsoon,
850 and oceanic rainfall regimes. *Geophysical Research Letters*, VOL. 39, L07802,
851 doi:10.1029/2012GL051242

852 Yoshimura, K., M. Kanamitsu, M. Dettinger., 2010. Regional downscaling for stable water
853 isotopes: A case study of an atmospheric river event, *J. Geophys. Res*., 115, D18114

854 Yu, W., Wei, F., Ma, Y., Liu, W., Zhang, Y., Luo, L., ... & Qu, D., 2016. Stable isotope
855 variations in precipitation over Deqin on the southeastern margin of the Tibetan Plateau
856 during different seasons related to various meteorological factors and moisture sources.
857 *Atmospheric Research*, *170*, 123-130.

858 Zongxing, L., Qi, F., Song, Y., Wang, Q. J., Yang, J., Yongge, L., ... & Xiaoyan, G., 2016).
859 Stable isotope composition of precipitation in the south and north slopes of Wushaoling
860 Mountain, northwestern China. *Atmospheric Research*, *182*, 87-101.

861

862 **Web references**

https://www.esrl.noaa.gov/psd/cgi-bin/data/composites/printpage.pl. Accessed on February 2018.

http://www.nwcsaf.org/web/guest/scientific-documentation. Accessed on November 2018

882 **List of Figures**

883 Figure 1. Map of the study area (Western Central Africa) with the location of GNIP stations
884 of Cotonou, Bangui, Douala and Sao-Tome.

885 Figure 2. Annual cycles of δ18O from 2006 to 2016. The blue line represents the mean
886 seasonal cycle while the red line corresponds to a given year

887 Figure 3. Monthly mean for δ18O (black line) and precipitation amounts (bars) at the GNIP
888 stations of Cotonou (2005-2012), Bangui (2009-2015), Douala (2006-2016) and Sao-Tome
889 (1962-1976). Summer enrichment phases are highlighted in pink and depletion phases in
890 spring and autumn are underlined in blue.

891 Figure 4. GPCP monthly mean precipitations (mm/day) distributions (colors) and back-
892 trajectories (dotted curves) during the period of 2006 to 2016. White color characterizes an
893 absence of precipitation. Monthly trajectories were calculated using monthly average mean
894 ERA-Interim reanalysis

895 Figure 5. Evolution of monthly mean GPCP precipitations (mm/day) along the back
896 trajectories over time (in hours) towards the Douala GNIP station in May, August, October
897 and January for the 2006-2016 period.

898 Figure 6. Monthly mean variations of δ18O (grey line) and average GPCP precipitations
899 (bars) recorded over the past 72h along the back trajectories for the 2006-2016 period.

900 Figure 7. Mean seasonal variations of (A) δD in precipitation (in grey) and in water vapor (in
901 black) at 900 hPa at Douala region as observed at the GNIP station (2006 to 2016) and by the
902 TES instrument (2004 to 2008) respectively; (B) δDP – δDv at Douala region

903 Figure 8. $\delta^{18}O$ in daily rainfall at Douala from March 2017 to August 2017.

Figure 9. Example of meteorological situations in the study region in 2017 (based on the SAFNWC cloud classification) during (A) spring and (B) summer periods. The backward trajectories (grey line) are plotted for each event.

Figure 10. Statistical distribution of daily rainfall duration at Douala as shown by box-and-whisker representation. The boxes have lines at the lower, median and upper quartile values. The whiskers are lines extending from each end of the box to 1.5 interquartile range. Red cross represents the mean and outliers are represented by black points above the maximum

924 **List of Tables**

925 Table 1. Characteristics of GNIP sampling sites in GOG and Central African regions. Data
926 from Cotonou, Bangui and Sao-Tome have been obtained online from the GNIP database
927 (AIEA/OMM 2018).

928 Table 2. Coefficient of determination (r^2) between $\delta^{18}O$ and local meteorological settings
929 (precipitation (P) and temperature (T)) for monthly GNIP stations of Cotonou, Bangui,
930 Douala and Sao-Tome, at different sampling periods.

931 Table3. Coefficient of determination (r^2) between δ18O and average GPCP precipitation in
932 average over the first day, two first days and three first days along the air parcel trajectory
933 before rainfall in Douala. Correlation coefficients ≥ 95% are highlighted in bold and
934 underlined.

935 Table 4. Information about Fland during the last 3 days along the air parcels trajectories for
936 the months of March, April and May; and its relationship (r^2) with δ18O, and upstream GPCP
937 precipitation. For the summer period, Fland corresponds to 0% for almost all the rainy days.
938 Correlation coefficients ≥ 95% are highlighted in bold and underlined.

939 Table 5. Information on the organization of convection (cloud types, cloud area and
940 local/upstream) and its influence on the isotopic composition of daily rainfall over the period
941 from March 2017 to August 2017. Cloud areas were only calculated for very high classes.
942 Correlation coefficients significant ≥ 95% are in bold and underlined.

943

944

945

Figures and captions.

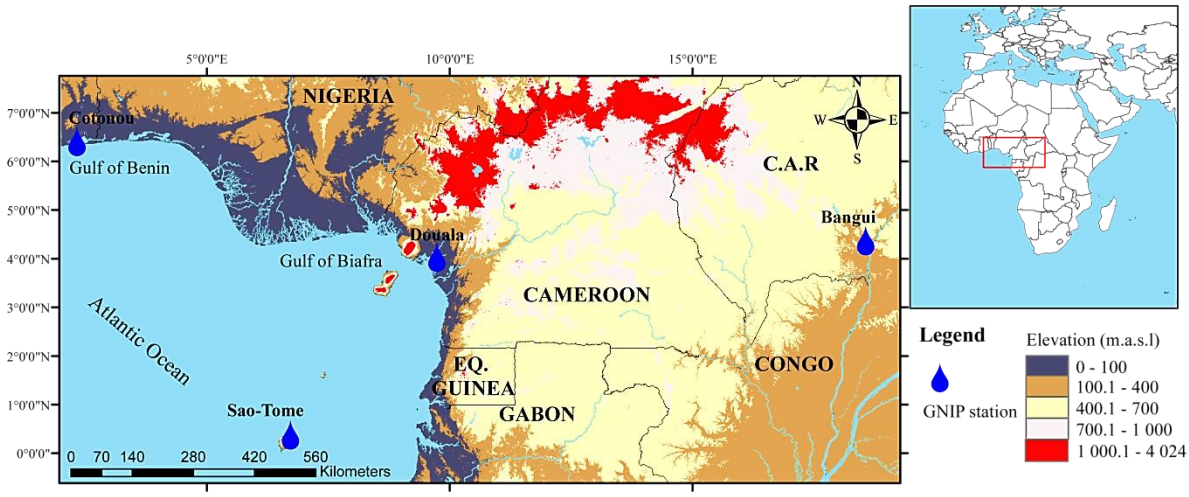

Figure 1. Map of the study area (Western Central Africa) with the location of GNIP stations of Cotonou, Bangui, Douala and Sao-Tome.

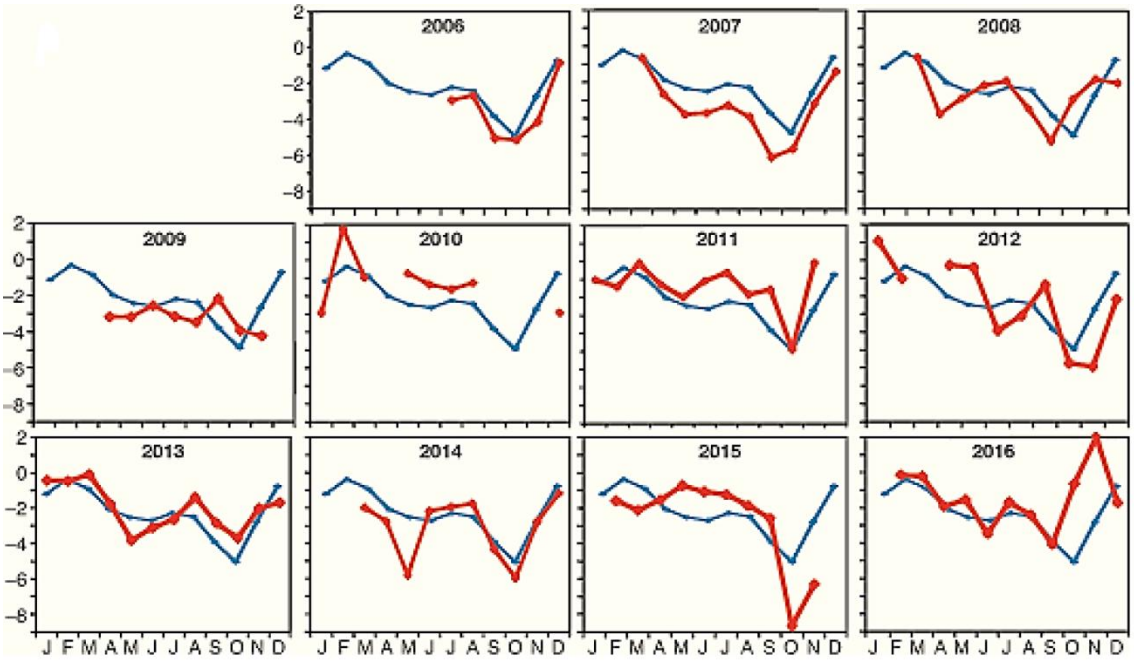

Figure 2. Annual cycles of $\delta^{18}O$ from 2006 to 2016. The blue line represents the mean seasonal cycle while the red line corresponds to a given year

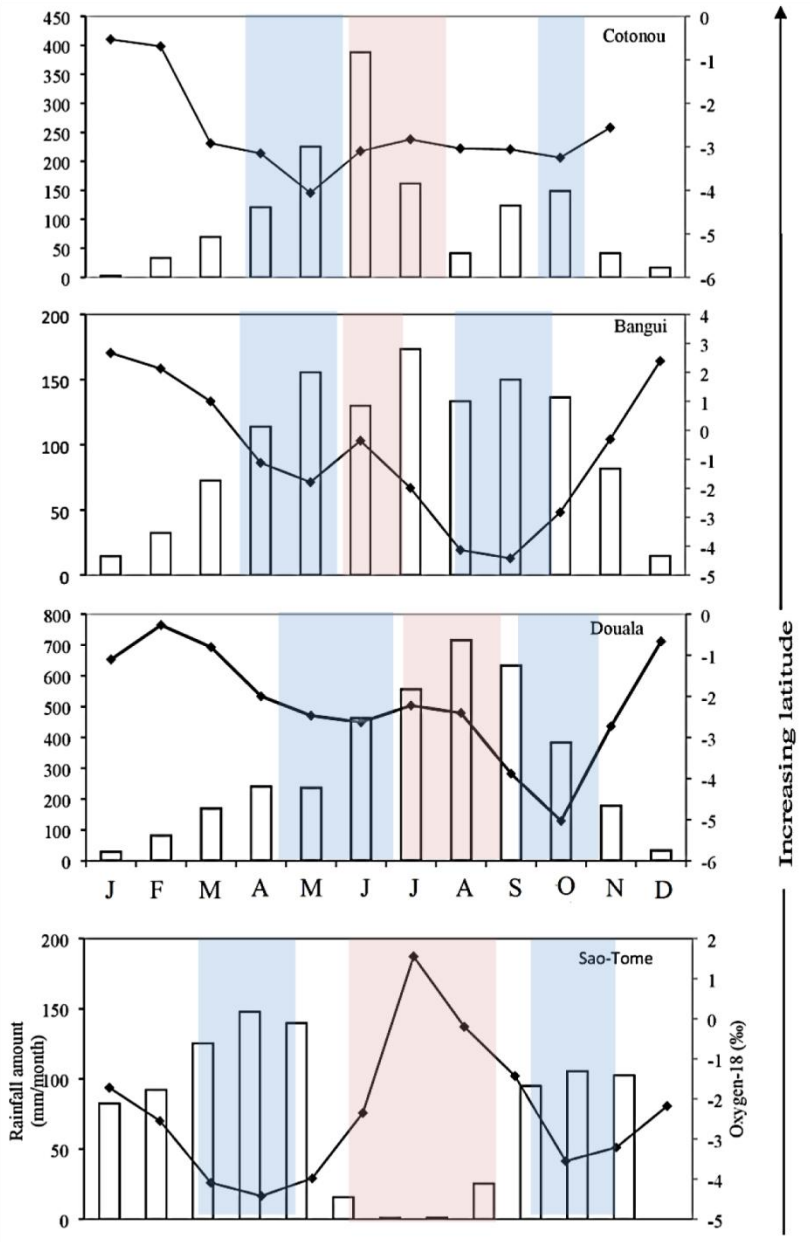

Figure 3. Monthly mean for $\delta^{18}O$ (black line) and precipitation amounts (bars) at the GNIP stations of Cotonou (2005-2012), Bangui (2009-2015), Douala (2006-2016) and Sao-Tome (1962-1976). Summer enrichment phase are highlighted in pink and depletion phases in spring and autumn are underlined in blue.

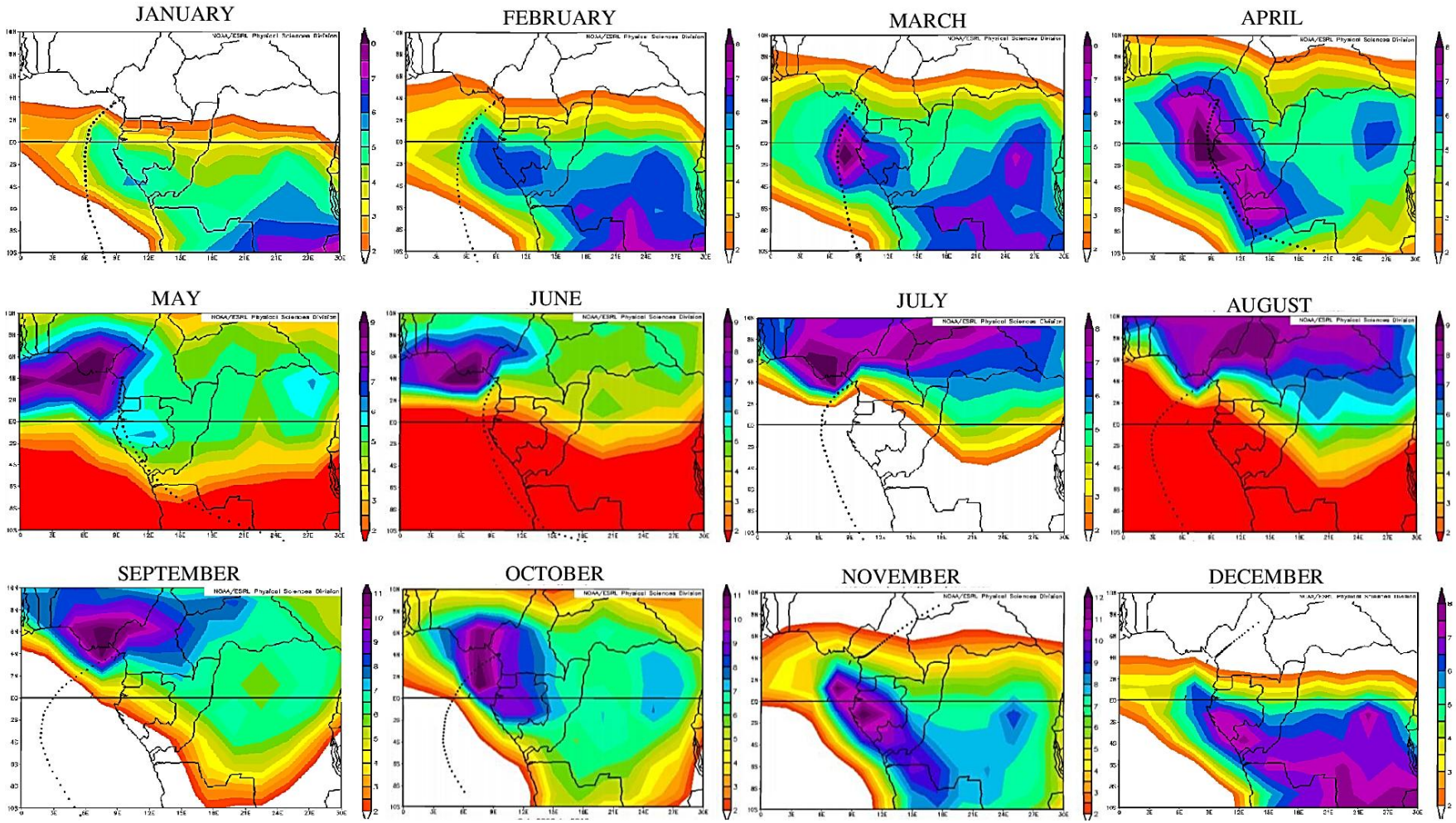

Figure 4. GPCP monthly mean precipitations (mm/day) distributions (colors) and back-trajectories (dotted curves) during the period of 2006 to 2016. White color characterizes an absence of precipitation. Monthly trajectories were calculated using monthly average mean ERA-Interim reanalysis

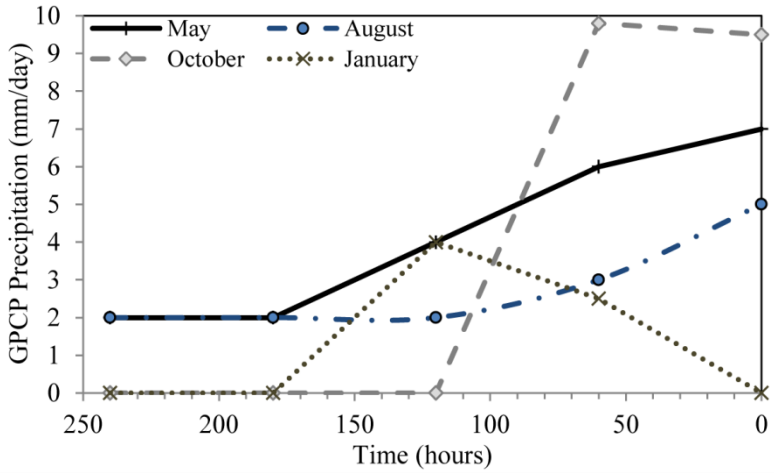

Figure 5. Evolution of monthly mean GPCP precipitations (mm/day) along the back trajectories over time (in hours) towards the Douala GNIP station in May, August, October and January for the 2006-2016 period.

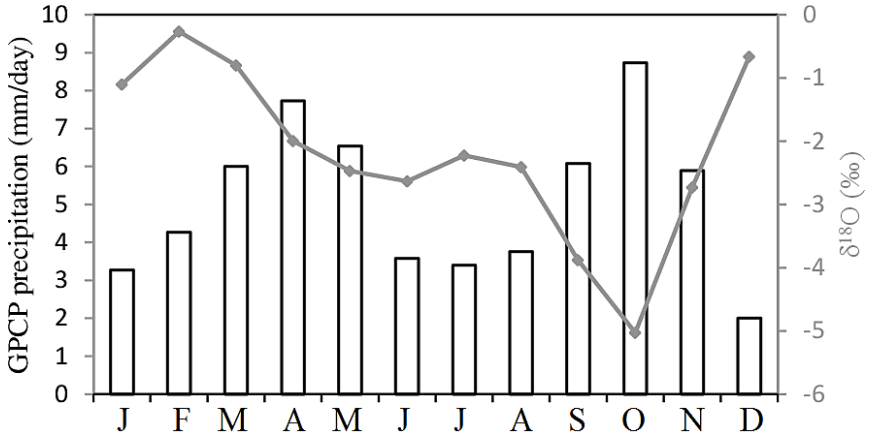

Figure 6. Monthly mean variations of $\delta^{18}O$ (grey line) and average GPCP precipitations (bars) recorded over the past 72h along the back trajectories for the 2006-2016 period.

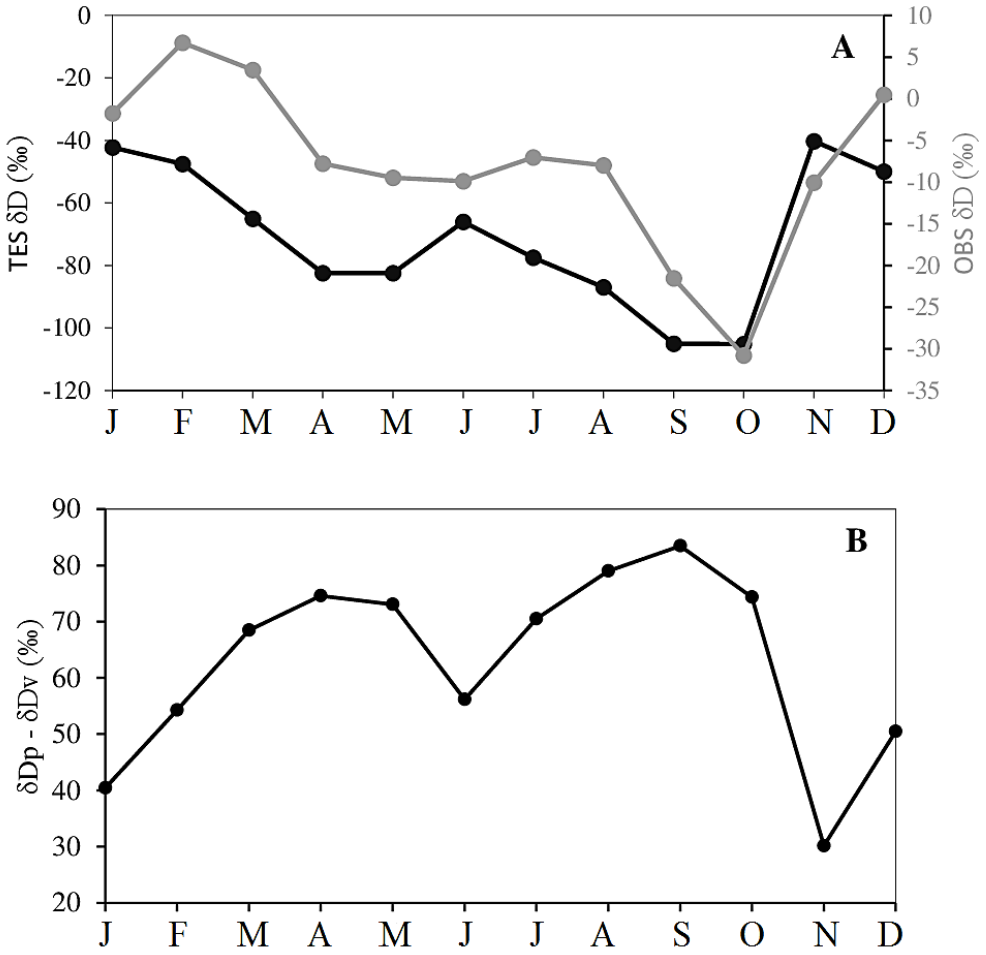

Figure 7. Mean seasonal variations of (A) δD in precipitation (in grey, Y-axis on the right) and in water vapor (in black, Y-axis on the left) at 900 hPa over Douala as observed at the GNIP station (2006 to 2016) and by the TES instrument (2004 to 2008) respectively; (B) δD_P – δD_v over Douala

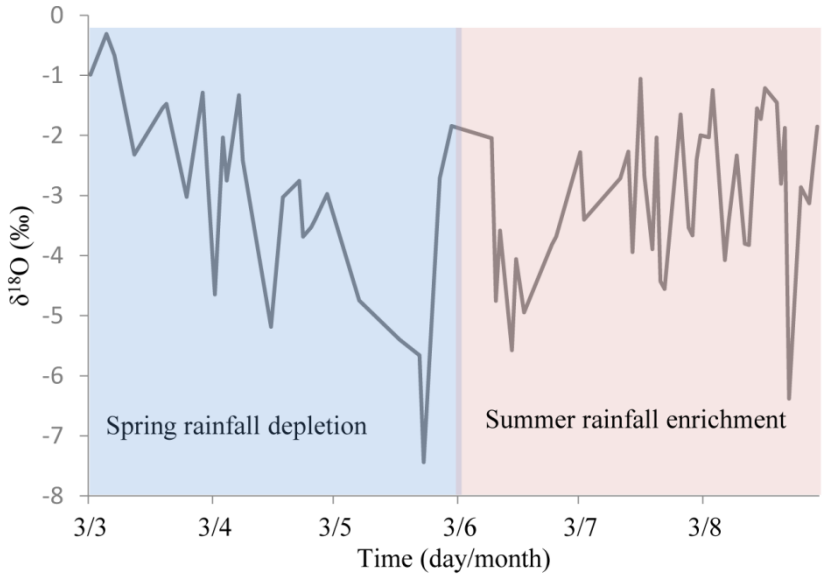

Figure 8. $\delta^{18}O$ in daily rainfall at Douala from March 2017 to August 2017.

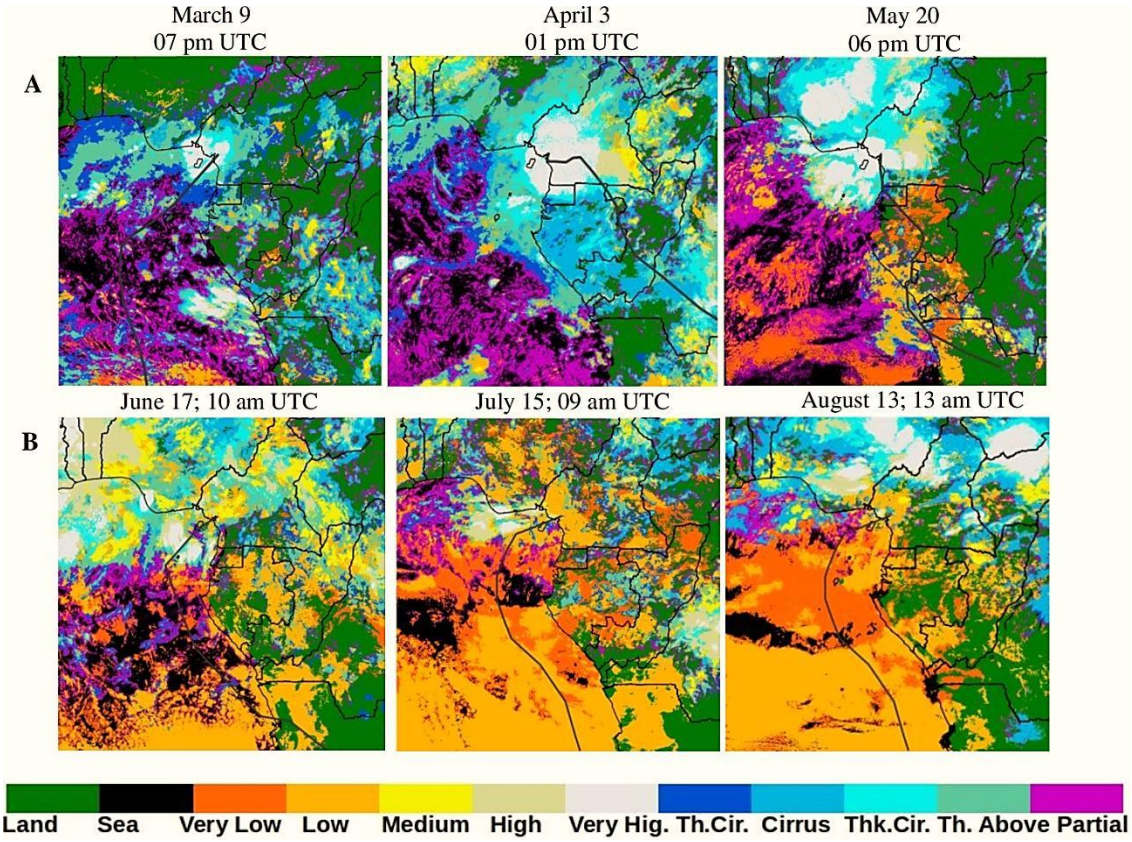

Figure 9. Example of meteorological situations in the study region in 2017 (based on the SAFNWC cloud classification) during (A) spring and (B) summer periods. The backward trajectories (grey line) are plotted for each event.

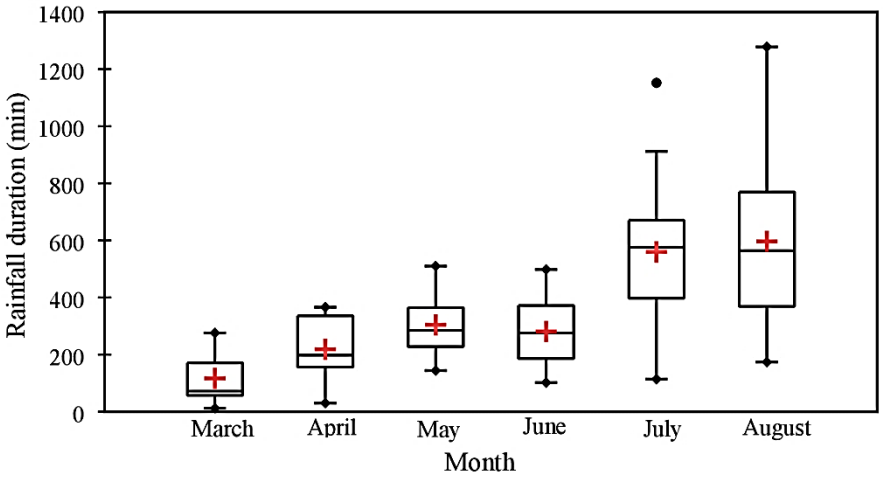

Figure 10. Statistical distribution of daily rainfall duration at Douala as shown by box-and-whisker representation. The boxes have lines at the lower, median and upper quartile values. The whiskers are lines extending from each end of the box to 1.5 interquartile range. Red cross represents the mean and outliers are represented by black points above the maximum

Tables

Table 1. Characteristics of GNIP sampling sites in GOG and Central African regions. Data from Cotonou, Bangui and Sao-Tome have been obtained online from the GNIP database (AIEA/OMM 2018).

Site	Country	Sampling period	Elevation (m.a.s.l)	Mean annual precip*(mm)	Vapor Pressure (hPa)	Mean annual T* (°C)
Cotonou	Benin	2005 - 2012	14	1395	28.3	27.1
Bangui	CAR*	2009 - 2015	363	1208	25.7	26.3
Douala	Cameroon	2006 - 2016	18	3720	30.5	27
Sao-Tome	Sao-Tome and Principe	1962-1976	8	933.7	26.2	25.2

* Precip. = Precipitation, T = temperatures; CAR= Central African Republic; dec. deg = decimal degrees

Table 2. Coefficient of determination (r^2) between $\delta^{18}O$ and local meteorological settings (precipitation (P) and temperature (T)) for monthly GNIP stations of Cotonou, Bangui, Douala and Sao-Tome, at different sampling periods.

Stations	Sampling period	r^2 $\delta^{18}O/P$	r^2 $\delta^{18}O/T$
Cotonou (n=95)	2005 - 2012	0.05	0.13
Bangui (n=81)	2009 - 2016	0.24	0.04
Douala (n=106)	2006 - 2016	0.12	0.09
Sao-Tome (n=123)	1962 - 1976	0.19	0.20

Table3. Coefficient of determination (r^2) between $\delta^{18}O$ and average GPCP precipitation in average over the first day, two first days and three first days along the air parcel trajectory before rainfall in Douala. Correlation coefficients ≥ 95% are highlighted in bold and underlined.

		March (n=08)	**April (n=12)**	**May (n=07)**	**June (n=09)**	**July (n=14)**	**August (n=20)**
$\delta^{18}O$ Vs GPCP Precipitation	One day before	**0.53**	**0.43**	0.40	0.03	0.14	0.15
	Two days before	**0.55**	0.23	0.28	0.14	0.03	**0.23**
	Three days before	**0.64**	0.16	0.44	0.00	0.11	**0.23**

Table 4. F_{land} statistics during the last 3 days along the air parcels trajectories for the months of March, April and May. Relationship (r^2) between F_{land}, $\delta^{18}O$, and upstream GPCP precipitation. For the summer period, F_{land} corresponds to 0% for almost all rainy days. Correlation coefficients ≥ 95% are in bold and underlined.

	March	**April**	**May**
F_{land} (%) *Minimum*	0	0	25
F_{land} (%) *Maximum*	100	100	100
F_{land} (%) *Mean*	25	69.45	70.83
F_{land} (%) *Median*	0	83.34	79.17
***r^2* (F_{land} *vs* $\delta^{18}O$)**	0.23	**0.33**	0.28
***r^2* (F_{land} *vs* GPCP precip.)**	0.51	0.42	0.85

Table 5. Information on the organization of convection (cloud types, cloud area and local/upstream) and its influence on the isotopic composition of daily rainfall over the period from March 2017 to August 2017. Cloud areas were only calculated for very high classes. Correlation coefficients significant ≥ 95% are in bold and underlined.

	March	**April**	**May**	**June**	**July**	**August**
Very low to low clouds (%)	0	0	0	0	71.43	54
Medium to high clouds (%)	0	0	18.18	72.73	21.43	40.5
Very high clouds (%)	100	100	81.82	27.27	7.14	5.5
Local without upstream convection (%)	75	27.27	0	22.29	7.14	0
Upstream and local convection (%)	25	72.73	100	77.71	92.86	100
Minimum cloud area (km^2)	5300 ± 100	4500 ± 100	63400 ± 100	2400 ± 100		-
Maximum cloud area (km^2)	35300 ±100	158100 ± 100	285600 ± 100	280000 ± 100	3077±100	615±100
Mean cloud area (km^2)	17800 ± 100	73700 ± 100	225100 ± 100	138500 ± 100	-	-
r^2 Clouds area *Vs* rainfall duration	**0.54**	**0.63**	**0.51**	0.34	-	-
r^2 Clouds area *Vs* $\delta^{18}O$	**0.44**	**0.55**	**0.97**	**0.90**	-	-
r^2 Clouds area *Vs* GPCP precipitation	0.30**	0.10**	0.01**	0.46**		
r^2 Rainfall duration *Vs* $\delta^{18}O$	**0.44**	**0.54**	**0.64**	0.24	0.00	0.07

***Anti-correlation*

Cover letter to Editor for revised manuscript

Ref: HYDROL31370

Bertil NLEND

Université de Bourgogne Franche-Comté
UMR 6249 Laboratoire Chrono-Environnement
16 route de Gray, Besançon Cedex
bertil.nlend@univ-fcomte.fr

December 09, 2019

Dear Editor,

Thank you for the opportunity to revise our manuscript entitled *Identification of processes that control the stable isotope composition of rainwater in the humid tropical West-Central Africa.* We appreciate your interest, the careful review and constructive suggestions made by reviewers. It is our belief that the manuscript is substantially improved after making the suggested edits.

Following this letter, are the reviewers comments with our responses in blue colour, including how and where the text was modified. The revision has been developed in consultation with all co-authors, and each author has given approval to the final form of this revision. The changes or/and added text are marked in the text by a yellow highlight.

We very much hope that the revised manuscript will be accepted for publication in Journal of Hydrology.

Thank you for your consideration.

Sincerely yours,

Bertil NLEND

on behalf of the authors

Response to Revision Request

The authors would like to thanks all the reviewers for their comments and suggestions for improvements which helped us to propose a new corrected version of the manuscript.

Here below is a point to point answer to comments.

Reviewer #2

1- I have some reservation about the explanation on the intra-seasonal time scale. For example, the authors have used the TES derived hydrogen vapor isotope data and compared their result of precipitation δ^2H variability. Though the absolute values of these two different datasets are not comparable as correctly mentioned by the authors, however a qualitative match is expected. According to Fig. 7 the seasonal characters are similar, but a considerable mismatch is observed during the later period of the year. For example, from Jan to Sep the precipitation isotope maintains a more or less constant positive offset relative to the vapor isotopic record, which is expected. But in the month of Oct the offset nearly vanishes and surprisingly in the month of Nov the offset value turns negative! This behavior defies the principle of isotopic fractionation. It may so happen that within the limits of analytical uncertainties, this negative offset is not significantly different from zero. But this aspect needs to be discussed in detail, especially why the offset values differ consistently in the months of Oct and Nov. Which atmospheric processes drive such kind of anomalous behavior?

In Figure 7, δD_V and δD_P do not have the same y-axis. For instance, in October (November) δD_V is approximately equal to -100‰ (-45‰) while δD_P equal to -30‰ (-10‰). So, there is always a positive offset between the isotopic composition of water vapor and precipitation despite the fact that we observe on Figure 7 that the two curves are bringing together. Moreover, once again, it is clearly mentioned in the text that we can't compare absolute values obtained from TES with observed precipitation isotopes. Concerning the processes involved in the variability of δD_V and δD_P, on Figure 7, the seasonal variability of δD_P - δD_V provides information on rainwater – water vapor interactions and it is demonstrated that post-condensational effects are negligible.

However, regarding this comment from the reviewer, to avoid misunderstanding, **we added in the title of Figure 7 a precision concerning the y-axis and precision in the text (lines 364-365) about the positive offset between δD_V and δD_P.**

Other issues

2- Line: 372: It is known that the process of condensation is an equilibrium process; if so, then why 'there is no reason for the precipitation to be in equilibrium with the vapor'?

We removed this sentence to avoid misunderstanding and confusion.

3- Line 376: Pls provide a complete description of the relationship between dDp and dDv. It has been reported that the slope for this kind of relation is closer to 1 (Conroy et al. 2016). But, the authors get a very high value of slope, 1.68. The reason for such a large deviation should be explained. In this context, it is also suggested to use the q-dD diagram (Conroy et al. 2016) in order to characterize the moisture sources.

Many thanks for bringing this to our attention and for the reference which has been taken in account (see lines 378 – 379). **We corrected it** and putted now the right value of the slope (see line 375).

4- In order to study the effect of continental recycling, the authors have calculated "the percentage of time of the air parcel over the continent during the last 3 days along the trajectory" (Line 404-405), termed as Fland. Two issues are important in this context. Firstly, the method of calculation of Fland is not provided. Secondly, and more importantly, at what height the trajectories have been calculated? If the trajectories have been calculated for a single height, then they do not necessarily represent a major amount of moisture transport to the sampling site, since moisture is typically transported at a spectrum of heights. A detailed quantitative calculation of moisture transport for different heights is expected to be presented here. Without this exercise the conclusion of 'poor continental recycling' could be misleading.

The method of calculation of F_{land} was added in the text; see lines 405-408. About the second issue, we thank the reviewer for his comment which helped us to improve this section of the manuscript. Indeed, **we calculated air back trajectories at different heights: 800, 850, 900, 950 and 980 hPa.** We have not performed investigation at more than 800 hPa because it is the boundary layer that feeds the convection and it is with the water vapor from the low layers that the rain is re-evaporated. By calculating trajectories at these different heights, we observed that there is no difference between them, especially since we focus only on air back trajectory at 3 days before Douala. Therefore, our conclusion of "poor continental recycling" in the study region can be considered as correct. **Detailed precision on this issue were added in section 4.3.2 (see lines 408 to 414).**

5- Line 457: how do you define the parameter "cloud surface"? How it is measured? How do you take care of the uncertainties in measurement?

Information concerning this is well detailed in section 3.3, line 238 and lines 240-241. Nevertheless thanks to this comment, to ensure the methodology described in the text is more understandable and robust, **we added more precision in lines 238, 240-241.**

6- One of the highlights "Local site precipitation <delta>18O of Douala was found to represent large-scale meteorology" may be confusing. I suggest rewording as 'Local site precipitation <delta>18O of Douala appears to respond to large-scale metrology".

Done.

7- The title of the MS is slightly misleading. Use of the word "and" in 'Western and Central Africa' may mean that the study sites are situated at both the western and central Africa. It

may be slightly modified as "Identification of processes that control the stable isotope composition of rainwater in the humid tropical West-Central Africa".

Done. Thank you for this suggestion.

Minor issues

8- Line 179: Ratios of d18O/d16O or d2D/D1H is not technically correct. Better use "ratios of 18O/16O or 2H/1H".

Done.

9- Line 212: Lekshmy et al. 2014 used TRMM derived rainfall data, not the GPCP products.

Corrected as suggested.

10- Line 270: Pls replace 'delta' by 'precipitation isotopes'.

Done. It is now line 269.

11- The MS is full of grammatical mistakes; use of the article is poorly done. I have mentioned some of them, but this is only an indicative list. It is suggested to get the MS examined by a native English speaker, or take the help of a professional service provider on the English language.

Done. Syntax errors have been corrected. In general, the English of the document has been improved and we thank the reviewer who encouraged us.

12- Line 282: 'regional scale' should be followed by "on a".

Done. It is now line 281

13- Line 296-97: please check for typos in the citations.

Done.

14- Line 311: English problem: "trajectories come…" is awkward. Trajectories are not object, but some kind of attribute. In this context, it may be replaced by moisture. Similar kind of errors is there in Line 313, 316, 318.

Corrected.

15- Line: 318: typo

Corrected.

16 - Line 321: "monsoon winds become less influent.." is not a good English. May be written as "strength of monsoon winds weaken.

Done.

17 - Line 327: The wording like "GPCP precipitation increases" may be replaced by 'the GPCP precipitation data show an increasing trend…'.

Done.

18 - Line 333: 'rainfall is most depleted' may mean that rainfall intensity is less. Better write "isotopic value of rainfall is depleted in spring….'.

Corrected as suggested. It is now line 332.

19 - Line 358: 'given' should be replaced by "provided".

Done. It is now line 357.

20 - Line 360: trajectories should be followed by 'the'.

Done. It is now line 359

Reviewer #3

1- Please avoid lumped references. Please talk about the specific points of each reference.

This remark has been considered and we would like to reassure the editors and the reviewers that each reference in the manuscript concerns a specific point or aspect.

2- How is the reproducibility of <delta>18O seasonal cycle from year to year?

This fact is clearly detailed and explained in section 4.1. The Figure 2 also discuss about it.

3- what is the correlation between monsoon and the transition to the dry season?

General comments on climate dynamic in the study area are given in section 2. There is no correlation between monsoon and the transition toward the dry season period, except that the second occurs when the first one ends. The monsoon is a SW wet wind which is most predominant at Douala from April to August. As the ITCZ begins its southward withdrawal in September until November the monsoon wind become less efficient, giving way to the Harmattan (NE dry wind) and the transition toward the dry period often correspond to the end of October – November. This is stated in section 2 and in section 4.2.2 by looking the pattern of air back trajectories.

Reviewer #4: Manuscript ID: HYDROL31370

Manuscript Title: Identification of processes that control the stable isotope composition of rainwater in the humid tropical Western and Central Africa

The paper is in order and can be recommended for publishing in present format.

Thank you very much for your positive comment.

List of Figures

Figure 1. Map of the study area (Western Central Africa) with the location of GNIP stations of Cotonou, Bangui, Douala and Sao-Tome.

Figure 2. Annual cycles of $\delta^{18}O$ from 2006 to 2016. The blue line represents the mean seasonal cycle while the red line corresponds to a given year

Figure 3. Monthly mean for $\delta^{18}O$ (black line) and precipitation amounts (bars) at the GNIP stations of Cotonou (2005-2012), Bangui (2009-2015), Douala (2006-2016) and Sao-Tome (1962-1976). Summer enrichment phases are highlighted in pink and depletion phases in spring and autumn are underlined in blue.

Figure 4. GPCP monthly mean precipitations (mm/day) distributions (colors) and back-trajectories (dotted curves) during the period of 2006 to 2016. White color characterizes an absence of precipitation. Monthly trajectories were calculated using monthly average mean ERA-Interim reanalysis

Figure 5. Evolution of monthly mean GPCP precipitations (mm/day) along the back trajectories over time (in hours) towards the Douala GNIP station in May, August, October and January for the 2006-2016 period.

Figure 6. Monthly mean variations of $\delta^{18}O$ (grey line) and average GPCP precipitations (bars) recorded over the past 72h along the back trajectories for the 2006-2016 period.

Figure 7. Mean seasonal variations of (A) δD in precipitation (in grey) and in water vapor (in black) at 900 hPa over Douala as observed at the GNIP station (2006 to 2016) and by the TES instrument (2004 to 2008) respectively; (B) $\delta D_P - \delta D_v$ over Douala

Figure 8. $\delta^{18}O$ in daily rainfall at Douala from March 2017 to August 2017.

Figure 9. Example of meteorological situations in the study region in 2017 (based on the SAFNWC cloud classification) during (A) spring and (B) summer periods. The backward trajectories (grey line) are plotted for each event.

Figure 10. Statistical distribution of daily rainfall duration at Douala as shown by box-and-whisker representation. The boxes have lines at the lower, median and upper quartile values. The whiskers are lines extending from each end of the box to 1.5 interquartile range. Red cross represents the mean and outliers are represented by black points above the maximum.

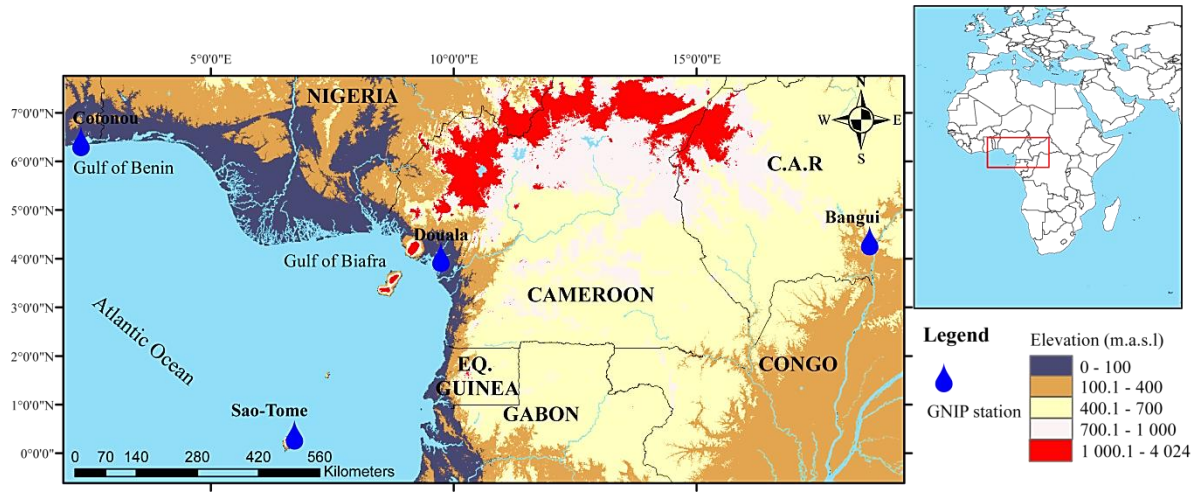

Figure 1. Map of the study area (Western Central Africa) with the location of GNIP stations of Cotonou, Bangui, Douala and Sao-Tome.

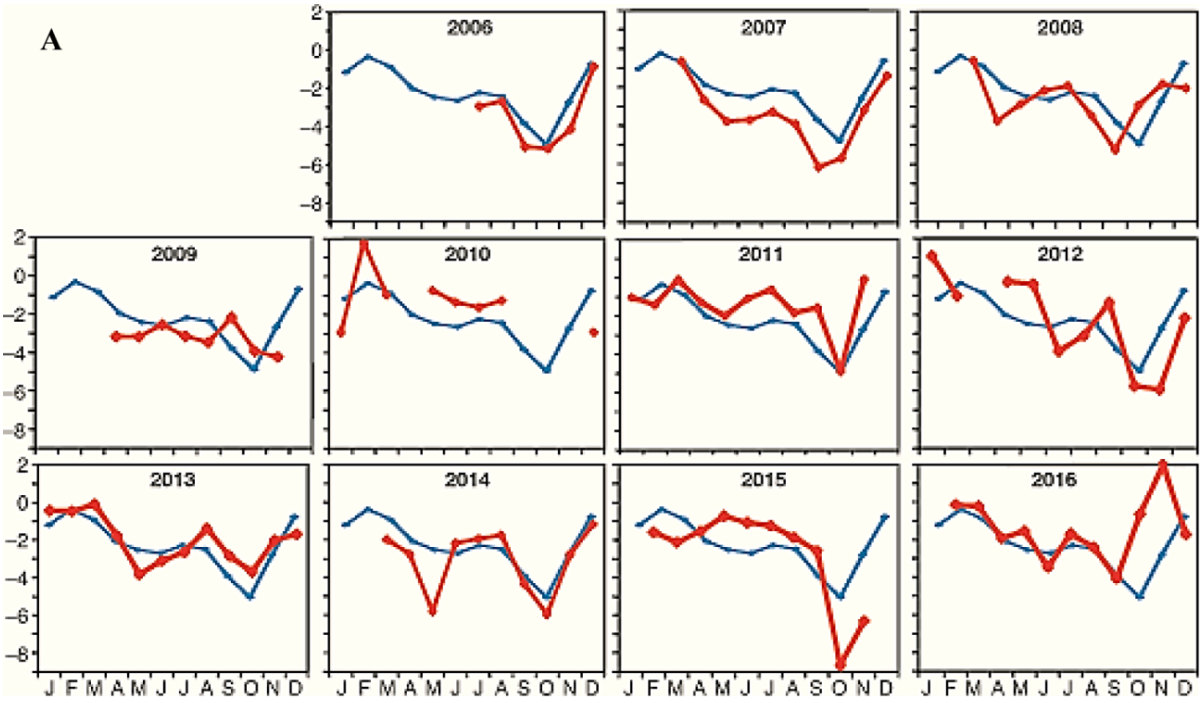

Figure 2. Annual cycles of $\delta^{18}O$ from 2006 to 2016. The blue line represents the mean seasonal cycle while the red line corresponds to a given year

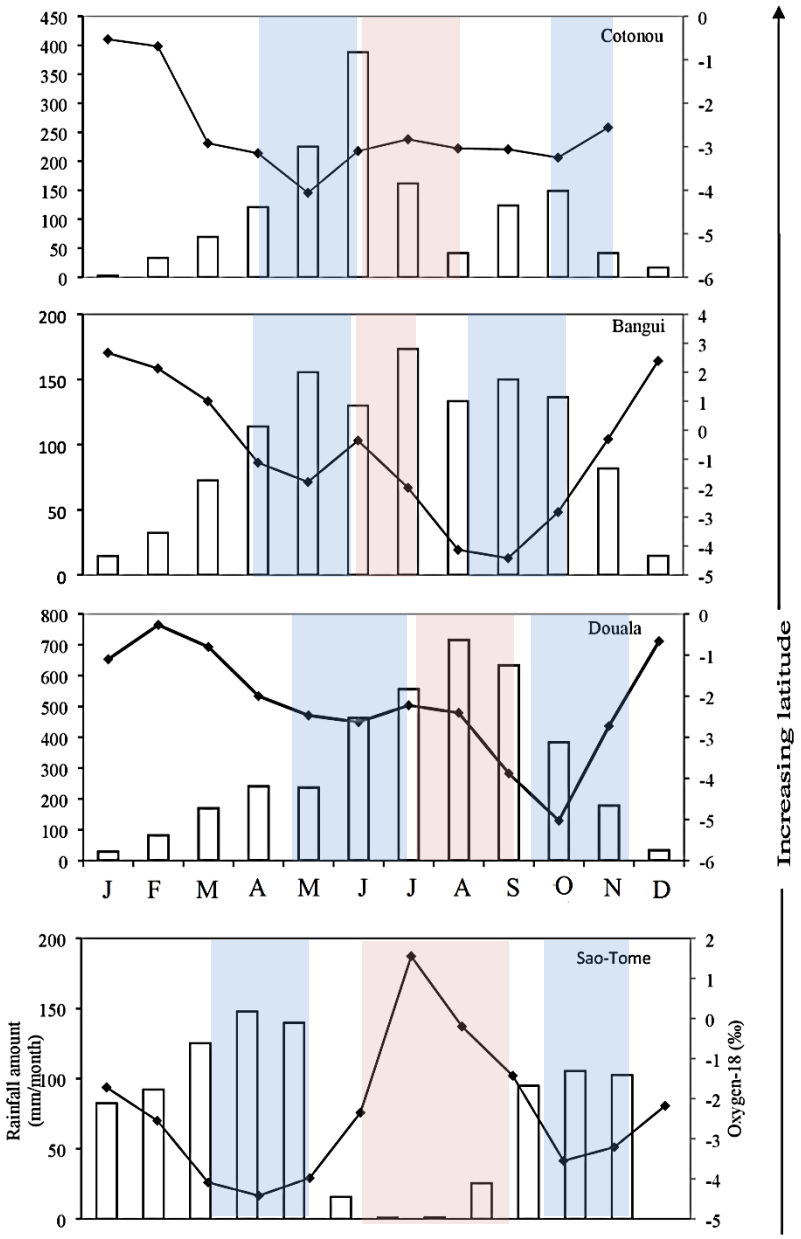

Figure 3. Monthly mean for $\delta^{18}O$ (black line) and precipitation amounts (bars) at the GNIP stations of Cotonou (2005-2012), Bangui (2009-2015), Douala (2006-2016) and Sao-Tome (1962-1976). Summer enrichment phases are highlighted in pink and depletion phases in spring and autumn are underlined in blue.

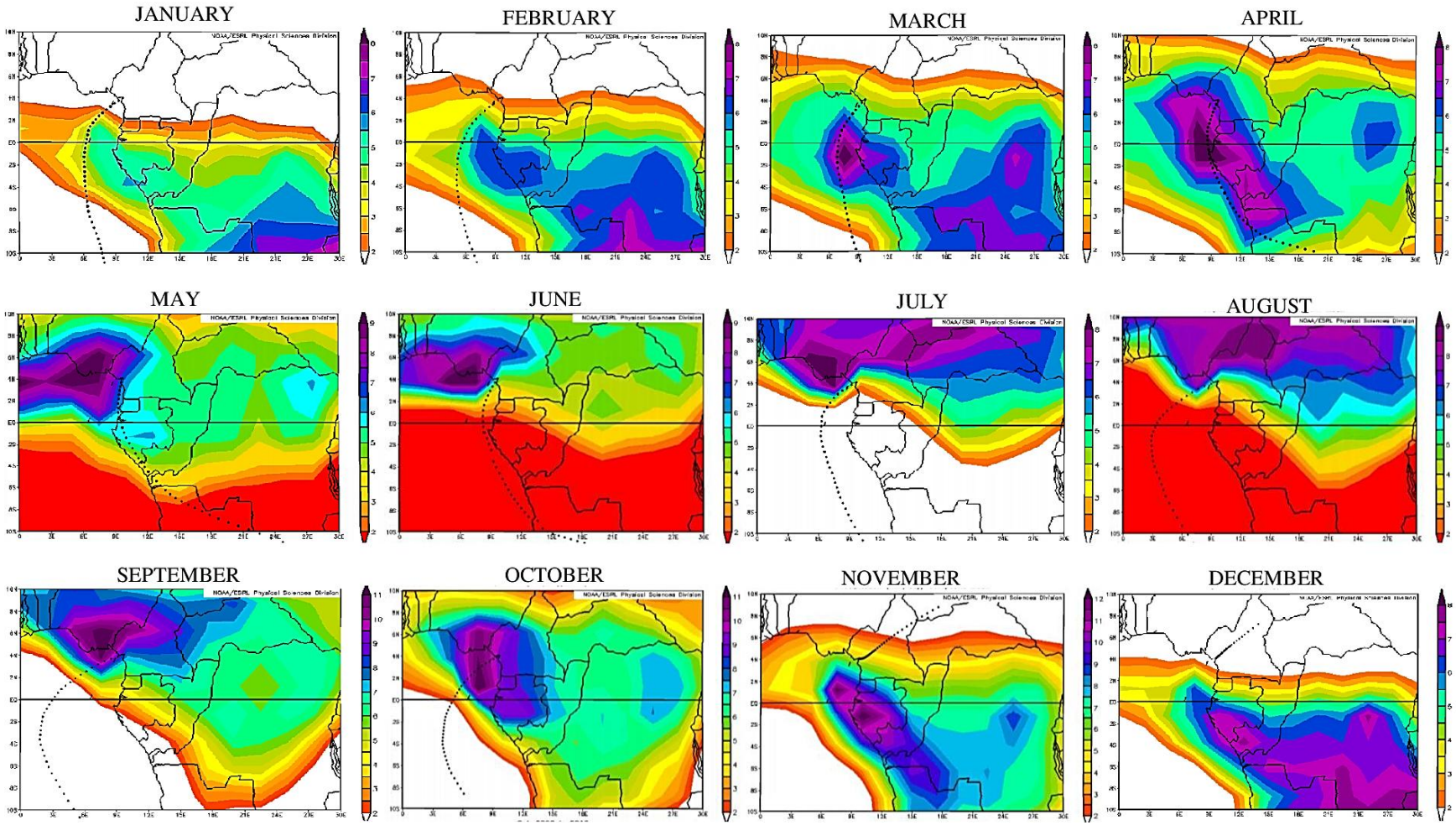

Figure 4. GPCP monthly mean precipitations (mm/day) distributions (colors) and back-trajectories (dotted curves) during the period of 2006 to 2016. White color characterizes an absence of precipitation. Monthly trajectories were calculated using monthly average mean ERA-Interim reanalysis

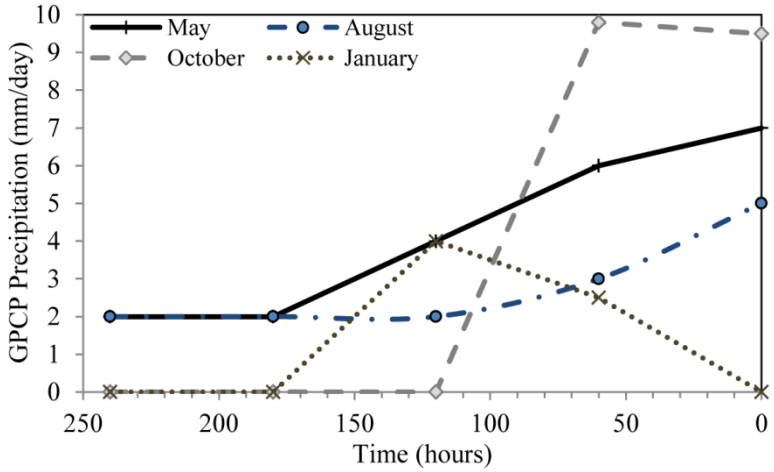

Figure 5. Evolution of monthly mean GPCP precipitations (mm/day) along the back trajectories over time (in hours) towards the Douala GNIP station in May, August, October and January for the 2006-2016 period.

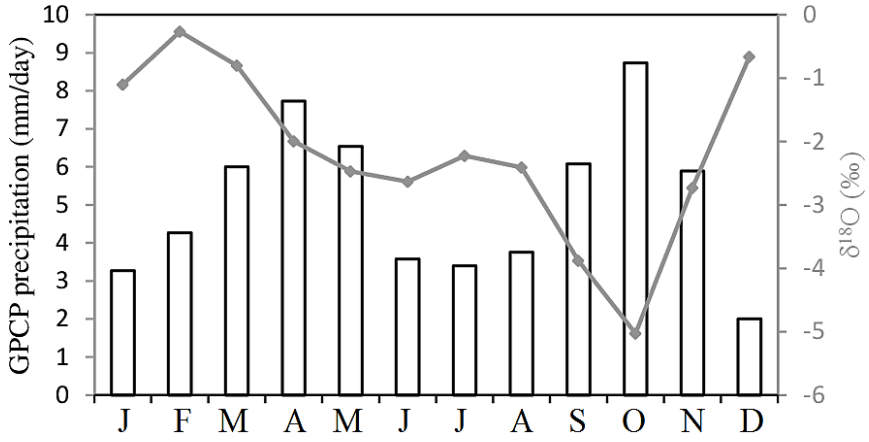

Figure 6. Monthly mean variations of $\delta^{18}O$ (grey line) and average GPCP precipitations (bars) recorded over the past 72h along the back trajectories for the 2006-2016 period.

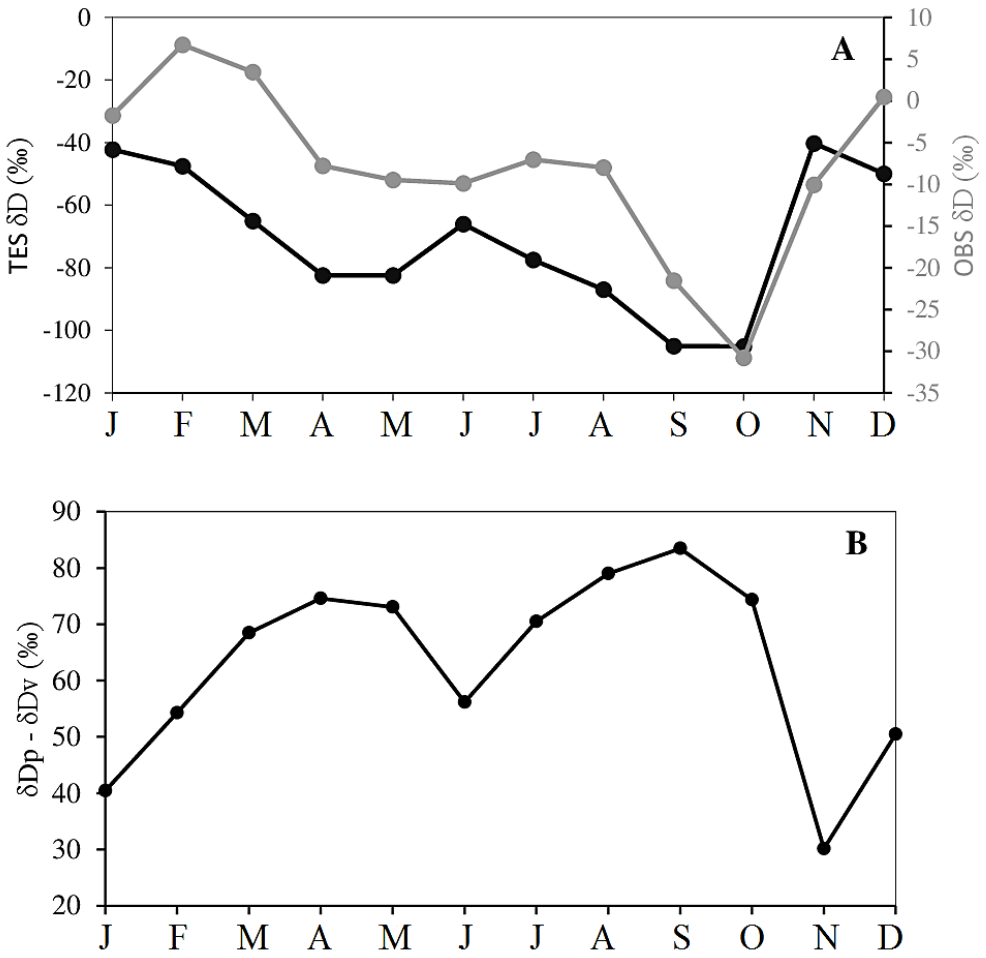

Figure 7. Mean seasonal variations of (A) δD in precipitation (in grey, Y-axis on the right) and in water vapor (in black, Y-axis on the left) at 900 hPa over Douala as observed at the GNIP station (2006 to 2016) and by the TES instrument (2004 to 2008) respectively; (B) δD_P – δD_v over Douala

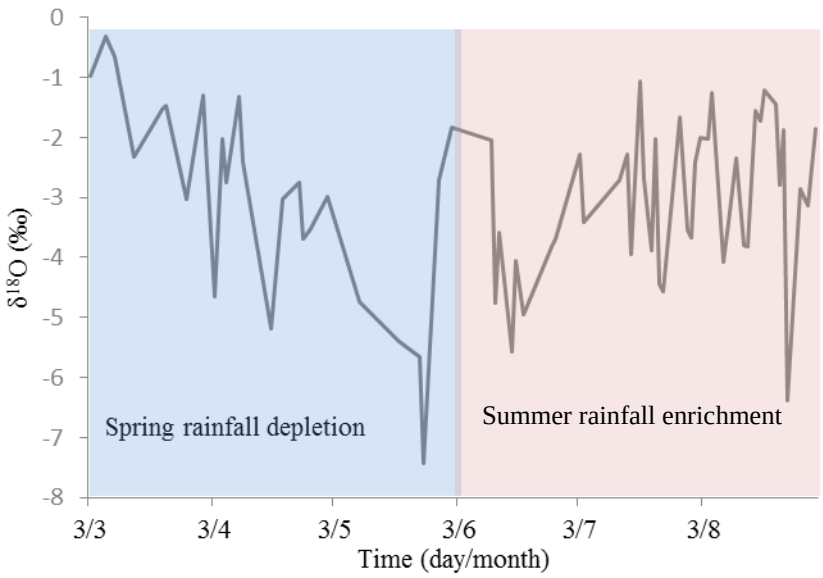

Figure 8. $\delta^{18}O$ in daily rainfall at Douala from March 2017 to August 2017.

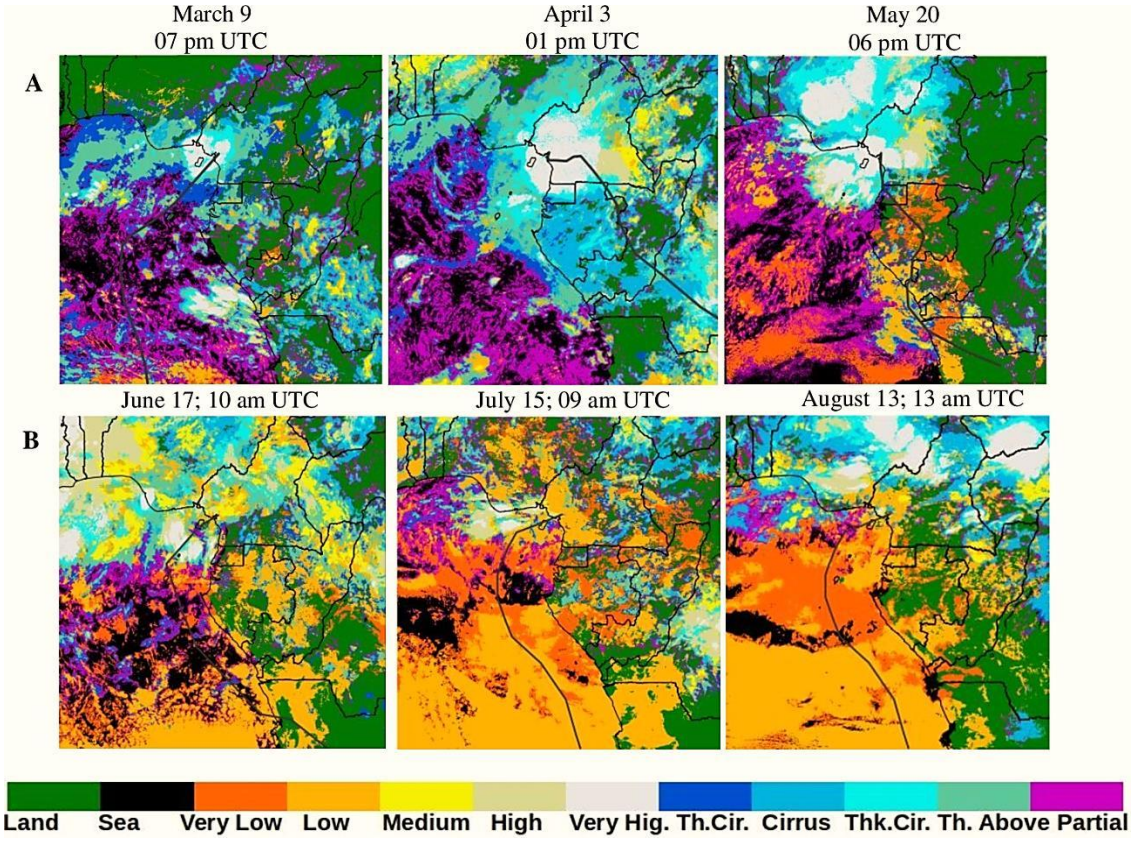

Figure 9. Example of meteorological situations in the study region in 2017 (based on the SAFNWC cloud classification) during (A) spring and (B) summer periods. The backward trajectories (grey line) are plotted for each event.

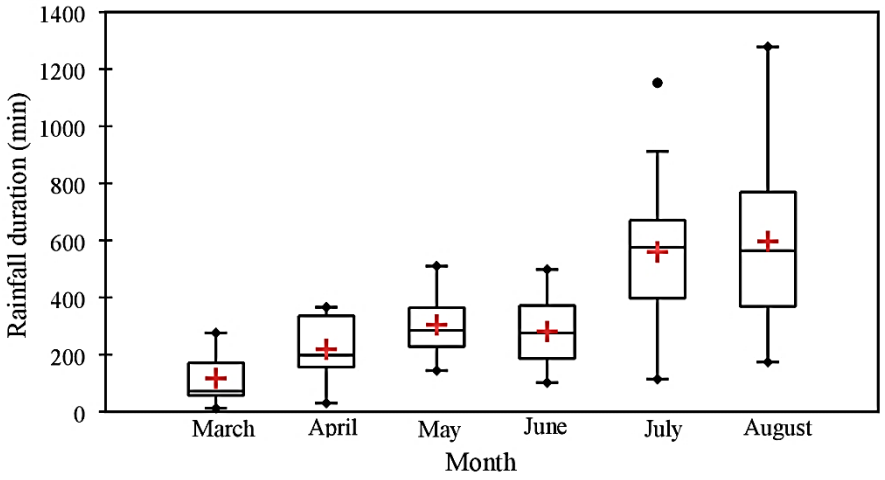

Figure 10. Statistical distribution of daily rainfall duration at Douala as shown by box-and-whisker representation. The boxes have lines at the lower, median and upper quartile values. The whiskers are lines extending from each end of the box to 1.5 interquartile range. Red cross represents the mean and outliers are represented by black points above the maximum

List of Tables

Table 1. Characteristics of GNIP sampling sites in GOG and Central African regions. Data from Cotonou, Bangui and Sao-Tome have been obtained online from the GNIP database (AIEA/OMM 2018).

Table 2. Coefficient of determination (r^2) between $\delta^{18}O$ and local meteorological settings (precipitation (P) and temperature (T)) for monthly GNIP stations of Cotonou, Bangui, Douala and Sao-Tome, at different sampling periods.

Table3. Coefficient of determination (r^2) between $\delta^{18}O$ and average GPCP precipitation in average over the first day, two first days and three first days along the air parcel trajectory before rainfall in Douala. Correlation coefficients ≥ 95% are highlighted in bold and underlined.

Table 4. F_{land} statistics during the last 3 days along the air parcels trajectories for the months of March, April and May. Relationship (r^2) between F_{land}, $\delta^{18}O$, and upstream GPCP precipitation. For the summer period, F_{land} corresponds to 0% for almost all rainy days. Correlation coefficients ≥ 95% are in bold and underlined.

Table 5. Information on the organization of convection (cloud types, cloud area and local/upstream) and its influence on the isotopic composition of daily rainfall over the period from March 2017 to August 2017. Cloud areas were only calculated for very high classes. Correlation coefficients significant ≥ 95% are in bold and underlined.

Table 1. Characteristics of GNIP sampling sites in GOG and Central African regions. Data from Cotonou, Bangui and Sao-Tome have been obtained online from the GNIP database (AIEA/OMM 2018).

Site	Country	Sampling period	Elevation (m.a.s.l)	Mean annual precip*(mm)	Vapor Pressure (hPa)	Mean annual T* (°C)
Cotonou	Benin	2005 - 2012	14	1395	28.3	27.1
Bangui	CAR*	2009 - 2015	363	1208	25.7	26.3
Douala	Cameroon	2006 - 2016	18	3720	30.5	27
Sao-Tome	Sao-Tome and Principe	1962-1976	8	933.7	26.2	25.2

* Precip. = Precipitation, T = temperatures; CAR= Central African Republic; dec. deg = decimal degrees

Table 2. Coefficient of determination (r^2) between $\delta^{18}O$ and local meteorological settings (precipitation (P) and temperature (T)) for monthly GNIP stations of Cotonou, Bangui, Douala and Sao-Tome, at different sampling periods.

Stations	Sampling period	r^2 $\delta^{18}O$/P	r^2 $\delta^{18}O$/T
Cotonou (n=95)	2005 - 2012	0.05	0.13
Bangui (n=81)	2009 - 2016	0.24	0.04
Douala (n=106)	2006 - 2016	0.12	0.09
Sao-Tome (n=123)	1962 - 1976	0.19	0.20

Table3. Coefficient of determination (r^2) between $\delta^{18}O$ and average GPCP precipitation in average over the first day, two first days and three first days along the air parcel trajectory before rainfall in Douala. Correlation coefficients ≥ 95% are highlighted in bold and underlined.

		March (n=08)	**April (n=12)**	**May (n=07)**	**June (n=09)**	**July (n=14)**	**August (n=20)**
$\delta^{18}O$ Vs GPCP Precipitation	**One day before**	**<u>0.53</u>**	**<u>0.43</u>**	0.40	0.03	0.14	0.15
	Two days before	**<u>0.55</u>**	0.23	0.28	0.14	0.03	**<u>0.23</u>**
	Three days before	**<u>0.64</u>**	0.16	0.44	0.00	0.11	**<u>0.23</u>**

Table 4. F_{land} statistics during the last 3 days along the air parcels trajectories for the months of March, April and May. Relationship (r^2) between F_{land}, $\delta^{18}O$, and upstream GPCP precipitation. For the summer period, F_{land} corresponds to 0% for almost all rainy days. Correlation coefficients ≥ 95% are in bold and underlined.

	March	**April**	**May**
F_{land} (%) *Minimum*	0	0	25
F_{land} (%) *Maximum*	100	100	100
F_{land} (%) *Mean*	25	69.45	70.83
F_{land} (%) *Median*	0	83.34	79.17
***r^2* (F_{land} *vs* $\delta^{18}O$)**	0.23	**<u>0.33</u>**	0.28
***r^2* (F_{land} *vs* GPCP precip.)**	0.51	0.42	0.85

Table 5. Information on the organization of convection (cloud types, cloud area and local/upstream) and its influence on the isotopic composition of daily rainfall over the period from March 2017 to August 2017. Cloud areas were only calculated for very high classes. Correlation coefficients significant ≥ 95% are in bold and underlined.

	March	**April**	**May**	**June**	**July**	**August**
Very low to low clouds (%)	0	0	0	0	71.43	54
Medium to high clouds (%)	0	0	18.18	72.73	21.43	40.5
Very high clouds (%)	100	100	81.82	27.27	7.14	5.5
Local without upstream convection (%)	75	27.27	0	22.29	7.14	0
Upstream and local convection (%)	25	72.73	100	77.71	92.86	100
Minimum cloud area (km^2)	5300 ± 100	4500 ± 100	63400 ± 100	2400 ± 100		-
Maximum cloud area (km^2)	35300 ±100	158100 ± 100	285600 ± 100	280000 ± 100	3077±100	615±100
Mean cloud area (km^2)	17800 ± 100	73700 ± 100	225100 ± 100	138500 ± 100	-	-
r^2 Clouds area *Vs* rainfall duration	**0.54**	**0.63**	**0.51**	0.34	-	-
r^2 Clouds area *Vs* $\delta^{18}O$	**0.44**	**0.55**	**0.97**	**0.90**	-	-
r^2 Clouds area *Vs* GPCP precipitation	0.30**	0.10**	0.01**	0.46**		
r^2 Rainfall duration *Vs* $\delta^{18}O$	**0.44**	**0.54**	**0.64**	0.24	0.00	0.07

***Anti-correlation*

Identification of processes that control the stable isotope composition of rainwater in the humid tropical West-Central Africa

B. Nlend [a,f,g*], H. Celle-Jeanton [a], C. Risi [b], B. Pohl [c], F. Huneau [d,e], S. Ngo Boum-Nkot [f], G. Seze [b] , P. Roucou [c], P. Camberlin [c], J. Etame [f], B. Ketchemen-Tandia [f]

[a] Université de Bourgogne Franche-Comté, CNRS, UMR 6249 Chrono-Environnement, 16 route de Gray, F-25030 Besançon cedex, France

[b] Laboratoire de Météorologie Dynamique, IPSL, Sorbonne Universités UPMC, CNRS, Paris, France

[c] Centre de Recherches de Climatologie, UMR 6282 Biogéosciences CNRS/Université de Bourgogne Franche-Comté, Dijon, France

[d] Université de Corse Pascal Paoli, Département d'Hydrogéologie, Campus Grimaldi, BP 52, F-20250 Corte, France

[e] CNRS, UMR 6134 SPE, BP 52, F-20250 Corte, France

[f] University of Douala, Faculty of Sciences, P.O BOX 24157, Douala, Cameroon

[g] Cameroonian Institute for Geological and Mining Research, Hydrological Research Center, P.O BOX 4110, Yaoundé, Cameroon

*Corresponding author:
Bertil NLEND
Université de Bourgogne Franche-Comté,
CNRS, UMR 6249 Chrono-Environnement,
16 route de Gray, F-25030 Besançon cedex, France
Tel: 03 81 66 20 10 / 06 33 59 01 04
(from abroad: +33 3 81 66 20 10 / +33 6 33 59 01 04)
e-mail: bertil.nlend@univ-fcomte.fr / Nlendbertil@yahoo.fr

Abstract

This study interprets 11 years (2006 to 2016) and 6 months (March to August in 2017) of respectively monthly and daily isotopic (δD and $\delta^{18}O$) monitoring of rain at Douala (Cameroon), a humid tropical station in Western Africa. The main scope is to analyze the climate controls on precipitation isotopes at different timescales. Firstly, we examine the annual cycles of $\delta^{18}O$. Over the 11 years of survey, the annual cycle exhibits a W shape that is quite reproducible from year to year, with two minima in spring and autumn periods. Based on back trajectory calculations and remote sensing observations of water vapor isotopic composition, we show that the observed depletion in spring and autumn is due to strong convective activity along air mass trajectories. The same effect of convective activity can be observed at the daily timescale. At seasonal and daily time scales, the isotopic composition is also strongly tied to the convective organization and cloud types. More depleted precipitation is associated with larger areas of high clouds. Very low to low clouds are observed in July-August, mid-level to high clouds are dominant in June and high to very high clouds characterize March-April-May, thus explaining the enriched (depleted) values in summer (spring). Finally, this paper highlights the importance of large scale meteorological conditions controls on precipitation stable isotope composition in the Gulf of Guinea.

Keywords: $\delta^{18}O$, water vapor, convective activity, GPCP precipitation, air back trajectory.

1. Introduction

The atmosphere is an essential hydrological environment. It contains all the water vapor (0.001% of all the water of the Earth; Delmas et al. 2005) that forms the clouds by condensation which can then generate precipitations (liquid/solid) as a function of air temperature. The atmosphere is also an essential place of transfer and exchange for the global functioning of the Earth system. Its multiple interactions with the oceans, the continent and the biosphere make it an important study environment for understanding global changes. According to IPCC (1998), these global changes must affect tropical regions which are among the most vulnerable to possible anthropogenically induced climatic changes.

During the last decade, the scientific community, environmental institutions, governments, and local communities have increased their awareness of the importance of current tropical climate variability, based on the premise that, under increasing anthropogenic influence on the climate, changes in regional and global circulation may lead to an intensification of extreme events (i.e. floods or severe droughts: e.g., Pohl et al. 2017). In parallel, the use of stable isotopes of water, both δD and $\delta^{18}O$ has provided insights in the study of atmospheric water cycle (e.g., Rozanski et al. 1993, Araguas - Araguas et al. 2000, Celle-Jeanton et al. 2004); the key to understand the future climate changes or global changes. Relationship between δD and $\delta^{18}O$ in natural meteoric waters serves as a foundational reference to determine regional and local deviations from equilibrium processes and the potential origin of the water vapor. Moreover, water losses due to evaporation, incorporation of recycled atmospheric moisture, and/or mixing between isotopically distinct reservoirs leave a unique water fingerprint that can be used for climate-reconstructions (Moerman et al. 2013). Recently, isotopic composition of tropical meteoric water has also proven its usefulness as an indicator of modern climate variability (Vuille and Werner 2005; Ishizaki et al. 2012; Sanchez-Murillo 2015).

84 While in extra-tropical climates, stable isotope variations in meteoric
85 waters have been successfully explained by air temperature variability (Dansgaard 1964;
86 Rozanski et al. 1993), the case of tropical humid regions proved to be very much complex
87 since temperature variability is much weaker. The amount effect occurs as a result of
88 convective precipitation and can be nonlocal (Vimeux et al. 2005; He et al. 2015). The degree
89 of organization of convective systems has been shown to impact the atmospheric conditions at
90 the large-scale (Tobin et al. 2012; Wing et al. 2017). Consistently, it also impacts the isotopic
91 composition of water vapor and precipitation. Many additional factors can potentially play a
92 role, such as orographic effects, continental recycling or moisture origin combined with
93 complex microclimates (Rozanski et al. 1993, Lachniet and Paterson 2009).

94 These problematics are of major importance for the paper. What are the key factors
95 controlling stable isotope ratios of meteoric waters in humid tropical areas of West and
96 Central Africa? Answers to this question will contribute to the understanding of atmospheric
97 processes in the study region. Unlike arid and semi-arid African areas, where isotopic
98 variability has already been assessed in previous work (e.g; Taupin et al. 1997, Celle-Jeanton
99 et al. 2001; Risi et al. 2008b, 2010; Lutz et al. 2011, Tremoy 2012; Tremoy et al. 2014), the
100 Gulf of Guinea (GOG) region and tropical humid areas in Central Africa (Figure 1) are still
101 under-documented in isotopic data. There, the atmospheric cycle of water remains poorly
102 documented and isotopic data may help improve their knowledge. Indirectly, the paper will
103 help to understand rainfall variability in Douala and the origin of precipitated water through
104 isotopic analysis. In this objective, we took advantage of the long term monthly monitoring
105 set up in Douala, Cameroon (Figure 1) as part of the Global Network for Isotopes in
106 Precipitation (GNIP) framework (IAEA/WMO 2018) from 2006. In parallel, a daily sampling
107 has been carried out in 2017. This article represents the first valuation of precipitation isotope
108 data in the region. Datasets of other GNIP stations in the GOG and Central Africa (Figure 1)

109 are also integrated in this study, together with remote sensing data that document water vapor
110 isotopic composition, convective activity and cloud properties.

111

112 Figure 1.

113

114 **2. Regional climate: the West African Monsoon (WAM) dynamic**

115 Seasonality in the tropics is mostly determined by the seasonal migrations of the Inter
116 Tropical Convergence Zone (ITCZ, Preston-White and Tyson 1988; Schott et al. 2003), a
117 highly energetic feature of earth climate that is associated with deep convection. The ITCZ or
118 meteorological equator in Africa is the result of convergence between the Harmattan
119 (northeasterly dry wind) and Monsoon (southwesterly wet wind) in low levels of the
120 atmosphere (Sultan and Janicot 2000, Fink et al. 2018). Nicholson and Grist (2003) have
121 shown that the rain belt over Western and Central Africa is positively correlated with the
122 migration of the ITCZ. During the boreal spring (Mar-Apr-May), ITCZ holds a position of
123 about 5°N; half of the rain belt is located over the continent and the other one on the ocean
124 (Waliser and Gautier 1993). The mean rainfall amount calculated for this period, according to
125 GNIP measurements, is 232 mm for Douala, 138.4 mm for Cotonou, 137.7 mm for Sao-Tome
126 and 114.1 mm for Bangui. The relative humidity increases significantly over the continent
127 and sea surface temperatures (SST) present their annual peak (>27°C) during this period
128 (Dezfuli and Nicholson 2013). Then, ITCZ abruptly shifts from 5°N to 10°N in June-July
129 (Sultan and Janicot 2003). The so-called monsoon jump causes a subsidence in the southern
130 part of the GOG and the development of a cold tongue complex (Gu and Adler 2004). Low
131 SSTs suppress then partly or totally rainfall as e.g. in Sao-Tome (Figure 3). However, in the

Gulf of Biafra (Figure 1), SSTs remain high enough (>26°C) to partly maintain convection (Odekunle and Eludoyin 2008). Moisture increases over land and enhances rainfall there. Simultaneously, convective activity migrates to the North, and the monsoon flow crosses the Equator from South (GOG) to North (Guinean and then Sahelian Africa). At this time of the year (Jun-Jul-Aug), a rainfall peak is observed (Figure 3) in Douala (618.3 mm) and Bangui (145.5 mm). In Cotonou, Ogu et al. (2016) have also shown a good correlation between SSTs and precipitation, connecting rainfall amount in June to anomalously warm waters of the Gulf of Benin.

The abruptness of the northward progression of the ITCZ is in sharp contrast to its withdrawal, which appears as a more progressive southward progression. Like most regions in the equatorial latitudes, the Guinean Coast/Central Africa thus benefits from a double passage of the ITCZ in spring and autumn.

The unimodal distribution and the highest rainfall amount (~ 4000 mm/year) observed in Douala (Figure 3) is very particular as the whole region is generally characterized by a bimodal distribution with two precipitation maxima in April-May (or May-June) and October-November (or September-October), with a total amount lower than 2000 mm/year. The concave shape of the Gulf of Biafra may induce a convergence of southwesterly winds and topographic ascents forced by the relief of Mount Cameroon (> 4000 m, Figure. 1). This mesoscale convergence and orographic influence (Vondou et al. 2017) are all the more marked if the monsoon flow is intense and thick, which is the case in the core of the summer monsoon, when the ITCZ is far to the North. These regional features can explain the unimodal regime observed at Douala while further west (in Cotonou), and in southern hemisphere (Sao-Tome), the annual cycle is bimodal.

155 ## 3. Data and methods

156 ### *3.1. Rainfall sampling and isotopes analyses*

157 This paper makes use of the 106 monthly samples of rainwater that have been collected from
158 July 2006 to December 2016 at the GNIP station of Douala (see details of the GNIP stations
159 in Table 1 and Figure 1). The sampling followed the standard protocols (IAEA 2012).
160 Samples were collected by using a rain gauge which consists of a plastic funnel (diameter =
161 10 cm) coupled with a filter mesh to prevent contaminations by debris. A 5 cm layer of
162 mineral oil has been systematically added into the rain collector to avoid fractionation of the
163 collected rainwater. For each month, total rainfall was collected. Samples were taken
164 regularly, stored in a totalizer and kept at 4°C before being transferred in 50 ml amber glass
165 bottles, tightly capped and sent to the International Atomic Energy Agency (IAEA) laboratory
166 in Vienna, Austria for stable isotopes determinations. Stable isotopes of hydrogen and oxygen
167 were then analyzed by laser absorption spectroscopy following the method described by
168 Penna et al. (2010).

169 Table 1

170

171 The rainwater daily survey was conducted from March to August 2017 at the campus of the
172 University of Douala (X= 9.7461; Y= 4.062; Z= 17 m.a.s.l.), approximately at 7 km from the
173 GNIP station. Seventy samples were collected using a Palmex rain gauge that presents the
174 advantage to avoid evaporation without using medicinal paraffin oil (Gröning et al. 2012).
175 Daily samples were stored using the same protocols as for monthly rainfall. Isotopes analyses
176 were performed at the Hydrogeology Department of the University of Corsica, France, by

using a liquid-water stable isotope analyzer DLT-100 Los Gatos Research (Aggarwal et al. 2006; Penna et al. 2010).

Ratios of $^{18}O/\delta^{16}O$ and $^{2}H/^{1}H$ are expressed in delta units (‰, parts per mil) relative to Vienna Standard Mean Ocean Water (V-SMOW). The analytical precision is ±0.1‰ for oxygen-18 and ±1‰ for deuterium.

Local meteorological settings (precipitation amount and duration, air temperatures, vapor pressure) were provided by the National Weather Direction of Cameroon.

3.2. Tropospheric Emission Spectrometer (TES) data

With the advent of new technology in stable water isotopes, such as spectrometer on-board satellite, it has become easier to analyze isotopic composition of water vapor based on indirect laser measurement (Aemisegger et al. 2012). TES instrument on board on the Aura satellite is a nadir-viewing infrared Fourier transform spectrometer from which the deuterium content of water vapor (δD_v) can be retrieved (Worden et al. 2006; Worden et al 2007). The sensitivity of the retrieval is typically larger between 900 hPa and 400 hPa with a peak at 700 hPa. On average, δDv retrieved over these levels has a precision of 1.5% or about 15 parts per thousand (per mile) relative to Standard Mean Ocean Water. Uncertainties are reduced by averaging several measurements (Worden et al. 2006; Risi et al. 2013). Then the precision is sufficient for characterizing the global distribution of evaporation and condensation processes (Worden et al. 2006).

There is on average 1.8 degrees of freedom for δDv retrievals in the tropics (Worden et al. 2012), meaning that vertical profiles bear information on more than one level. To ensure good data quality, we selected only the measurements for which the quality flag is set to unity and for which the degree of freedom of the signal is higher than 0.5 (Risi et al. 2013). Here, to document the water vapor composition as close as possible to the surface, we use the δD

values retrieved by TES at 900 hPa from 2004-2008 at a monthly scale and we focus on a multi-year mean seasonal cycle and temporal variations rather than absolute values.

3.3. Convection and cloud datasets

Convective activity associated with the West African Monsoon (WAM) was analyzed using the Global Precipitation Climate Project one degree daily (GPCP-1dd; Huffman et al. 2001) data. The same dataset is used for both monthly and daily analyses. Data were retrieved from the National Oceanic and Atmospheric Administration (NOAA) website (https://www.esrl.noaa.gov/psd/cgi-bin/data/composites/printpage.pl). The robustness of GPCP products has been demonstrated in many studies (e.g.; Huffman et al. 1995, 1997; Adler et al. 2017) through a comparison with other proxies of convection or by multi-proxy studies: OLR (Outgoing Longwave Radiation) and TRMM (Tropical Rainfall Measurement Mission). GPCP products are a combination of precipitation data provided by a multiple sources of satellite-gauge (SG). They are obtained by optimally merging precipitation estimates computed from microwave, infrared, sounder data observed by the international constellation of precipitation-related satellites, and rain gauge analyses, taking advantage of the strengths of each data type. Mean SG products are computed by combining multi-satellite estimates with rain gauge analysis (Huffman et al. 2001). In this study, we use the GPCP-1dd (1-degree grid over the entire globe at 1-day) both for monthly and daily analyses.

To document the cloud types and convection organization in Western Central Africa, we use a cloud type (CT) product issued from geostationary MSG (Meteosat Second generation) satellite data and developed by SAFNWC (Satellite application facilities in support to nowcasting) /MSG algorithms (for more information see http://www.nwcsaf.org/web/guest/scientific-documentation). Clouds types are determined from their top temperature or pressure and, for high level clouds from their opacity (Dommo

et al. 2018; Seze 2015). The SAFNWC CT offers a classification of clouds into 12 classes: free land, free sea, very low clouds, low clouds, medium clouds, high clouds, very high clouds, thin cirrus, medium cirrus, thick cirrus, fractional clouds and semi-transparent above low or medium clouds, at 3-km spatial resolution for regions close to MSG sub-satellite point (0N, 0E) and a time step of 15-min. For our study purposes, focus is given to the altitude of clouds (low, medium, high, etc.) and their organization (as measured by the spatial extent of connected cloud pixels) to seek links with the isotopic contents of rainfall. Data are extracted for the region bounded by latitudes 10S–10N and longitudes 0E–20E, for the period from March to June 2017.

Based on these images, very high clouds areas (corresponding to very organized convective system) around Douala were calculated for each event using ArcGis mapping software, through the tool "measure". Indeed, since the contours of cloud masses or pixels are approximated to geometric forms (circle, rectangular, trapezoidal shape, etc.), the areas were calculated based on these forms. This calculation was performed after a zoom of the image at 100% in order to limit uncertainties or errors by using the tool of the software. For events with duration of more than 15 min, we have taken the maximum cloud area throughout the duration of rainfall.

3.4. Back trajectories

In order to assess the influence of air masses pathways on the isotopic composition of precipitation, and the importance of the location of convective activity in the region, we compute air back trajectories at 6h time steps, 10 days prior to arrival in the sampling site. This operation was performed for monthly and daily scales when isotopic data is available. Winds (at 900 hPa) were simulated by using the general circulation model LMDZ5A (Hourdin et al. 2013) guided by reanalysis products (ERA-Interim, Dee et al. 2011) of the

European Centre for Medium-Range Weather Forecasts (ECMWF). Back trajectories (speed and direction) were then computed with a 2D algorithm (similar to Vimeux et al. 2005) in order to approximate the moisture transport near the ground surface.

4. Results and discussion

4.1.Annual cycles of isotopes (δ) in precipitation of Douala

Figure 2 presents the seasonal variations of $\delta^{18}O$ from 2006 to 2016. The annual cycle of δ is quite reproducible from year to year. It exhibits a W shape most of the time, with minima in spring and autumn periods. Because of this rather good reproducibility of $\delta^{18}O$ seasonal cycle from year to year; we further consider a multi-year mean seasonal cycle in the section 4.2, and investigate the factors associated with this W cycle of δ.

However, the magnitude varies widely from one year to another for a given month. Such inter-annual variability could either reflect variations (i) in the climate seasonal background, or (ii) in synoptic / intra-seasonal variability, which could modify seasonal mean fields through upscaling processes, or eventually affect isotopic variations. These hypotheses are tested and discussed below.

Figure 2.

4.2. Factors responsible for precipitation isotopes variations at seasonal scale

4.2.1. Highlighting of a regional context

Seasonal variations of $\delta^{18}O$ and precipitation amount for GNIP stations in GOG and Central Africa region are presented in Figure 3.

Figure 3.

Similarities can be observed in the seasonal evolution of $\delta^{18}O$ at Cotonou, Bangui, Douala and Sao-Tome (Figure 3): (i) from January-February to April-May, $\delta^{18}O$ decreases; (ii) an enrichment in isotopic content is observed in summer (in June, July or August depending on the station); (iii) isotope contents then decrease until September or October and (iv) a new increase occurs until December. This relative homogeneity suggests that isotopic seasonality is controlled by mechanisms of, at least, on regional scale.

Correlation coefficients between $\delta^{18}O$, precipitation and temperature are very low for all the stations (Table 2). The weak correlation between $\delta^{18}O$ and air temperature (Table 2) highlights the lack of temperature effect in the GOG and Central Africa regions. Despite the fact that, in tropical maritime stations, a local amount effect is often observed (Rozanski et al. 1993), the poor correlation between $\delta^{18}O$ and local precipitation amount shows that this effect does not dominate the isotopic seasonality in Central Western Africa. Therefore, it is clear that, the local climate parameters do not control the seasonal variation of δ in precipitation. Thus we hypothesize that convective activity at the regional scale could be involved. This hypothesis is tested in the next section for the Douala station.

Table 2.

4.2.2. Influence of regional convective activity

Many studies in China (e.g., Gao et al. 2013; He et al. 2015 ; Yu et al. 2016; Guo et al. 2017; Shao et al. 2017; Gao et al. 2018), India and Indo-Pacific region (e.g., Chakraborty et al. 2015; Rahul and Gosh 2016; Cai et al. 2016; He et al. 2018), South America (e.g., Hoffmann et al. 2003;Vimeux et al. 2005; Villacis et al. 2008, Samuels-Crow et al. 2014) and Sahelian Africa (e.g., Risi et al. 2008b; Risi et al. 2010b; Tremoy et al. 2012) based on both

observations and models, have shown that convective activity, that occurs upstream the pathway of air parcels, is a major control of rainwater isotope composition in the tropics at daily, seasonal and inter-annual timescales.

Convective activity is known to deplete water vapor through 3 main processes: i) precipitating downdrafts, either at the convective-scale or at the meso-scale (Risi et al. 2008a, Kurita 2013), bring down depleted water vapor from the mid-troposphere to the boundary layer; ii) rain evaporation, when concerning a small proportion of each raindrop, adds depleted water vapor to the lower troposphere (Worden et al. 2007, Risi et al. 2010); iii) rain-vapor diffusive exchanges in a saturated atmosphere can also deplete the water vapor (Lawrence et al. 2004).

GPCP precipitations are used to examine convective activity upstream the sampling site of Douala. Figure 4 presents monthly mean precipitation and back trajectories calculated for each month. As expected, moisture comes from the Atlantic Ocean most of the time and precipitation, at this timescale, is entirely controlled by the seasonal migration of the ITCZ.

In November and December, moisture comes from the North-East without undergoing any convection. From December to January, there is an abrupt shift of air parcel from North-Easterly to South-Westerly, in line with the beginning of long northward migration of the ITCZ. From March to May (spring season), air masses undergo strong convective activity over the Gulf of Guinea. During the period June - August, air parcels still travel over the Gulf of Guinea, but air masses undergo a weak convective activity because the ITCZ has shifted further north over the Sahel region. From September to October (autumn period), the ITCZ retreats to the South so that air masses undergo strong convective activity once again. The shift between October and November trajectories marks the transition to the dry season when the strength of monsoon winds weakens.

Figure 5 by presenting the variability of monthly mean GPCP precipitation along the back trajectory over time (in hours), towards Douala station for May (spring period), August

(summer period), October (autumn period) and January (winter period) shows a quantitative analysis. It reveals where, along the trajectories, convective activity becomes higher and thus impacts $\delta^{18}O$ of Douala rainfall. Overall, the GPCP precipitation data show an increasing trend from the Southern Atlantic to Douala. Along the air back trajectories, at 7 days (168 hours) to the sampling site, precipitation is higher in August and May. First significant changes are observable at 120 hours, when a decrease (increase) of GPCP precipitation occurs in January (October). It substantially increases in May and August. At 3 days (72 hours) before Douala, convective activity is stronger in October (and to a lesser extent in May) than August and January. Since isotopic value of rainfall is depleted in spring and autumn (Figures 2-3), $\delta^{18}O$ seems to be mostly sensitive to convective activity only in the past few days before reaching Douala. This is consistent with the "memory" of convection in the isotopic composition of water as discussed by Risi et al (2008a), Tuinenburg et al (2015) and Gao et al (2013). Stable isotopes are imprint of convection along air parcel trajectories, and in the case of Douala, precipitation seems to acquire its signature on average 72h before reaching the station. Figure 6 shows the precipitation averaged over the past 72h (3 days) along the backward trajectories, for each month. The precipitation $\delta^{18}O$ is significantly anti-correlated with this average precipitation (r^2=0.60). This supports our hypothesis that convective activity along trajectories significantly controls the seasonality of precipitation $\delta^{18}O$ in Douala.

In summary, the moisture "source" at Douala is most of the year in the GOG. Two seasonal precipitation maxima along the trajectories (Figure 6) are related to the seasonal migration of the ITCZ. Thus, even if precipitation in Douala shows a unimodal regime with a rainfall peak in August, $\delta^{18}O$ records bimodal cycle as in the "source" area. This suggests that the regional convective activity is the main control of the isotopic composition of precipitation in Douala.

In the following section, we use the isotopic information of the water vapor to provide additional insights about the main processes controlling the isotopic composition of precipitation.

Figure 4.

Figure 5.

Figure 6.

4.2.3. Information from the isotopic composition of water vapor (δv)

The isotopic composition of the water vapor provided by the TES instrument can help to understand the variation of δ in precipitation: it allows separating the relative effect of processes acting along the trajectories of the water vapor (δDv) and local post-condensational processes (δDp – δDv) following the equation below:

$$\delta Dp = \delta Dv + (\delta Dp - \delta Dv) \quad (1).$$

δD_v and δD_P (Figure 7a) show a similar seasonality (r^2 = 0.57). Both δD_v and δD_P present depleted values in April-May and September-October (Figure 7a), corresponding to more active convection in the GOG. In addition, there is always a positive offset between the isotopic composition of water vapor and precipitation. Thus, the isotopic information on the advected water vapor is preserved in the isotopic composition of the rain.

Figure 7.

However, absolute values of δDp and TES δDv should not be directly compared. TES was calibrated using in-situ measurements on local sites (Worden et al 2012) but not specifically in West Africa. In addition, TES data at 900hPa represent an average over several vertical levels in the lower troposphere. Therefore, focus is given instead to temporal variability. Yet, assuming that the vertical δD gradient between 1000 and 900hPa is constant, δDp-δDv variations can be interpreted as variations in the rain-water vapor interaction processes.

The regression between δD_p and δD_v gives a slope of a1 = 1 whereas the values for δD_p and δD_p-δD_v are a2 = -0.68 and r^2 = 0.18. This insignificant r^2 attests that the rain-water vapor interaction processes do not control the δDp variations. Based on the slope a1, δD_v accounts for 100% of the δD_p variability. A similar case has been reported in western tropical Pacific (Conroy et al. 2016). This confirms that the seasonal variability of the isotopic composition of rainfall is predominantly influenced by δD_v, i.e. by the processes that affect water vapor along the trajectories. This means that the variability of δD_p-δD_v acts only to dampen and to blur the variability of δD_p. For instance, the evolution of δDp-δDv presents a maximum in spring (Figure 7b) and autumn, when δDv is most depleted.

4.3. Main controls of precipitation isotopic composition at daily scale

4.3.1. Temporal evolution of δ and link with upstream convection

Daily $\delta^{18}O$ in Douala varies from -0.3‰ to -7.4‰, with a mean value of -3.0‰ close to the monthly weighted mean of -2.8‰ calculated for the 2006-2016 period. These daily data appear then to be representative of the 2006-2016 mean seasonal cycles. Moreover, as for the seasonal scale, daily rainwater (Figure 8) is most depleted in spring (April-May) and more enriched in summer (July-August).

Figure 8.

In order to investigate upstream convection effects, we calculated the correlation between the $\delta^{18}O$ of rainfall and the precipitation recorded at 1 to 3 days earlier, along back trajectories (Table 3). In March, April and August, the correlations are significant (≥ 95%), suggesting that, like for the seasonal timescale, the daily evolution is driven by convection along trajectories. Yet, this mechanism is insufficient to explain completely the variability of δ in daily precipitation, especially in May, June and July.

Table 3.

4.3.2. Factors besides the upstream convection intensity: continental recycling and organization of convective systems

Continental recycling?

The goal of this section is to test whether continental recycling has significant influence on $\delta^{18}O$ at the daily time scale. To that end, we calculated the percentage of time of the air parcel over the continent during the last 3 days (72h) along the trajectory, hereafter F_{land}. This calculation was relatively simple since air back trajectories have been computed at 6h time steps and then for instance, the travel time of 36h of air mass over the continent will correspond to F_{land} equal to 50%. However, for this issue, we calculated air back trajectories at different heights: 800, 850, 900, 950 and 980 hPa since moisture is typically transported at a spectrum of heights. As it is the boundary layer that feeds the convection and it is with the water vapor from low layers that the rain is re-evaporated, investigation was not performed above 800 hPa. Results from this quantitative calculation (not shown here) of moisture transport for different heights show that there is no difference between them, especially since we focus only on air back trajectory at 3 days before Douala. In June, July and August, F_{land} is 0% for all rainy days (except on June 11th when F_{land} = 25%). Table 4 presents the detailed

results for spring period and shows an anti-correlation between $\delta^{18}O$ and F_{land}. Precipitation are thus more depleted, when the transit time of air parcels over the continent is long, during the last 3 days along the back trajectory This is in contradiction with the expected effect of a continental recycling.

Table 4.

Since δ is controlled in spring by a convection upstream the sampling site, the fact that $\delta^{18}O$ is more depleted with the increase of F_{land}, suggests a significant influence of convection intensity over the continent. Indeed, Xu and Zipser (2012) demonstrated that convection is generally more intense over the land than over the ocean. The more intense the convection along trajectories, the more depleted the water vapor. Therefore, moisture origin has only an indirect effect on isotopic composition of precipitation, depending on whether air mass goes through regions of a strong convection. The positive and significant correlation between F_{land} and GPCP precipitation confirms this mechanism.

Therefore, we suggest that, δ variations at a daily timescale are partly controlled by the intensity of the convection along air parcel trajectories and that continental recycling is not involved.

Influence of the organization of convective systems?

Several studies have shown that convective systems deplete the low-level water vapor more efficiently when they are more organized (Lawrence et al. 2004, Risi et al. 2008, Tremoy et al 2014), probably because moister air in larger systems allows for more efficient rain-vapour diffusive exchanges (Risi et al. 2008a). In addition, convective systems deplete more vapor as they extend to the upper troposphere (Lacour et al 2018) and as the extent of their anvils

(measured by the fraction of stratiform clouds) is large (Aggarwal et al. 2016). These features are typically associated with higher degrees of organization.

Here, we test whether the type of convective organization has a significant impact on the $\delta^{18}O$ observed at Douala. By using satellite image from the SAF classification, we define 3 classes of clouds in the region from March to August according to their altitude: (i) very low to low; (ii) medium to high and (ii) very high clouds. The low cloud class is mostly observed in July-August (Table 5 and Figure 9). The mid-level to high cloud class is dominant in June and the very high clouds are mostly present in spring (Figure 9). The area of cloud systems increases throughout spring, reaching a maximum in May, and decreases again from June. In July-August, the areas are too small to be calculated.

Figure 9.

Spatial organization of convective systems also determines rainfall event duration. The latter increases globally from March to August (Figure 10), ranging from 12 minutes to 1278 min (i.e. more than 21 hours).

Figure 10.

Combining this information on cloud altitude, cloud area and rainfall duration; we can infer that in March-April, most convective systems correspond to deep mesoscale convective systems (MCS; Mapes and Houze 1993; Laing and Fritsch 1997; Mathon et al. 2001; Fink et al. 2006; Tremoy et al. 2014). In May-June, convective systems are MCS that become even larger and organized, but extend less deep in altitude (in June). In contrast, in July-August,

462 convective systems are isolated; characterized by small cumulonimbus in the middle of low-
463 to-medium clouds (Figure 9b) that follow one another throughout the day, explaining the
464 apparent long durations of rain events.

465 The type of convective organization emerges then as an important control on the precipitation
466 isotopic composition. Cloud surface shows a significant negative correlation with
467 precipitation $\delta^{18}O$ from March to June (Table 5). The larger the cloud area, the more depleted
468 the precipitation. In addition, the more the convective system is organized, the longer is the
469 duration of the event (Laurent and Machado 2002, Fiolleau et al. 2013). Consistently, event-
470 scale $\delta^{18}O$ is anti-correlated with event duration in March (r^2 = 0.44), April (r^2 = 0.54), May
471 (r^2 = 0.64) and more weakly in June (r^2 = 0.34). The longer is the convective system, the more
472 depleted is the precipitation.

473 These different types of convective organization can also explain the isotopic evolution at the
474 seasonal scale. In spring, the organized, deep MCS deplete the water vapor efficiently,
475 leading to the observed precipitation $\delta^{18}O$ minimum. In contrast, in July-August, the
476 shallower, small isolated cumulonimbus clouds deplete the water vapor less efficiently,
477 leading to the observed precipitation $\delta^{18}O$ maximum in spite of the local precipitation
478 maximum observed at Douala.

479 Surprisingly, the r^2 between cloud area and $\delta^{18}O$ are close and even higher (in May and June)
480 than that observed between $\delta^{18}O$ and upstream precipitation (Table 3). After verifying that
481 upstream convection (GPCP precipitation recorded at 72h to Douala along the trajectory) and
482 cloud area are uncorrelated (Table 5), we can assert that two independent parameters control
483 $\delta^{18}O$: upstream convection intensity and the size of the convective system (both at local scale
484 and at upstream, see the Table 5).

Table 5.

5. Conclusion and outlook

This study aims at investigating the processes controlling the year-to-year (inter-annual), month-to-month (seasonality) and day-to-day (intra-seasonal) variability of rainfall isotopic composition in the Gulf of Guinea (GOG) region and especially in Douala (Cameroon). We observed that the annual cycle of δ is quite reproducible. Most years presents a W shape with minima in spring and autumn. $\delta^{18}O$ and δD_v appear to be mainly controlled by upstream convection and by the size of convective systems. We identified that the continental recycling doesn't impact the rainwater isotopes in the humid tropical area of the GOG. In particular, the $\delta^{18}O$ minima in spring and autumn are associated with strong convective activity in the GOG and large, long-lived and deep mesoscale convective systems, whereas the $\delta^{18}O$ maximum in July-August is associated with reduced convective activity in the GOG and isolated shallow convective systems. The importance of upstream convective activity in controlling the $\delta^{18}O$ of precipitation at various time scales is in line with a large body of recent research in different tropical regions influenced by a monsoon system. The importance of the type of convective system (size, organization, vertical extension) is also consistent with a growing number of recent studies but this is the first time that it is demonstrated through a detailed analysis of such a large number of individual convective systems. The findings of this study (obtained by integrating in situ and satellite measurements) advance our understanding of the temporal variation of precipitation stable isotopes in humid tropical area such as Douala, and shed a

new light on the importance of large scale meteorological conditions controls on precipitation stable isotope composition in the GOG.

Notwithstanding, numerical climate modelling could be a useful complementary approach to further analyse the factors controlling rainfall isotopic composition in and around Douala

Moreover, the climate in Douala being representative of a small area with monomodal rainfall regime surrounded by area with bimodal rainfall, high resolution modelling is necessary to correctly capture such particularity. More robust conclusions could be obtained with larger samples, which could be obtained by extending the length of the record. To better understand the role of convective organization on the isotopic composition, sampling at the intra-event scale is necessary. Finally, measuring the isotopic composition in the water vapor in addition to precipitation would be useful to isolate the post-condensation effects.

Acknowledgements

This paper constitutes a part PhD study of the first author, who was supported by a doctoral scholarship from the French Ministry of Foreign Affairs. The authors thank the French Embassy to the Republic of Cameroon for all mobility facilities provided during the study. Thanks also to the anonymous reviewers whose comments have substantially helped to improve the manuscript.

Funding: This research did not receive any specific grant from funding agencies in the public, commercial, or not-for-profit sectors.

References

Adler, R.F., Sapiano, M.R.P., Huffman, G.J., Wang, J., Gu, G., Bolvin. D., Chiu, L., Schneider, U., Becker, A., Nelkin, E., Xie, P., Ferraro, R., Shin, D-B., 2017. The Global Precipitation Climatology Project (GPCP) Monthly Analysis (New Version 2.3) and a Review of 2017 Global Precipitation. *Atmosphere* 2018, 9, 138; doi:10.3390/atmos9040138

Aemisegger, F., Sturm, P., Graf, P., Sodemann, H., Pfahl, S., Knohl,A., and Wernli, H.: 2012. Measuring variations of $\delta^{18}O$ and $\delta^{2}H$ in atmospheric water vapour using two commercial laser-based spectrometers: an instrument characterization study, *Atmos. Meas.Tech*., 5, 1491–1511, doi:10.5194/amt-5-1491-2012, 2012

Aggarwal, P., Ahmad, T., Gröning, M., Manish, G., Owano, Th., Baer, D., 2006. Laser spectroscopic analysis of stable isotopes in natural waters: a low-cost, robust technique for the use of environmental isotopes in hydrological and climate studies. *AGU Fall Meeting* Abstracts.

Aggarwal, P. K., Romatschke, U., Araguas-Araguas, L., Belachew, D., Longstaffe, F. J., Berg, P., ... & Funk, A. (2016). Proportions of convective and stratiform precipitation revealed in water isotope ratios. *Nature Geoscience, 9*(8), 624.

Aemisegger, F., Pfahl, S., Sodemann, H., Lehner, I., Seneviratne, S.I., Wernli, H., 2014. Deuterium excess as a proxy for continental moisture recycling and plant transpiration. *Atmos. Chem. Phys*. 14, 4029–4054

Araguas-Araguas, L., Froehlich, K., Rozanski, K., 2000. Deuterium and oxygen-18 isotope composition of precipitation and atmospheric moisture. *Hydrol. Process*. 14, 230-244

Benetti, M., Reverdin, G., Pierre, C., Merlivat, L., Risi, C., Steen-Larsen, H. C., & Vimeux, F., 2014. Deuterium excess in marine water vapor: Dependency on relative humidity and

surface wind speed during evaporation. *Journal of Geophysical Research: Atmospheres*, *119*(2), 584-593.

Benetti, M., Lacour, J. L., Sveinbjörnsdóttir, A. E., Aloisi, G., Reverdin, G., Risi, C., & Steen Larsen, H. C., 2018. A framework to study mixing processes in the marine boundary layer using water vapor isotope measurements. *Geophysical Research Letters*, *45*(5), 2524-2532.

Bony, S., Risi, C., and Vimeux, F., 2008. Influence of convective processes on the isotopic composition ($\delta^{18}O$ and δD) of precipitation and water vapor in the tropics: 1. Radiative-convective equilibrium and Tropical Ocean-Global Atmosphere-Coupled Ocean-Atmosphere Response Experiment (TOGA-COARE) simulations, *J. Geophys. Res*., 113, D19305, doi:10.1029/2008JD009942

Cai, Z., & Tian, L., 2016. Processes governing water vapor isotope composition in the Indo-Pacific region: convection and water vapor transport. *Journal of Climate*, *29*(23), 8535-8546.

Celle-Jeanton, H., Zouari, K., Travi, Y., Daoud, A., 2001. Caractérisation isotopique des pluies en Tunisie. Essai de typologie dans la région de Sfax. *C. R. Acad. Sci*. Paris, Sciences de la Terre et des planètes / Earth and Planetary Sciences 333 (2001) 625–631

Celle-Jeanton, H., Gonfiantini, R., Travi, Y., Sol B., 2004. Oxygen-18 variations of rainwater during precipitation: Application of the Rayleigh model to selected rainfalls in Southern France. *J. Hydrol*.289: 165–177

Chakraborty, S., Sinha, N., Chattopadhyay, R., Sengupta, S., Mohan, P.M., Datye, A., 2016. Atmospheric controls on the precipitation isotopes over the Andaman Islands, Bay of Bengal. *Scientific Reports* | 6:19555 | DOI: 10.1038/srep19555.

576 Conroy, J. L., Noone, D., Cobb, K.M., Moerman, J.W. & Konecky, B.L., (2016), Paired
577 stable isotopologues in precipitation and vapor: A case study of the amount effect within
578 western tropical Pacific storms, J. Geophys. Res. Atmos., 121, 3290-3303,
579 doi:10.1002/2015JD023844.

580 Dansgaard, W., 1964. Stable isotopes in precipitation. *Tellus* 16 (4), 436-468.

581 Dee, D.P., Uppala, S.M., Simmons, A.J., Berrisford, P., Poli, P., Kobayashi, S., Andrae, U.,
582 Balmaseda, M.A., Balsamo, G., Bauer, P., Bechtold, P., Beljaars, A.C.M., van de Berg, L.,
583 Bidlot, J., Bormann, N., Delsol, C., Dragani, R., Fuentes, M., Geer, A.J., Haimberger, L.,
584 Healy, S.B., Hersbach, H., Hólm, E.V., Isaksen, L., Kållberg, P., Köhler, M., Matricardi,
585 M., Mcnally, A.P., Monge-Sanz, B.M., Morcrette, J.J., Park, B.K., Peubey, C., de Rosnay,
586 P., Tavolato, C., Thépaut, J.N., Vitart, F., 2011. The ERA-interim reanalysis:
587 configuration and performance of the data assimilation system. Q. J. R. Meteorol. Soc.
588 137, 553–597. https://doi.org/10.1002/qj.828

589 Delmas, R., Mégie, G., & Peuch, V-H., 2005. Physique et chimie de l'atmosphère. Belin

590 Derrien, M., and Le Gléau, H., 2005. MSG/SEVIRI cloud mask and type from SAFNWC. *Int.*
591 *J. Remote Sens*., 26, 4707–4732, https://doi.org/10.1080/01431160500166128D

592 ——, and ——, 2010: Improvement of cloud detection near sunrise and sunset by temporal-
593 differencing and region-growing techniques with real-time SEVIRI. *Int. J. Remote Sens*.,
594 31, 1765–1780, https://doi.org/10.1080/01431160902926632.

595 Dezfuli, A.K., Nicholson, S.E., 2013. The Relationship of Rainfall Variability in Western
596 Equatorial Africa to the Tropical. *Journal of Climate,* Vol 26. DOI: 10.1175/JCLI-D-11-
597 00686.1

598 Dommo, A., Philipon, N., Vondou, D.A., Seze, G., Eastman, R., 2018. The June–September
599 Low Cloud Cover in Western Central Africa: Mean Spatial Distribution and Diurnal
600 Evolution, and Associated Atmospheric Dynamics. *JCLI*, 1-19; DOI: 10.1175/JCLI-D-17-
601 0082.1

602 Fiolleau, T., and Roca, R., 2001. Composite life cycle of tropical mesoscale convective
603 systems from geostationary and low Earth orbit satellite observations: Method and
604 sampling considerations. *Quart. J. Roy. Meteor. Soc*., 139, 941–953,
605 doi:https://doi.org/10.1002/qj.2174.

606 Fink A., Vincent D., Ermert V., 2006. Rainfall types in the West African Sudanian zone
607 during the summer monsoon 2002. *Mon. Wea. Rev*., 134(8) : 2143–2164.

608 Fink AH., Engel T., Ermert V., Van der Linden R., Schneidewind M., Redl R., Afiesimama
609 E., Thiaw W., Yorke C., Evans M., Pohl B., Camberlin B. & Roucou P., 2018. «Chapitre
610 1 : Climat Moyen et Cycle Annuel » dans DJ Parker et M Diop-Kane (Eds.), Météorologie
611 de l'Afrique de l'Ouest Tropicale, Manuel du Prévisionniste. EDP Sciences, pp. 27-82
612 (ISBN: 978-2-7598-2108-2)

613 Gao, J., Masson-Delmotte, V., Risi, C., He, Y., and Yao, T., 2013. What controls precipitation
614 δ18O in the southern Tibetan Plateau at seasonal and intra-seasonal scales? A case study
615 at Lhasa and Nyalam, *Tellus B*, 65, 21043, doi:10.3402/tellusb.v65i0.21043

616 Gao, J., He, Y., Masson-Delmotte, V., & Yao, T., 2018. ENSO effects on annual variations of
617 summer precipitation stable isotopes in Lhasa, southern Tibetan Plateau. *Journal of*
618 *Climate*, *31*(3), 1173-1182.

619 Gat, J. R. and Matsui, E., 1991. Atmospheric water balance in the Amazon basin: An isotopic
620 evapotranspiration model, *J. Geophys. Res*, 96, 13179–13188, doi:10.1029/91JD00054,
621 1991.

622 Gimeno, L., Drumond, A., Nieto, R., Trigo, R. M., and Stohl, A., 2010. On the origin of
623 continental precipitation, *Geophysical Research Letters*, 37, 2010

624 Gonfiantini, R., 1996. « On the isotopic composition of precipitation ». In Jean Charles
625 Fontes (1936-1994), Un Souvenir, Proceedings, International Symposium, déc. 1995.
626 European Geologist, 2: 5-8.

627 Gröning, M., Lutz, H.O., Roller-Lutz, Z., Kralik, M., Gourcy, L., Pöltenstein, L., 2012. A
628 simple rain collector preventing water re-evaporation dedicated for δ18O and δ2H analysis
629 of cumulative precipitation samples. *Journal of Hydrology* 448–449 (2012) 195–200

630 Gu, G., and Adler, R.F., 2004. Seasonal evolution and variability associated with the West
631 African Monsoon System. *J. Climate* 17: 3364–3377.

632 Guo, X., Tian, L., Wen, R., Yu, W., & Qu, D. (2017). Controls of precipitation δ18O on the
633 northwestern Tibetan Plateau: A case study at Ngari station. *Atmospheric Research*, *189*,
634 141-151.

635 Gupta, P., Noone, D., Galewsky, J., Sweeney, C., Vaughn, B.H., 2009. Demonstration of
636 high-precision continuous measurements of water vapor isotopologues in laboratory and
637 remote field deployments using wavelength-scanned cavity ring-down spectroscopy (WS-
638 CRDS) technology. Rapid Commun. Mass Spectrom. 23 (16), 2534-2542.
639 http://dx.doi.org/10.1002/rcm.4100

640 He, Y., Risi, C., Gao, J., Masson-Delmotte, V., Yao, T., Lai, Ch-T., Ding, Y., Worden, J.,
641 Frankenberg, Ch., Chepfer, H., Cesana, G., 2015. Impact of atmospheric convection on

642 south Tibet summer precipitation isotopologue composition using a combination of in situ
643 measurements, satellite data and atmospheric general circulation modeling, *J. Geophys.*
644 *Res. Atmos*., 120, 3852–3871, doi:10.1002/2014JD022180

645 He, S., Goodkin, N. F., Kurita, N., Wang, X., & Rubin, C. M., 2018. Stable isotopes of
646 precipitation during tropical Sumatra Squalls in Singapore. *Journal of Geophysical*
647 *Research: Atmospheres*, *123*(7), 3812-3829.

648 Hoffmann, G., Ramirez, E., Taupin, J.-D., Francou, B., Ribstein, P., Delmas, R., Durr, H.,
649 Gallaire, R., Simoes, J., Schoterer, U., Stievenard, M. and Werner, M., 2003. "Coherent
650 Isotope History of Andean Ice Cores over the Last Century". *Geophys. Res. Lett*., 30(4),
651 1179, doi:10.1029/2002GL014870.

652 Hourdin, F., Foujols, MA., Codron, F. et al. 2013. Impact of the LMDZ atmospheric grid
653 configuration on the climate and sensitivity of the IPSL-CM5A coupled model *Clim Dyn*
654 (2013) 40: 2167. https://doi.org/10.1007/s00382-012-1411-3

655 Huffman, G. J., Adler, R. F., Rudolf, B., Schneider, U., & Keehn, P. R., 1995. Global
656 precipitation estimates based on a technique for combining satellite-based estimates,
657 rain-gauge analysis, and Nwp model precipitation information. *Journal of Climate*, 8(5),
658 1284–1295.

659 Huffman, G. J., Adler, R. F., Arkin, P., Chang, A., Ferraro, R., Gruber, A., Janowiak, J.,
660 McNab, A., Rudolf, B. and Schneider, U., 1997. The Global Precipitation Climatology
661 Project (GPCP) Combined Precipitation Dataset. *Bulletin of the American Meteorological*
662 *Society*, 78(1), 1997, pp. 5-20.

663 Huffman, G.J.; Adler, R.F.; Morrissey, M.; Bolvin, D.; Curtis, S.; Joyce, R.; McGavock, B.;
664 Susskind, J., 2001. Global Precipitation at One-Degree Daily Resolution from Multi-
665 Satellite Observations. *J. Hydrometeorol*. 2001, 2, 36–50.

666 IAEA, 2012. Technical Procedures for GNIP Stations. Vienna, Austria, p. 12. Available at.
667 http://www-naweb.iaea.org/napc/ih/IHS_resources_gnip.html.

668 IAEA/WMO, 2018. Global Network of Isotopes in Precipitation. The GNIP Database.
669 Accessible at: https://nucleus.iaea.org/wiser

670 Ishizaki, Y., Yoshimura, K., Kanae, S., Kimoto, M., Kurita, N., Oki, T., 2012. Interannual
671 variability of H18 2 O in precipitation over the Asian monsoon region. *J. Geophys. Res*.
672 117, D16308. http://dx.doi.org/10.1029/2011JD015890.

673 IPCC 1998. The regional impacts of climate change'. A special report of IPCC Working
674 Group II. Eds. R. T. Watson, M. C. Zinyow-era, R. H. Moss and D. J. Dokken. Cambridge
675 University Press

676 Kurita, N., 2013. Water isotopic variability in response to mesoscale convective system over
677 the tropical ocean, *J. Geophys. Res*., 118, 10,376-10,390, doi:10.1002/jgrd.50754

678 Lachniet, M., Paterson, W., 2009. Oxygen isotope values of precipitation and surface waters
679 in northern Central America (Belize and Guatemala) are dominated by temperature and
680 amount effects. *Earth Planet. Sci. Lett*. 284, 435-446.

681 Lacour, J.-L., Clarisse, L., Worden, J., Schneider, M., Barthlott, S., Hase, F., Risi,
682 C.,Clerbaux, C., Hurtmans, D., Coheur, P.-F., 2015. Cross-validation of IASI/MetOp
683 derived tropospheric δD with TES and ground-based FTIR observations. *Atmos. Meas.*
684 *Tech*. 8, 1447–1466. https://doi.org/10.5194/amt-8-1447-2015.

685 Lacour, J-L., Risi, C., Worden, J., Clerbaux, C., Coheur, P.F., 2018. Importance of depth and
686 intensity of convection on the isotopic composition of water vapor as seen from IASI and
687 TES δD observations. *Earth and Planetary Science Letters* 481: 387–394.
688 https://doi.org/10.1016/j.epsl.2017.10.048.

689 Laing, A., and J. M. Fritsch, 1997: The global population of mesoscale convective complexes.
690 *Quart. J. Roy. Meteor. Soc*.,123,389–405.

691 Laurent, H., and Machado, L.A.T., 2002. Characteristics of the convective cloud system
692 organization during WETAMC/LBA – Comparison with West African convective
693 systems. Second international LBA science conference, Manaus, 7-10 July 2002.

694 Lawrence, J. R., Gedzelman, S.D., Dexheimer, D., Cho, H.K., Carrie, G.D., Gasparini, R.,
695 Anderson, C. R., Bowman, K. P., and Biggerstaff, M. I., 2004. Stable isotopic
696 composition of water vapor in the tropics, *J. Geophys. Res*., 109,
697 D06115,doi:10.1029/2003JD004046

698 Lee, JE., Fung, I., 2008. 'Amount effect' of water isotopes and quantitative analysis of post
699 condensation processes. *Hydrol. Processes* 22: 1–8.

700 Lutz, A., Thomas, J.M., Panorska, A., 2011. Environmental controls on stable isotope
701 precipitation values over Mali and Niger, West Africa. *Environ Earth Sci* (2011) 62:1749–
702 1759. DOI 10.1007/s12665-010-0655-7

703 Mathon, V., and Laurent, H., 2001. Life cycle of Sahelian mesoscale convective cloud
704 systems. *Q. J. R. Meteorol. Soc*., 127(572): 377–406.

705 Mapes, B. E., and Houze, Jr., 1993. Cloud clusters and superclusters over the Oceanic warm
706 pool, *Mon. Wea. Rev*., 121, 1398–1415.

Merlivat, L., and Jouzel, J., 1979. Global climatic interpretation of the deuterium-oxygen 18 relationship for precipitation, *J. Geophys. Res*., 84, 5029–5033

Moerman, J.W., Cobb, K.M., Adkins, J.F., Sodemann, H., Clark, B., Tuen, A., 2013. Diurnal to interannual rainfall δ18O variations in northern Borneo driven by regional hydrology. *Earth Planet. Sci. Lett*. 369e370, 108-119. http://dx.doi.org/ 10.1016/j.epsl.2013.03.014

Moyer, E. J., Irion, F.W., Yung, Y.L., and. Gunson, M. R., 1996. ATMOS stratospheric deuterated water and implications for troposphere-stratosphere transport, *Geophys. Res. Lett*., 23(17), 2385–2388, doi:10.1029/96GL01489.

Nicholson, S.E., Grist, J.P., 2003. The seasonal evolution of the atmospheric circulation over west africa and equatorial Africa. *J Climate* 16(7):1013–1030

Odekunle, T.O. and Eludoyin, A.O., 2008. Sea Surface Temperature Patterns in the Gulf of Guinea: Their Implications for the Spatio-Temporal Variability of Precipitation in West Africa. *International Journal of Climatology*, 28, 1507-1517. http://dx.doi.org/10.1002/joc.1656

Ogou, F.K., Batebana, K., Ogwang, B.A., Sein, Z.M.M., Ongoma, V., Ngarukiyimana, J.P., 2016. Investigation of the influence of Atlantic Ocean on rainfall variability over Benin Republic, West Africa. *Ethiopian Journal of Environmental Studies & Management* 9 (1): 70 – 79, 2016. ISSN:1998-0507 doi: http://dx.doi.org/10.4314/ejesm.v9i1.7

Penna, D., Stenni, B., Sanda, M., Wrede, S., Bogaard, T.A., Gobbi, A., Borga, M., Fischer, B.M.C., Bonazza, M., Charova, Z., 2010. On the reproducibility and repeatability of laser absorption spectroscopy measurements for δ^2H and $\delta^{18}O$ isotopic analysis. *Hydrol. Earth Syst. Sci. Discuss*., 7, 2975–3014, 2010. www.hydrol-earth-syst-sci-discuss.net/7/2975/2010/doi:10.5194/hessd-7-2975-2010

730 Pfahl, S., and Wernli, H., 2009. Lagrangian simulations of stable isotopes in water vapor – an
731 evaluation of non-equilibrium fractionation in the Craig-Gordon model, *J. Geophys. Res*.,
732 114, D20108, doi:10.1029/2009JD012054.

733 Pohl, B., Macron, C., & Monerie, P.A., 2017. Fewer rainy days and more extreme rainfall by
734 the end of the century in Southern Africa. Sci. Rep. 7, 46466; doi: 10.1038/srep46466.

735 Preston-Whyte, R., Tyson, P., 1988. The atmosphere and weather of Southern Africa. *Oxford*
736 *University Press*, Cape Town, pp 334

737 Rahul, P., Ghosh, P., & Bhattacharya, S. K., 2016. Rainouts over the Arabian Sea and
738 Western Ghats during moisture advection and recycling explain the isotopic composition
739 of Bangalore summer rains. *Journal of Geophysical Research: Atmospheres*, *121*(11),
740 6148-6163.

741 Ren, W., Yao, T., & Xie, S.,2017. Key drivers controlling the stable isotopes in precipitation
742 on the leeward side of the central Himalayas. *Atmospheric Research*, *189*, 134-140.

743 Risi, C., Bony, S., Vimeux, F., 2008a. Influence of convective processes on the isotopic
744 composition (δ18O and δD) of precipitation and water vapor in the tropics: 2. Physical
745 interpretation of the amount effect. *J. Geophys. Res*. 113, D19306.
746 http://dx.doi.org/10.1029/2008JD00943

747 Risi, C., Bony, S., Vimeux, F., Descroix, L., Ibrahim, B., Lebreton, E., Mamadou I., Sultan,
748 B., 2008b. What controls the isotopic composition of the African monsoon precipitation?
749 Insights from event-based precipitation collected during the 2006 AMMA field campaign.
750 *Geophysical Research Letters*, Vol. 35, L24808, doi: 10.1029/2008GL035920

Risi, C., S. Bony, F. Vimeux, M. Chong, L. and Descroix, L., 2010a. Evolution of the water stable isotopic composition of the rain sampled along Sahelian squall lines, *Quart. J. Roy. Meteor. Soc*., 136, 227–242.

Risi, C., Bony, S., Vimeux, F., Frankenberg, C., Noone, D., & Worden, J., 2010b. Understanding the Sahelian water budget through the isotopic composition of water vapor and precipitation. *Journal of Geophysical Research: Atmospheres*, *115*(D24).

Risi, C., Noone, D., Worden, J., Frankenberg, C., Stiller, G., Kiefer, M., Funke, B., Walker, K., Bernath, P., Schneider, M., Wunch, D., Sherlock, V., Deutscher, N., Griffith, D.,. Wennberg, P.O., Strong, K., Smale, D., Mahieu, E., Barthlott, S., Hase, F., García, O., Notholt, J., Warneke, T., Toon, G., Sayres, D., Bony, S., Lee, J., Brown, D., Uemura, R., and Sturm, C., 2012.Process evaluation of tropospheric humidity simulated by general circulation models using water vapor isotopologues: 1. Comparison between models and observations, *J. Geophys. Res*., 117, D05303

Risi, C., Noone, D., Frankenberg, C., and Worden, J., 2013. Role of continental recycling in intraseasonal variations of continental moisture as deduced from model simulations and water vapor isotopic measurements, *Water Resour. Res*., 49, 4136–4156, doi:10.1002/wrcr.20312.

Rozanski, K., Araguas-Araguas, L., and Gonfiantini, R., 1993. Isotopic patterns in modern global precipitation, in Climate Change in Continental Isotopic Records, *Geophys. Monogr. Ser*., vol. 78, edited by P. K. Swart et al., pp. 1 –36, AGU, Washington, D. C

Salamalikis, V., Argiriou, A. A., & Dotsika, E., 2015. Stable isotopic composition of atmospheric water vapor in Patras, Greece: A concentration weighted trajectory approach. *Atmospheric research*, *152*, 93-104.

774 Salati, E., Dall'Olio, A., Matsui, E., and Gat, J., 1979. Recycling of water in the Amazon
775 basin: An isotopic study, *Water Resour. Res*, 15, 1250–1258, doi:
776 10.1029/WR015i005p01250.

777 Samuels Crow, K. E., Galewsky, J., Hardy, D. R., Sharp, Z. D., Worden, J., & Braun, C.,
778 2014. Upwind convective influences on the isotopic composition of atmospheric water
779 vapor over the tropical Andes. *Journal of Geophysical Research: Atmospheres*, *119*(12),
780 7051-7063.

781 Sanchez-Murillo, R., Birkel, C., Welsh, K., Esquivel-Hernandez, G., Corrales-Salazar, C.,
782 Boll, J., Brooks, E., Roupsard, E., Saenz-Rosales, O., Katchan, I., Arce-Mesen, R.,
783 Soulsby, C., Araguas-Araguas, L.J., 2015. Key drivers controlling stable isotope
784 variations in daily precipitation of Costa Rica: Caribbean Sea versus Eastern Pacific
785 Ocean moisture sources, *Quaternary Science Reviews*
786 http://dx.doi.org/10.1016/j.quascirev.2015.08.028

787 Schott, F., Carton, J., Hazeleger, W., Johns, W., Kushnir, Y., Reason, C., Xie, SP., 2003.
788 White paper on a tropical atlantic climate experiment (t.a.c.e.) CLIVAR Atlantic
789 Implementation Panel, US Clivar, Washington

790 Sèze, G., Pelon, J., Derrien, M., Le Gléau, H., Six, B., 2015. Evaluation against CALIPSO
791 lidar observations of the multigeostationary cloud cover and type dataset assembled in the
792 framework of the Megha-Tropiques mission. *Quart. J. Roy. Meteor. Soc*., 141, 774–797,
793 https://doi.org/10.1002/qj.2392.

794 Shao, L., Tian, L., Cai, Z., Cui, J., Zhu, D., Chen, Y., & Palcsu, L., 2017. Driver of the
795 interannual variations of isotope in ice core from the middle of Tibetan Plateau.
796 *Atmospheric Research*, *188*, 48-54.

797 Stewart, M. K., 1975. Stable isotope fractionation due to evaporation and isotopic exchange
798 of falling water drops: Applications to atmospheric processes and evaporation of lakes.
799 *Journal of Geophysical Research*, *80*(9), 1133-1146.

800 Sultan. B., Janicot, S., 2000. Abrupt shift of the ITCZ over West Africa and intra-seasonal
801 variability. *Geophys Res Lett* 27:3353–3356

802 Sultan, B., Janicot, S., 2003. The West African monsoon dynamics. Part II: the ‘‘pre-onset’’
803 and ‘‘onset’’ of the summer monsoon. *J Clim* 16:3407–3427

804 Taupin, J.-D., R. Gallaire, and Y. Arnaud., 1997. Analyses isotopiques et chimiques des
805 précipitations sahéliennes de la région de Niamey au Niger: Implications climatologiques,
806 Hydrochemistry, 244, 151– 164, *IAH Congress*.

807 Tobin, I., Bony, S., & Roca, R., 2012. Observational evidence for relationships between the
808 degree of aggregation of deep convection, water vapor, surface fluxes, and radiation.
809 *Journal of Climate*, *25*(20), 6885-6904.

810 Tremoy, G., 2012. Etude de la composition isotopique (deutérium et oxygène 18) de la vapeur
811 d’eau à Niamey (Niger): vers une meilleure compréhension des processus atmosphériques
812 en Afrique de l’Ouest, Ph.D. thesis, Université de Versailles Saint-Quentinen-Yvelines

813 Tremoy, G., Vimeux, F., Mayaki, S., Souley, I., Cattani, O., Risi, C., ... & Oi, M., 2012b. A 1
814 year long $\delta^{18}O$ record of water vapor in Niamey (Niger) reveals insightful atmospheric
815 processes at different timescales. *Geophysical Research Letters*, *39*(8).

816 Tremoy, G., Vimeux, F., Soumana, S., Souley, I., Risi, C., Favreau, G., Oï, M., 2014.
817 Clustering mesoscale convective systems with laser-based water vapor $\delta^{18}O$ monitoring in
818 Niamey (Niger). doi: 10.1002/2013JD020968

819 Tuinenburg, O. A., Risi, C., Lacour, J.L., Schneider, M., Wiegele, A., Worden, J., Kurita, N.,
820 Duvel, J.P; Deutscher, N; Bony, S,.Coheur, P.F., and C. Clerbaux., 2015. Moist processes
821 during MJO events as diagnosed from water isotopic measurements from the IASI
822 satellite, *J. Geophys. Res. Atmos*., 120, 10,619–10,636, doi:10.1002/2015JD023461.

823 Villacís, M., Vimeux, F. and Taupin, J.-D., 2008. "Analysis of the Climate Controls on the
824 Isotopic Composition of Precipitation (d18O) at Nuevo Rocafuerte, 74.58W, 0.98S, 250
825 m, Ecuador." *C. R. Geosciences* 340(1): 1-9

826 Vimeux, F., Gallaire, R., Bony, S., Hoffmann, G., Chiang, J., Fuertes, R., 2005. What are the
827 climate controls on isotopic composition (δD) of precipitation in Zongo Valley (Bolivia)?
828 Implications for the Illimani ice core interpretation, *Earth Planet. Sci. Lett*. 240 (2005)
829 205–220

830 Vondou, D.A., Yepdo, Z.D., Djiotang Tchotchou, L.A., 2017. Diurnal Cycle of Convective
831 Cloud Occurrences over Cameroon during June–August. *Journal of the Indian Society of*
832 *Remote Sensing* https://doi.org/10.1007/s12524-017-0747-x

833 Vuille, M., Wermer, M., 2005. Stable isotopes in precipitation recording South American
834 summer monsoon and ENSO variability: observations and model results. Clim. Dyn. 25,
835 401-413. http://dx.doi.org/10.1007/s00382-005-0049-9.

836 Wing, A. A., Emanuel, K., Holloway, C. E., & Muller, C. (2017). Convective self-
837 aggregation in numerical simulations: a review. In *Shallow Clouds, Water Vapor,*
838 *Circulation, and Climate Sensitivity* (pp. 1-25). Springer, Cham.

839 Worden, J., and Coauthors. 2006. Tropospheric Emission Spectrometer observations of the
840 tropospheric HDO/H2O ratio: Estimation approach and characterization. *J. Geophys. Res*.,
841 111, D16309,

Worden, J, D. Noone, K. Bowman, and the Tropospheric Emission Spectrometer science team & data contributors. 2007. Importance of rain evaporation and continental convection in the tropical water cycle, *Natur*e, 445, doi:10.1038.

Worden, J., Kulawik, S., Frankenberg, C., Payne, V., Bowman, K., Cady-Pereira, K., Wecht, K., Lee, J.-E., Noone, D., 2012. Profiles of CH4, HDO, H2O, and N2O with improved lower tropospheric vertical resolution from aura TES radiances. *Atmos.Meas. Tech*. 5, 397–411. https://doi.org/10.5194/amt-5-397-2012.

Xu, W. and Zipser, E.J., 2012. Properties of deep convection in tropical continental, monsoon, and oceanic rainfall regimes. *Geophysical Research Letters*, VOL. 39, L07802, doi:10.1029/2012GL051242

Yoshimura, K., M. Kanamitsu, M. Dettinger., 2010. Regional downscaling for stable water isotopes: A case study of an atmospheric river event, *J. Geophys. Res*., 115, D18114

Yu, W., Wei, F., Ma, Y., Liu, W., Zhang, Y., Luo, L., ... & Qu, D., 2016. Stable isotope variations in precipitation over Deqin on the southeastern margin of the Tibetan Plateau during different seasons related to various meteorological factors and moisture sources. *Atmospheric Research*, *170*, 123-130.

Zongxing, L., Qi, F., Song, Y., Wang, Q. J., Yang, J., Yongge, L., ... & Xiaoyan, G., 2016). Stable isotope composition of precipitation in the south and north slopes of Wushaoling Mountain, northwestern China. *Atmospheric Research*, *182*, 87-101.

Web references

https://www.esrl.noaa.gov/psd/cgi-bin/data/composites/printpage.pl. Accessed on February 2018.

http://www.nwcsaf.org/web/guest/scientific-documentation. Accessed on November 2018

882 **List of Figures**

883 Figure 1. Map of the study area (Western Central Africa) with the location of GNIP stations
884 of Cotonou, Bangui, Douala and Sao-Tome.

885 Figure 2. Annual cycles of δ18O from 2006 to 2016. The blue line represents the mean
886 seasonal cycle while the red line corresponds to a given year

887 Figure 3. Monthly mean for δ18O (black line) and precipitation amounts (bars) at the GNIP
888 stations of Cotonou (2005-2012), Bangui (2009-2015), Douala (2006-2016) and Sao-Tome
889 (1962-1976). Summer enrichment phases are highlighted in pink and depletion phases in
890 spring and autumn are underlined in blue.

891 Figure 4. GPCP monthly mean precipitations (mm/day) distributions (colors) and back-
892 trajectories (dotted curves) during the period of 2006 to 2016. White color characterizes an
893 absence of precipitation. Monthly trajectories were calculated using monthly average mean
894 ERA-Interim reanalysis

895 Figure 5. Evolution of monthly mean GPCP precipitations (mm/day) along the back
896 trajectories over time (in hours) towards the Douala GNIP station in May, August, October
897 and January for the 2006-2016 period.

898 Figure 6. Monthly mean variations of δ18O (grey line) and average GPCP precipitations
899 (bars) recorded over the past 72h along the back trajectories for the 2006-2016 period.

900 Figure 7. Mean seasonal variations of (A) δD in precipitation (in grey) and in water vapor (in
901 black) at 900 hPa at Douala region as observed at the GNIP station (2006 to 2016) and by the
902 TES instrument (2004 to 2008) respectively; (B) δDP – δDv at Douala region

903 Figure 8. $\delta^{18}O$ in daily rainfall at Douala from March 2017 to August 2017.

Figure 9. Example of meteorological situations in the study region in 2017 (based on the SAFNWC cloud classification) during (A) spring and (B) summer periods. The backward trajectories (grey line) are plotted for each event.

Figure 10. Statistical distribution of daily rainfall duration at Douala as shown by box-and-whisker representation. The boxes have lines at the lower, median and upper quartile values. The whiskers are lines extending from each end of the box to 1.5 interquartile range. Red cross represents the mean and outliers are represented by black points above the maximum

List of Tables

Table 1. Characteristics of GNIP sampling sites in GOG and Central African regions. Data from Cotonou, Bangui and Sao-Tome have been obtained online from the GNIP database (AIEA/OMM 2018).

Table 2. Coefficient of determination (r^2) between $\delta^{18}O$ and local meteorological settings (precipitation (P) and temperature (T)) for monthly GNIP stations of Cotonou, Bangui, Douala and Sao-Tome, at different sampling periods.

Table3. Coefficient of determination (r^2) between δ18O and average GPCP precipitation in average over the first day, two first days and three first days along the air parcel trajectory before rainfall in Douala. Correlation coefficients ≥ 95% are highlighted in bold and underlined.

Table 4. Information about Fland during the last 3 days along the air parcels trajectories for the months of March, April and May; and its relationship (r^2) with δ18O, and upstream GPCP precipitation. For the summer period, Fland corresponds to 0% for almost all the rainy days. Correlation coefficients ≥ 95% are highlighted in bold and underlined.

Table 5. Information on the organization of convection (cloud types, cloud area and local/upstream) and its influence on the isotopic composition of daily rainfall over the period from March 2017 to August 2017. Cloud areas were only calculated for very high classes. Correlation coefficients significant ≥ 95% are in bold and underlined.

Figures and captions.

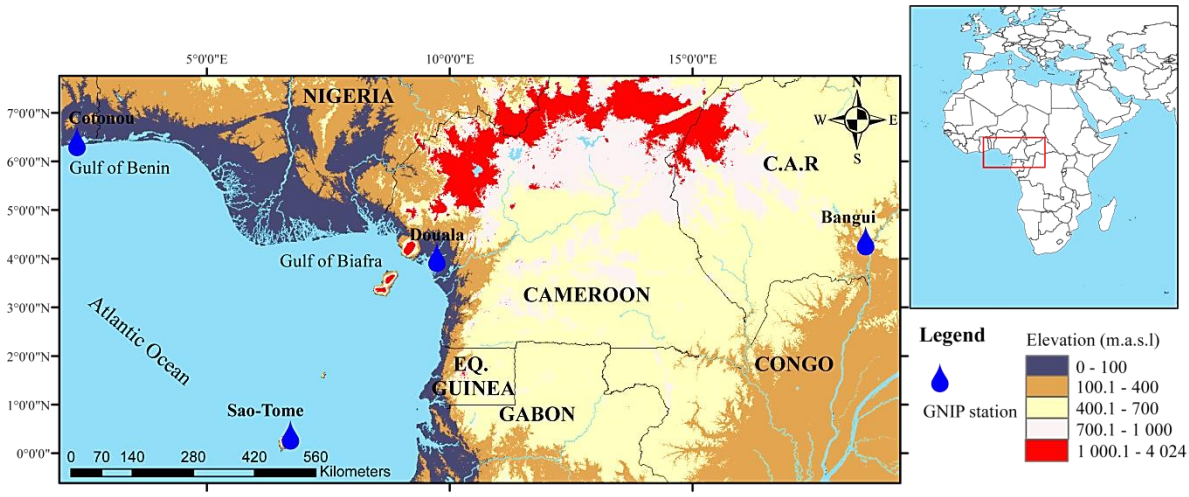

Figure 1. Map of the study area (Western Central Africa) with the location of GNIP stations of Cotonou, Bangui, Douala and Sao-Tome.

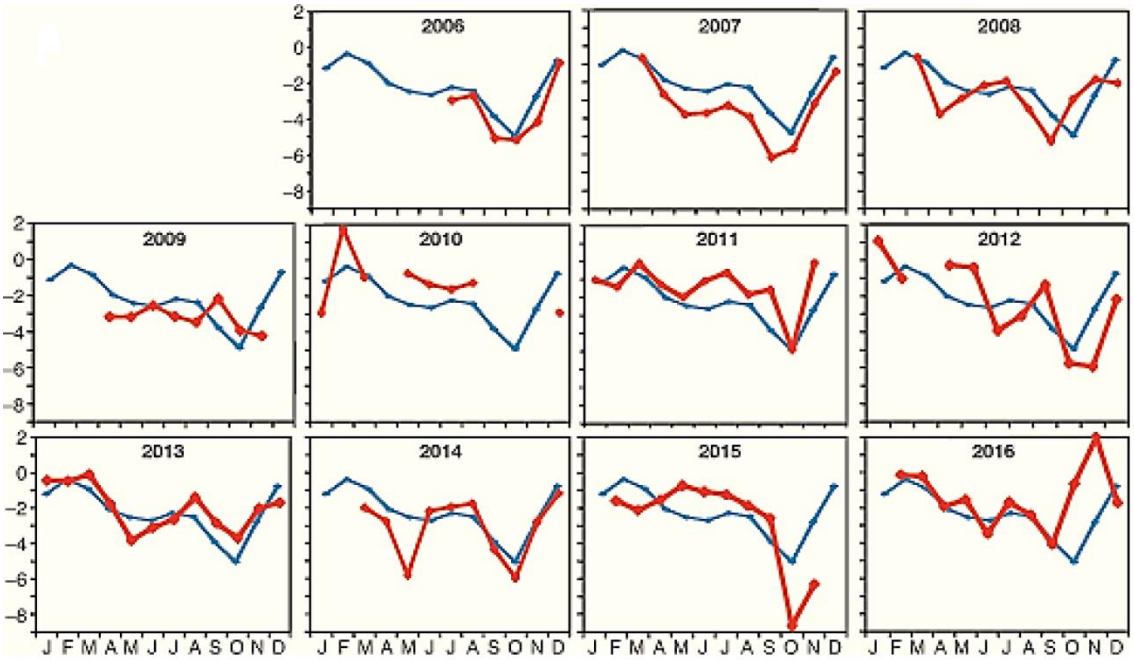

Figure 2. Annual cycles of $\delta^{18}O$ from 2006 to 2016. The blue line represents the mean seasonal cycle while the red line corresponds to a given year

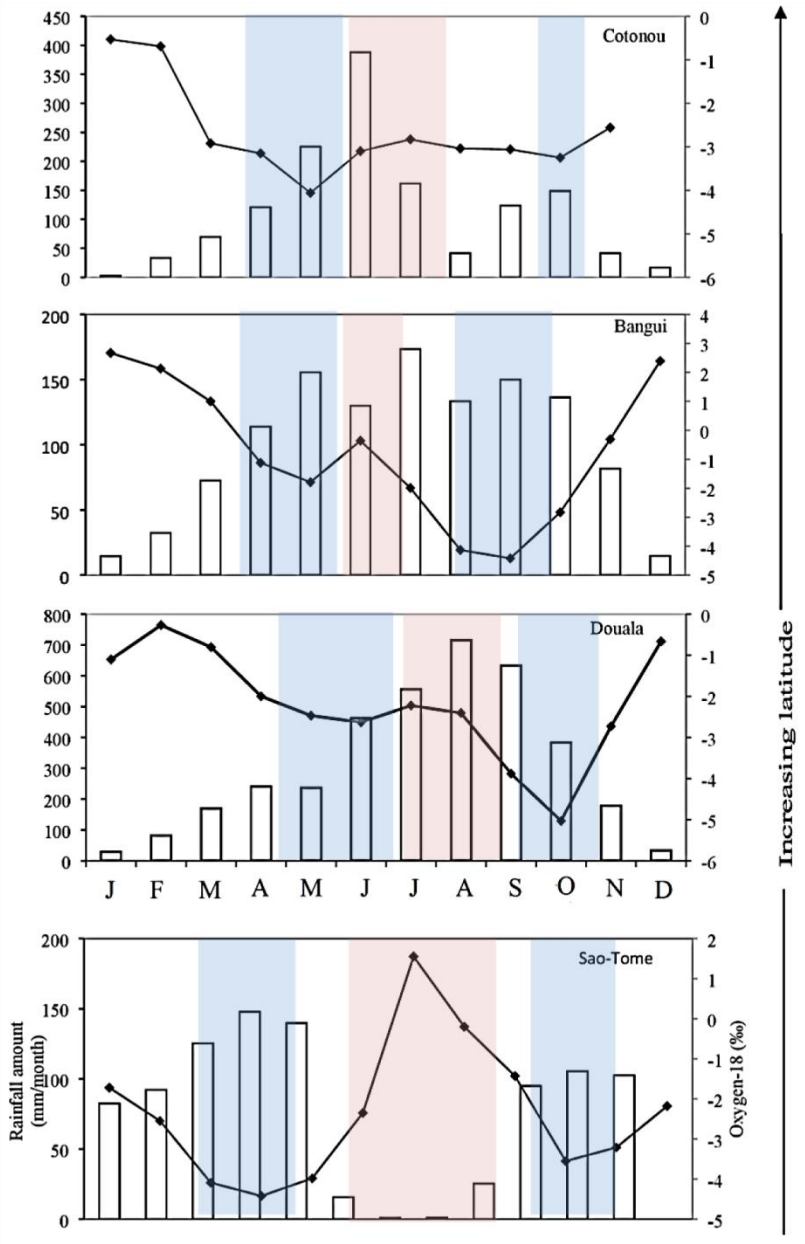

Figure 3. Monthly mean for $\delta^{18}O$ (black line) and precipitation amounts (bars) at the GNIP stations of Cotonou (2005-2012), Bangui (2009-2015), Douala (2006-2016) and Sao-Tome (1962-1976). Summer enrichment phase are highlighted in pink and depletion phases in spring and autumn are underlined in blue.

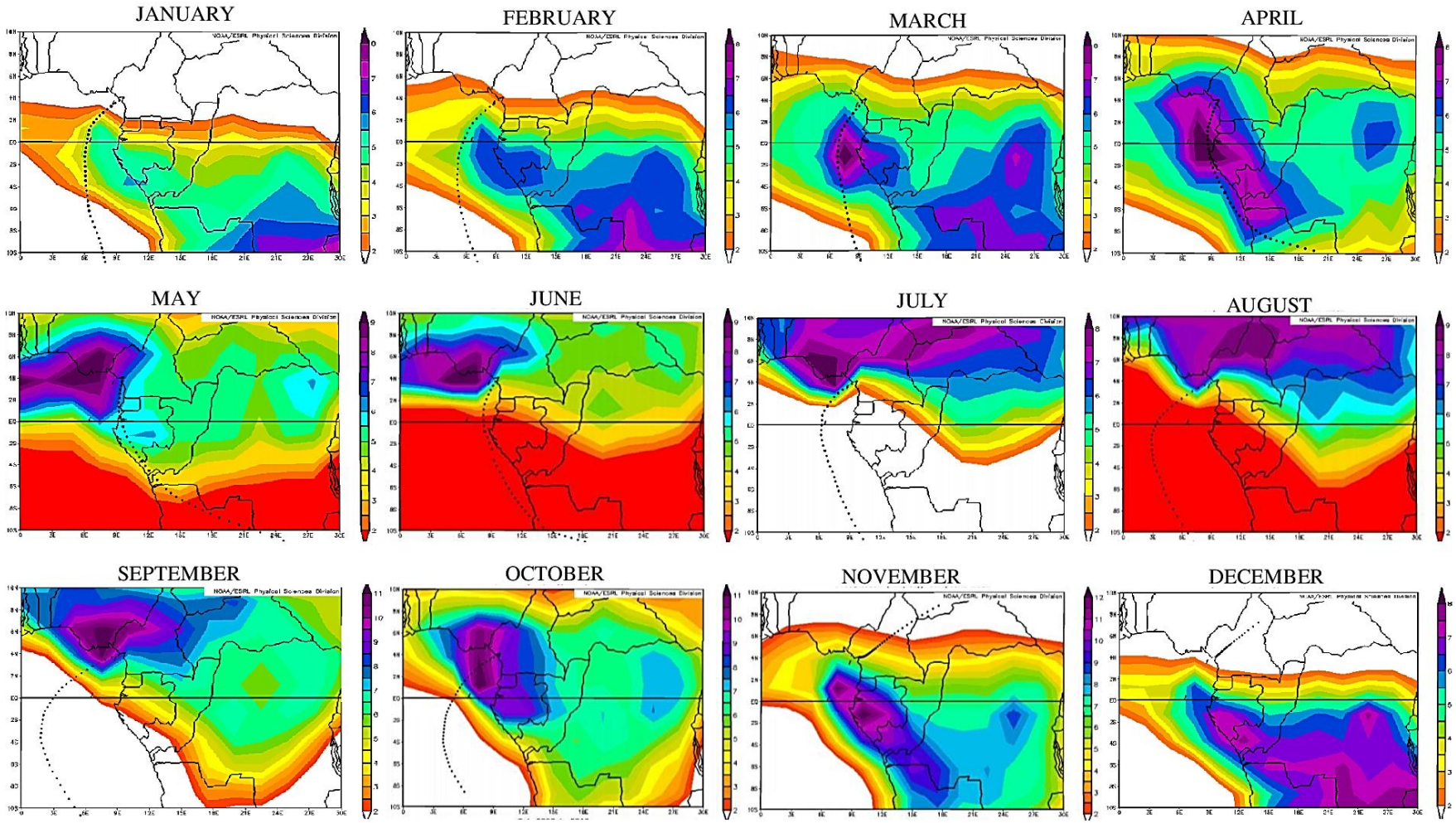

Figure 4. GPCP monthly mean precipitations (mm/day) distributions (colors) and back-trajectories (dotted curves) during the period of 2006 to 2016. White color characterizes an absence of precipitation. Monthly trajectories were calculated using monthly average mean ERA-Interim reanalysis

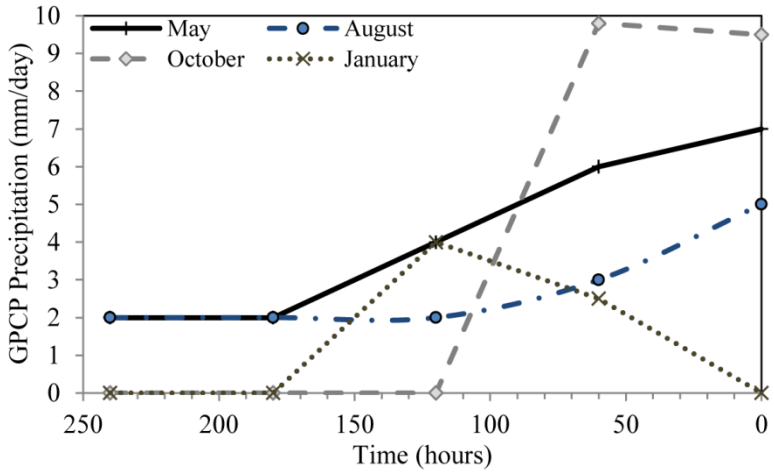

Figure 5. Evolution of monthly mean GPCP precipitations (mm/day) along the back trajectories over time (in hours) towards the Douala GNIP station in May, August, October and January for the 2006-2016 period.

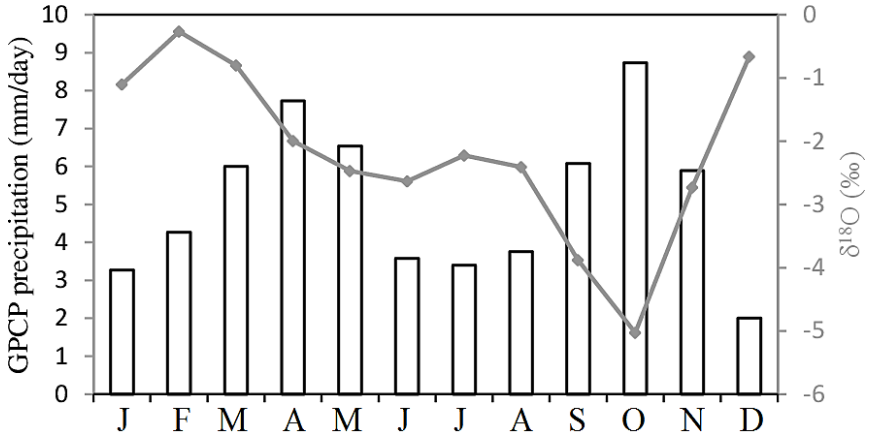

Figure 6. Monthly mean variations of $\delta^{18}O$ (grey line) and average GPCP precipitations (bars) recorded over the past 72h along the back trajectories for the 2006-2016 period.

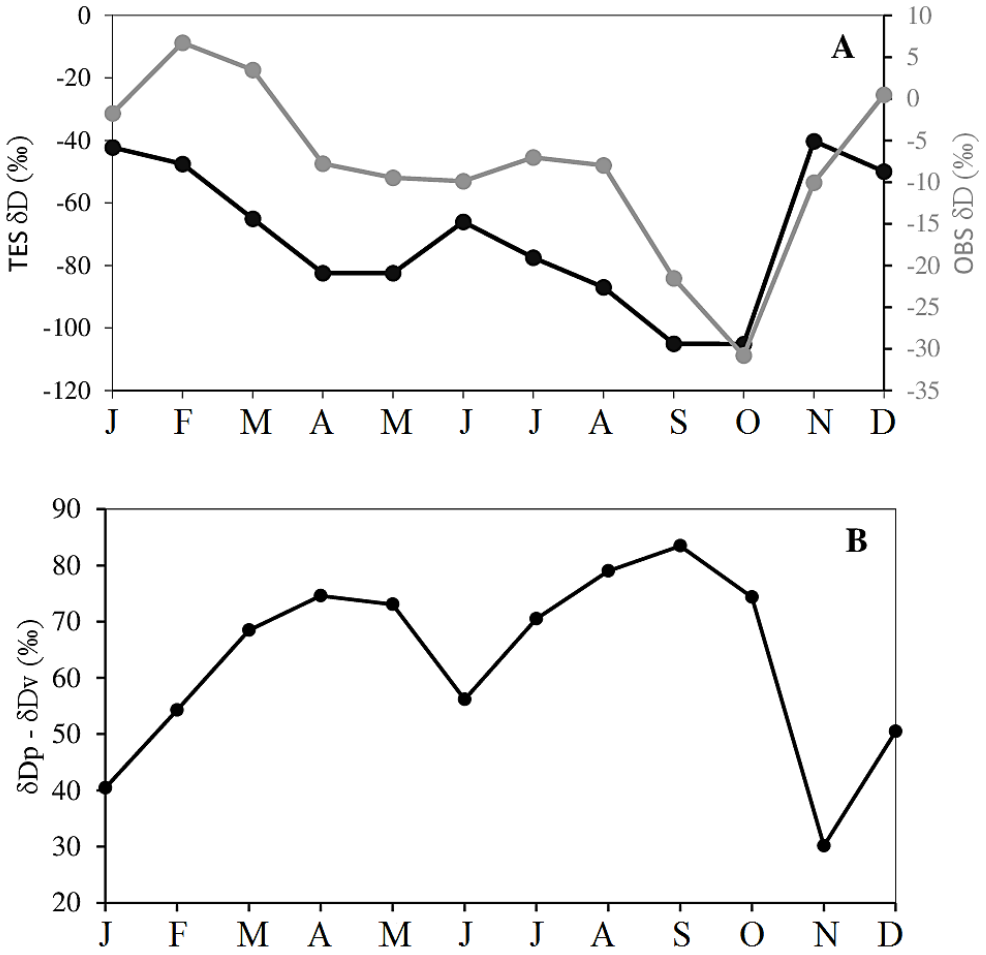

Figure 7. Mean seasonal variations of (A) δD in precipitation (in grey, Y-axis on the right) and in water vapor (in black, Y-axis on the left) at 900 hPa over Douala as observed at the GNIP station (2006 to 2016) and by the TES instrument (2004 to 2008) respectively; (B) δD_P – δD_v over Douala

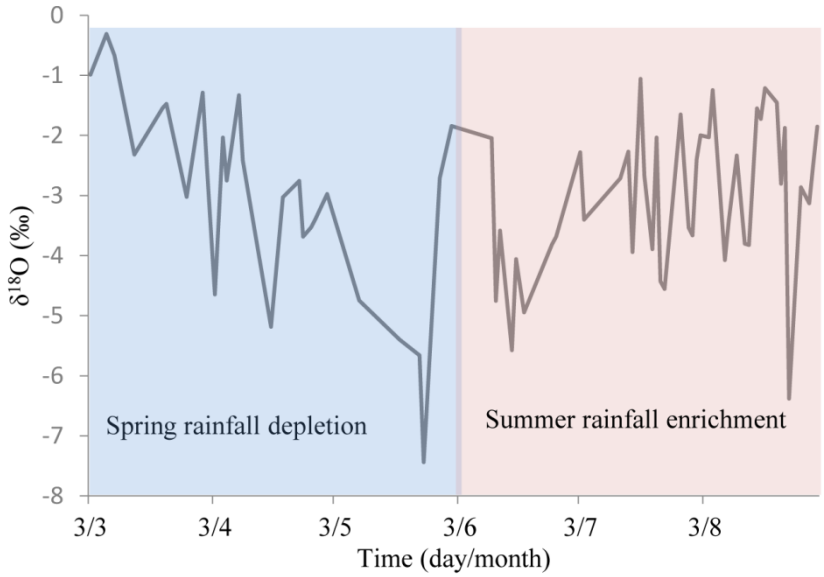

Figure 8. $\delta^{18}O$ in daily rainfall at Douala from March 2017 to August 2017.

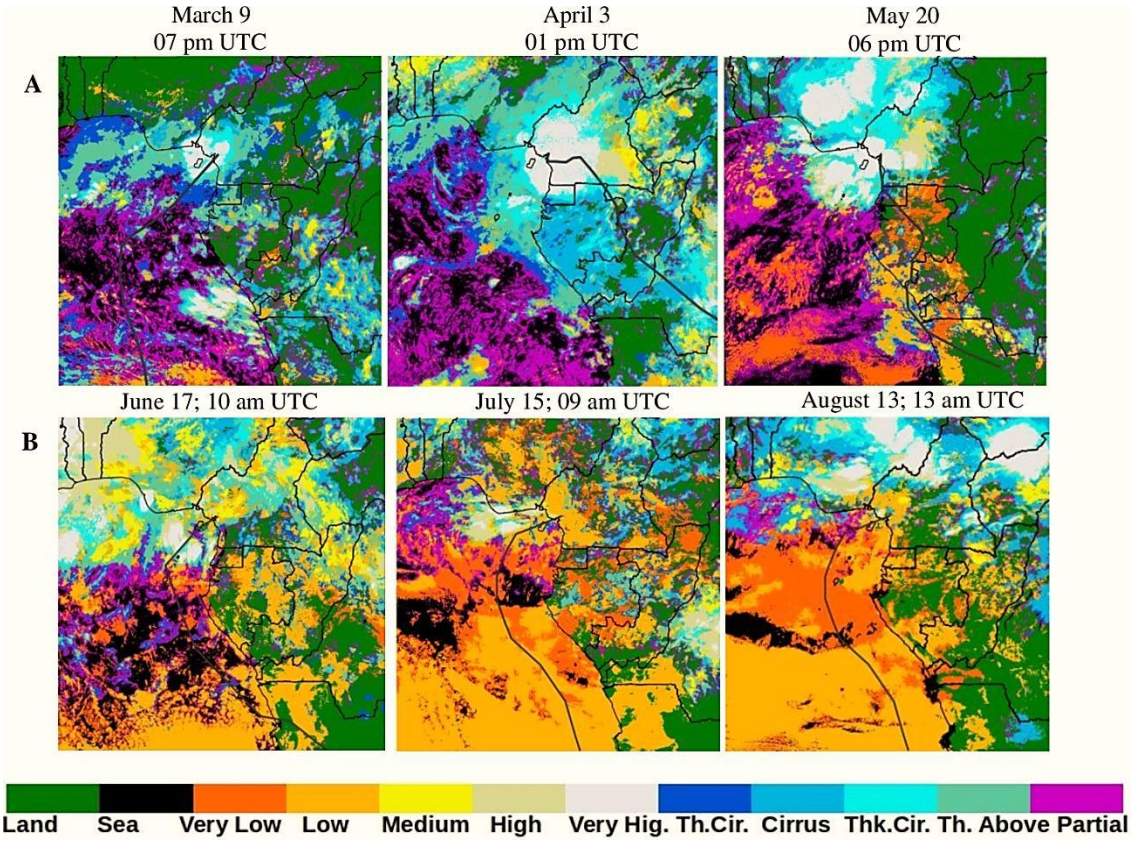

Figure 9. Example of meteorological situations in the study region in 2017 (based on the SAFNWC cloud classification) during (A) spring and (B) summer periods. The backward trajectories (grey line) are plotted for each event.

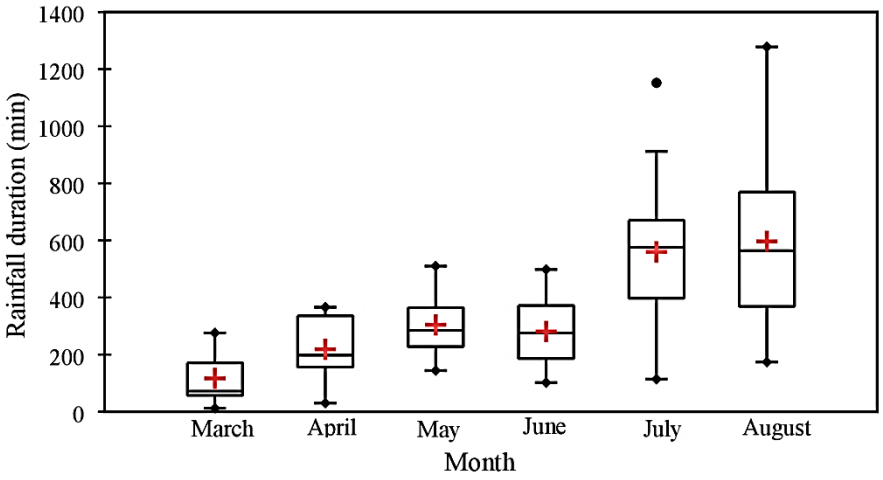

Figure 10. Statistical distribution of daily rainfall duration at Douala as shown by box-and-whisker representation. The boxes have lines at the lower, median and upper quartile values. The whiskers are lines extending from each end of the box to 1.5 interquartile range. Red cross represents the mean and outliers are represented by black points above the maximum

Tables

Table 1. Characteristics of GNIP sampling sites in GOG and Central African regions. Data from Cotonou, Bangui and Sao-Tome have been obtained online from the GNIP database (AIEA/OMM 2018).

Site	Country	Sampling period	Elevation (m.a.s.l)	Mean annual precip*(mm)	Vapor Pressure (hPa)	Mean annual T* (°C)
Cotonou	Benin	2005 - 2012	14	1395	28.3	27.1
Bangui	CAR*	2009 - 2015	363	1208	25.7	26.3
Douala	Cameroon	2006 - 2016	18	3720	30.5	27
Sao-Tome	Sao-Tome and Principe	1962-1976	8	933.7	26.2	25.2

* Precip. = Precipitation, T = temperatures; CAR= Central African Republic; dec. deg = decimal degrees

Table 2. Coefficient of determination (r^2) between $\delta^{18}O$ and local meteorological settings (precipitation (P) and temperature (T)) for monthly GNIP stations of Cotonou, Bangui, Douala and Sao-Tome, at different sampling periods.

Stations	Sampling period	r^2 $\delta^{18}O/P$	r^2 $\delta^{18}O/T$
Cotonou (n=95)	2005 - 2012	0.05	0.13
Bangui (n=81)	2009 - 2016	0.24	0.04
Douala (n=106)	2006 - 2016	0.12	0.09
Sao-Tome (n=123)	1962 - 1976	0.19	0.20

Table3. Coefficient of determination (r^2) between $\delta^{18}O$ and average GPCP precipitation in average over the first day, two first days and three first days along the air parcel trajectory before rainfall in Douala. Correlation coefficients ≥ 95% are highlighted in bold and underlined.

		March (n=08)	**April (n=12)**	**May (n=07)**	**June (n=09)**	**July (n=14)**	**August (n=20)**
$\delta^{18}O$ Vs GPCP Precipitation	One day before	**0.53**	**0.43**	0.40	0.03	0.14	0.15
	Two days before	**0.55**	0.23	0.28	0.14	0.03	**0.23**
	Three days before	**0.64**	0.16	0.44	0.00	0.11	**0.23**

Table 4. F_{land} statistics during the last 3 days along the air parcels trajectories for the months of March, April and May. Relationship (r^2) between F_{land}, $\delta^{18}O$, and upstream GPCP precipitation. For the summer period, F_{land} corresponds to 0% for almost all rainy days. Correlation coefficients ≥ 95% are in bold and underlined.

	March	**April**	**May**
F_{land} (%) *Minimum*	0	0	25
F_{land} (%) *Maximum*	100	100	100
F_{land} (%) *Mean*	25	69.45	70.83
F_{land} (%) *Median*	0	83.34	79.17
***r^2* (F_{land} *vs* $\delta^{18}O$)**	0.23	**0.33**	0.28
***r^2* (F_{land} *vs* GPCP precip.)**	0.51	0.42	0.85

Table 5. Information on the organization of convection (cloud types, cloud area and local/upstream) and its influence on the isotopic composition of daily rainfall over the period from March 2017 to August 2017. Cloud areas were only calculated for very high classes. Correlation coefficients significant ≥ 95% are in bold and underlined.

	March	**April**	**May**	**June**	**July**	**August**
Very low to low clouds (%)	0	0	0	0	71.43	54
Medium to high clouds (%)	0	0	18.18	72.73	21.43	40.5
Very high clouds (%)	100	100	81.82	27.27	7.14	5.5
Local without upstream convection (%)	75	27.27	0	22.29	7.14	0
Upstream and local convection (%)	25	72.73	100	77.71	92.86	100
Minimum cloud area (km^2)	5300 ± 100	4500 ± 100	63400 ± 100	2400 ± 100		-
Maximum cloud area (km^2)	35300 ±100	158100 ± 100	285600 ± 100	280000 ± 100	3077±100	615±100
Mean cloud area (km^2)	17800 ± 100	73700 ± 100	225100 ± 100	138500 ± 100	-	-
r^2 Clouds area *Vs* rainfall duration	**0.54**	**0.63**	**0.51**	0.34	-	-
r^2 Clouds area *Vs* $\delta^{18}O$	**0.44**	**0.55**	**0.97**	**0.90**	-	-
r^2 Clouds area *Vs* GPCP precipitation	0.30**	0.10**	0.01**	0.46**		
r^2 Rainfall duration *Vs* $\delta^{18}O$	**0.44**	**0.54**	**0.64**	0.24	0.00	0.07

***Anti-correlation*

Author contribution statements

B. Nlend , H. Celle-Jeanton , C. Risi , B. Pohl , F. Huneau , S. Ngo Boum-Nkot , G. Seze , P. Roucou c, P. Camberlin , J. Etame f and B. Ketchemen-Tandia conceived the presented paper,. developed the theory and performed the computations.

F. Huneau was particulary in charge of analytical methods.

G. Seze , C. Risi and H. Celle-Jeanton encouraged B. Nlend to investigate cloud type products.

B. Pohl, P. Camberlin and P. Roucou contribute to the understanding and redaction of the climate context.

B. Pohl provided a significant help to improve the English.

All authors discussed the results and contributed to the final manuscript.